

**IMPROVING CAR RADIATOR PERFORMANCE BY USING TiO₂-WATER
NANOFLUID**

**A THESIS SUBMITTED TO
FACULTY OF TECHNOLOGY SCIENCES OF
KARABUK UNIVERSITY**

BY

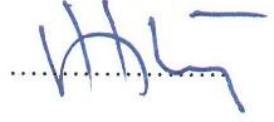
SIRAJ ALI AHMED

**IN PARTIAL FULFILLMENT OF THE REQUIREMENTS FOR
THE DEGREE OF DOCTOR OF SCIENCE IN
DEPARTMENT OF ENERGY SYSTEMS ENGINEERING**

January 2019

I certify that in my opinion the thesis submitted by Siraj Ali AHMED titled “IMPROVING CAR RADIATOR PERFORMANCE BY USING TIO₂-WATER NANOFLUID” is fully adequate in scope and quality as a thesis for the degree of Doctor of Philosophy.

Prof. Dr. Mehmet ÖZKAYMAK
Thesis Advisor, Department of Energy Systems Engineering



This thesis is accepted by the examining committee with a unanimous vote in the Department of Energy Systems Engineering as a Doctor of Philosophy thesis. January 18, 2019

Examining Committee Members (Institutions)

Signature

Chairman: Prof. Dr. Kurtuluş BORAN (GU)



Member : Prof. Dr. Mehmet ÖZKAYMAK (KBU)



Member : Prof. Dr. Tayfun MENLİK (GU)



Member : Doç. Dr. Muhammet KAYFECİ (KBU)



Member : Doç. Dr. Engin GEDİK (KBU)



..... / / 2019

The degree of Doctor of Philosophy by the thesis submitted is approved by the Administrative Board of the Graduate School Natural and Applied Sciences, Karabük University.

Prof. Dr. Filiz ERSÖZ
Head of Graduate School Natural and Applied Sciences





“I announce that all the data inside this proposal has been assembled and displayed in understanding with scholarly directions and moral standards and I have agreeing to the prerequisites of these directions and standards cited all those which don't start in this work as well.”

Siraj Ali AHMED

ABSTRACT

Ph.D. Thesis

IMPROVING CAR RADIATOR PERFORMANCE BY USING TiO₂-WATER NANOFLUID

Siraj Ali Ahmed

Karabük University

Graduate School of Natural and Applied Science

The Department of Energy Systems Engineering

Thesis Advisor:

Prof. Dr. Mehmet ÖZKAYMAK

January 2019, 99 pages

The foremost later improvements in nanotechnology have lead to changes in unique employments of nanofluids in car motor cooling. Within the display ponder, upgrade of car motor radiator by TiO₂-water nanofluid as a coolant of car motor radiator was explored tentatively. In arrange to decide the impact of TiO₂-water nanofluid on radiator's execution, tests were performed with immaculate water and TiO₂-water nanofluid independently and comes about were compared with other considers on vehicle engine framework FIAT DOBLO 1.3 MJTD ENG. The most objective was to check the viewpoints of warm exchange of the TiO₂-water nanofluid as a substitution to the standard coolant framework. For this reason, tests were carried out employing a TiO₂ nanofluid with 0.1, 0.2 and 0.3% volume concentrations with stream rates of 0.097 and 0.68 m³/h in laminar floe locale, where Reynolds number extended from 560 to 1650. Our comes about appear that the grinding calculate diminishes when Reynolds number and the volume concentration

are expanded. Besides, TiO₂-water nanofluid with 0.2% concentration can upgrade the viability of car radiator by 47% as compared to 0.1 and 0.3% concentrations and unadulterated water as a coolant. At last, the normal warm exchange coefficient was specifically influenced by the increment in Reynolds number and volume concentration division of the nanofluid.

Key Words : Car radiator, Nanofluids, Performance, Reynolds number, TiO₂ - water

Science Code : 928.1.065



ÖZET

Yüksek Lisans Tezi

TiO₂-SU NANOAKIŞKAN KULLANARAK ARABA RADYATÖR PERFORMANSININ GELİŞTİRİLMESİ

Siraj Ali Ahmed

**Karabük Üniversitesi
Fen Bilimleri Enstitüsü
Teknoloji Fakültesi**

Tez Danışmanı:

Prof. Dr. Mehmet ÖZKAYMAK

Ocak 2019, 99 sayfa

Nanoteknolojideki en son gelişmeler, araba motor soğutmasında nanoakışkanların orijinal kullanımlarında iyileşmelere yol açmıştır. Bu çalışmada, otomobil motoru radyatörünün bir radyatör olarak TiO₂-su nanofluid tarafından araba motor radyatörünün geliştirilmesi deneysel olarak incelenmiştir. TiO₂-su nano-akışkanının radyatörün performansı üzerindeki etkisini belirlemek için, deneyler saf su ve TiO₂-su nanofluid ile ayrı ayrı gerçekleştirilmiş ve sonuçlar, taşıt motoru sistemi ile ilgili diğer çalışmalarla karşılaştırılmıştır. FIAT DOBLO 1.3 MJTD ENG. Temel amaç, TiO₂-su nanoakışkanının geleneksel soğutma sistemine bir ikame olarak ısı transferinin yönlerini kontrol etmektir. Bu amaçla, Reynolds sayısı 560 ile 1650 arasında değişen laminar akış bölgesinde 0.097 ve 0.68 m³/h akış hızları ile 0.1, 0.2 ve 0.3 hacim hacimli bir TiO₂ nanofluid kullanılarak gerçekleştirilmiştir. Reynolds sayısı ve hacim konsantrasyonu arttığında sürtünme faktörü azalır.

Ayrıca, % 0.2'lik konsantrasyona sahip TiO_2 -su nanofluid, araba radyatörünün etkinliğini % 47 ve % 0,3 konsantrasyona ve bir soğutucu olarak saf suya kıyasla % 47 oranında artırabilir. Son olarak, ortalama ısı transfer katsayısı, nanoakışkanın Reynolds sayısı ve hacim konsantrasyon fraksiyonundaki artıştan doğrudan etkilenmiştir.

Anahtar Kelimeler : Araba radyatörü, Nanoakışkanlar, Performans, Reynolds sayısı, TiO_2 – su

Bilim Kodu : 928.1.065



ACKNOWLEDGMENT

Firstly I would like to thank my boss, help. Prof. Dr. Mehmet ÖZKAYMAK. Thank you for sharing your riches of information and encounter and for giving accommodating counsel on my investigate. The opportunity to work with you and in an connected workforce environment has been a benefit. Thank you for helping me to create a firm establishment of information and expertise to set out on my inquire about career. I would also like to thank the support staff from the energy systems department that made this research possible.

I wish to amplify an extraordinary thanks to the management of energy systems department in Gazi University for their participation in this research project.

At long last, I would like to expand my most profound appreciation to my guardians, my family and companions for their bolster and support all through my thinks about.

CONTENTS

	<u>Page</u>
APPROVAL	ii
ABSTRACT.....	iv
ÖZET	vi
ACKNOWLEDGMENT	viii
CONTENTS.....	ix
LIST OF FIGURES	xii
LIST OF TABLES.....	xvi
SYMBOLS AND ABBREVIATIONS INDEX	xvii
CHAPTER 1	1
INTRODUCTION & OBJECTIVES.....	1
1.1. ESSENTIAL QUALITIES OF COOLANTS	3
1.2. HISTORICAL OVERVIEW.....	4
1.3. NANOFUIDS	5
1.4. SYNTHESIS OF NANOFUIDS.....	5
1.5. PARTICLE MATERIAL AND BASE FLUID	6
1.6. PARTICLE SIZE	6
1.7. PARTICLE SHAPE	7
1.8. PREPARATION OF NANOFUID.....	7
1.9. VISCOSITY OF NANOFUID.....	9
1.10. THERMAL CONDUCTIVITY OF NANOFUID	9
1.11. FRICTION FACTOR AND HEAT TRANSFER.....	9
1.12. ADVANTAGES OF NANOFUIDS	10
1.13. PROBLEM STATEMENT	10
1.14. AIM OR GOAL OF THIS WORK	11
1.15. ORGANIZATION OF THE THESIS	11

	<u>Page</u>
CHAPTER 2	13
LITERATURE REVIEW	13
2.1. BASE FLUID	23
2.2. METHODS OF PRODUCING NANOFLUIDS.....	25
2.3. APPLICATIONS OF NANOFLUIDS	25
2.4. SURFACTANT	27
2.6. SEDIMENTATION	29
2.7. PH ADJUSTMENT.....	29
2.8. TEMPERATURE.....	30
2.9. VOLUME FRACTION.....	32
2.10. CLUSTERING OF NANOPARTICLES	32
2.11. RHEOLOGICAL CHARACTERISTICS OF NANOFLUIDS	34
2.11.1. Viscosity	35
2.11.2. Nanofluid Viscosity Dependent on Nanoparticle Material	35
2.11.3. Nanofluid Thermal Conductivity Dependent on Nanoparticle Material	36
2.12. STABILITY OF NANOFLUIDS.....	38
2.13. OTHER EXPLORATORY INVESTIGATE ON NANOFLUID FOR ENGINE COOLING	39
 CHAPTER 3	 41
THEORETICAL ANALYSIS	41
3.1. THERMOPHYSICAL PROPERTIES OF THE NANOFLUID.....	41
3.2. VISCOSITY CALCULATION AND MEASUREMENT	41
3.3. SPECIFIC HEAT CAPACITY OF NANOFLUID.....	46
3.4. THERMAL CONDUCTIVITY OF NANOFLUID	46
3.5. CALCULATION OF HEAT TRANSFER COEFFICIENT.....	49
3.6. RELATIONSHIPS FOR NUSSELT NUMBER DETERMINATION FOR SINGLE PHASE FLUIDS	50
3.7. UNCERTAINTY ANALYSIS.....	50
3.7. FLOW METERS	51
3.8. THERMOCOUPLES	52

	<u>Page</u>
CHAPTER 4	54
PREPARATION AND CHARACTERIZATION OF NANOFLUID	54
4.1. EXPERIMENTAL WORK	54
4.2. CHARACTERISTICS OF EXPERIMENTAL TiO ₂ NANOPARTICLES	55
4.3. ARRANGEMENT OF TiO ₂ NANOFLUID	60
4.4. STABILITY OF NANOFLUID	62
4.5. EXPERIMENTAL SETUP	64
CHAPTER 5	68
RESULTS AND DISCUSSION	68
5.1. PROPERTIES OF NANOFLUID	68
5.2. VISCOSITY	71
5.3. THERMAL CONDUCTIVITY	71
5.4. HEAT TRANSFER COEFFICIENT	72
5.5. EFFECT OF REYNOLDS NUMBER ON NUSSELT NUMBER	74
5.6. EFFECT OF VOLUME FRACTION ON NUSSELT NUMBER	75
5.7. DENSITY OF NANOFLUID	76
5.8. SPECIFIC HEAT CAPACITY OF NANOFLUID	78
CHAPTER 6	82
CONCLUSION AND RECOMMENDATIONS	82
6.1. CONCLUSION	82
6.2. RECOMMENDATIONS FOR FUTURE WORK	82
REFERENCES	84
RESUME	99

LIST OF FIGURES

	<u>Page</u>
Figure 1.1. Automobile cooling system	2
Figure 1.2. Photograph of the real test set up.....	3
Figure 1.3. Essential qualities of Coolants.....	4
Figure 1.4. Nanofluid synthesis.	6
Figure 1.5. TiO ₂ -water nanofluid.....	6
Figure 1.6. Common basefluids, nanoparticles, and surfactants for synthesizing nanofluid.	8
Figure 1.7. Photograph of the Auto Lab	11
Figure 2.1. Number of distributions including TiO ₂ nanofluids within the writing concurring to distribution year.....	15
Figure 2.2. Some possible combinations of nanoparticles and base fluids.....	26
Figure 2.3. Schematic layout representing the clustering marvel	34
Figure 2.4. TEM nanograph of 15 nm TiO ₂ nanoparticles.	34
Figure 2.5. Nanoparticle repeat plot gotten from the composing think about.	36
Figure 3.1. Pycnometer used for measuring density of nanofluids.....	42
Figure 3.2. Brookfield Viscometer (DV-2 + Professional Programmable Viscometer).	45
Figure 3.3. Photographic view of Cone and plate assembly.....	45
Figure 3.4. KD2 Pro with KS-1 needle.....	47
Figure 3.5. Flow meters.	52
Figure 3.6. Pico-thermocouple (display: TC-08) and Testo-thermometer.....	53
Figure 4.1. Single step method.	54
Figure 4.2. Two-step method.	55
Figure 4.3. TiO ₂ nano powder.....	56
Figure 4.4. Weighing of TiO ₂ nano powder.	56
Figure 4.5. XRD.....	57
Figure 4.6. XRD analysis of TiO ₂ nano particles.	57
Figure 4.7. Ultrasonic stirrer.	58
Figure 4.8. Scanning Electron Microscope.....	59

	<u>Page</u>
Figure 4.9. SEM picture of TiO ₂ nanoparticles 20000X.....	59
Figure 4.10. SEM image of TiO ₂ nanoparticles 50000X.	60
Figure 4.11. SEM image of TiO ₂ nanoparticles 30000X.....	60
Figure 4.12. TiO ₂ -water nanofluid.....	63
Figure 4.13. TiO ₂ water nanofluid of sonication process.	63
Figure 4.14. Schematic representation of experimental setup.	64
Figure 4.15. Photograph of the real test set up.....	65
Figure 4.16. Schematic and dimensions of the radiator flat tube.....	65
Figure 4.17. Photograph of car radiator.	66
Figure 4.18. Pico-thermocouple (display: TC-08) and Testo-thermometer.....	66
Figure 4.19. The experiment with pure water.....	67
Figure 5.1. Real experimental setup.....	68
Figure 5.2. Nanoparticles Size distribution.....	69
Figure 5.3. SEM morphology of TiO ₂	70
Figure 5.4. TEM of the TiO ₂ nanoparticle.....	70
Figure 5.5. Viscosity of TiO ₂ -water nanofluid at different temperatures.....	71
Figure 5.6. Thermal conductivity of TiO ₂ nanofluid at different volume fraction. .	72
Figure 5.7. Average heat transfer coefficient as a function of Reynolds numbers..	73
Figure 5.8. The experimental data of MWCNT nanofluid	73
Figure 5.9. Nusselt Number verification.....	74
Figure 5.10. Nusselt number as a function of Reynolds numbers.	75
Figure 5.11. Nusselt number as a temperature of volume fractions.	76
Figure 5.12. Density of water-based TiO ₂ nanofluid as a function of temperatures.	77
Figure 5.13. Density of TiO ₂ nanofluid at different volume fraction	78
Figure 5.14. Specific heat of TiO ₂ - water nanofluid as a function of temperature..	79
Figure 5.15. Specific heat capacity of TiO ₂ nanofluid at different volume fraction.	80

LIST OF TABLES

	<u>Page</u>
Table 2.1. The articles on thermophysical properties of TiO ₂ nanofluids	14
Table 2.2. Application of nanofluids and description of the field of potential application.....	27
Table 2.3. Surfactants used for nanofluid stability	28
Table 2.4. Rundown of exploratory ponders of warm conductivity improvement... ..	37
Table 2.5. Exploratory thinks about of nanofluid for vehicle framework cooling. ..	39
Table 2.6. Outline of numerical thinks about on nanofluid for vehicle framework cooling.	40
Table 3.1. Viscosity models for TiO ₂ nanofluids.....	44
Table 3.2. Thermal conductivity models of TiO ₂ nanofluid.....	48
Table 3.3. Technical properties, precisions and total uncertainty analysis of the equipment.....	51
Table 4.1. Characteristics of TiO ₂ nanoparticles.	61
Table 4.2. Nanofluid stability for distinctive zeta potential values.	62
Table 4.3. The dimensions of the chosen car radiator.	65
Table 4.4. The dimensions of the car radiator tubes.	65
Table 5.1. The properties of pure water and TiO ₂	69

SYMBOLS AND ABBREVIATIONS INDEX

SYMBOLS

C_p : Specific heat capacity

Q : The heat transfer rate

C_p : Specific heat capacity

\dot{m} : Mass flow rate

D_h : Hydraulic diameter of the tube

N_u : Nusselt number

Re : Reynolds number

f : The friction factor

ϑ : Velocity at inlet radiator

ρ : Density

φ : Volume concentration

μ : Viscosity

h_{exp} : The heat transfer coefficient

Pr : Prandtl number

ABBREVIATIONS

nf : Nanofluid

SDS : Sodium dodecyl sulfate

MDS : Molecular Dynamic Simulations

CNTs : Carbon nanotubes

SEM : Scanning electron microscope

TEM : Transmission electron microscope

CTAB : Cetyl trimethyl ammonium bromide

XRD : X-ray Powder Diffraction

SDBS : Sodium dodecyl benzene sulfonate



CHAPTER 1

INTRODUCTION & OBJECTIVES

The main purposes of an engine's cooling system are removal of excess heat, keep it at its most efficient operating temperature, and finally, set it to its optimal temperature as soon as possible after the engine is started. Therefore, cooling of engine and its components is essential and at the same time, one of the biggest technical challenges in automotive design. Due to limited space around the engine, the size of the radiator used for cooling it is always limited, so the only option for more efficient cooling is the nature of the coolant, not its volume.

An engine coolant is a specific fluid used to remove excess heat from an internal combustion engine. Other important applications of the coolant are prevention of freezing, and most importantly, protection of engine and the radiator components from corrosion. Several researchers have carried out a number of thinks about to improve the heat transfer and corrosive properties of coolants, and their research shows that one of the best approaches is to mix in additives into normal coolants. Nano technology may be a progressive concept presented in 21st century that has the potential to progress the characteristics of materials utilized in numerous areas, including that of coolants in automotive industry. In particular, one very promising approach is that of using nano-sized particles as additives as an alternative to conventional coolants.

According to their areas of application, heat exchangers are manufactured in a assortment of configurations. They are generally classified according to the following factors:

1. Transfer processes
2. Heat transfer mechanism
3. Flow arrangement

4. Surface
5. Compactness
6. Construction
7. Number of fluids etc.

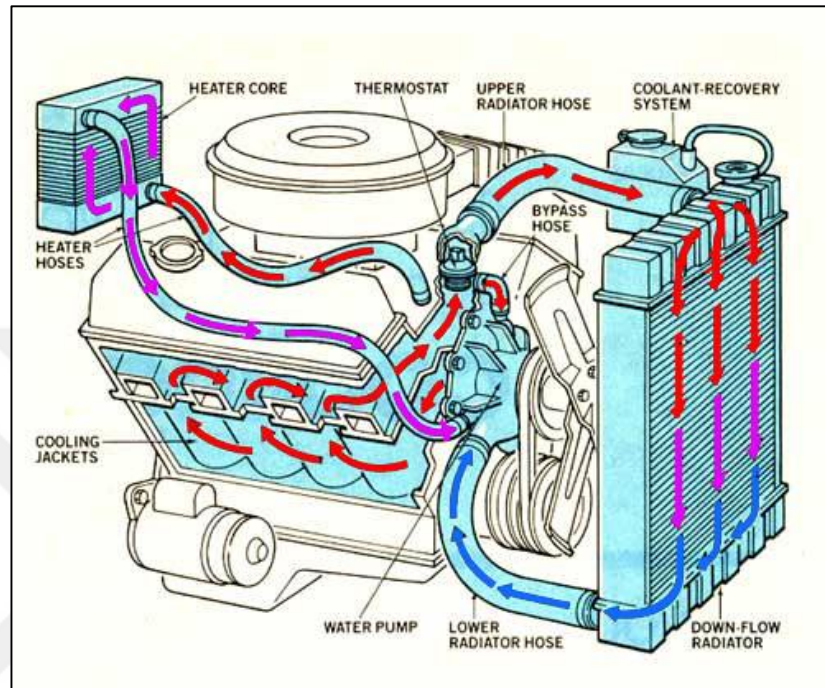


Figure 1.1. Automobile cooling system [1].

The way a typical vehicle cooling system works is heat transfer coefficient as follows: The liquid is directed to the engine block and heads via a number of passages, and on the way, it absorbs the heat produced by the engine as it is being operated. The returning hot liquid is then cooled in the radiator by the ramming air stream which enters into this compartment of the engine.

There are two ways for increasing the heat transfer coefficient, namely, heat transfer method where the size of the radiator has to be increased, or by moving forward the thermo-physical properties of the heat-transfer fabric. The first idea of progressing the thermo-physical properties of a liquid by adding solid particles such as metals, certain oxides, or particles of other compositions, belongs to Maxwell and it has been studied since the 19th century. Nanofluids are a modern course of coolants based on Maxwell's original idea but using nanometer-sized materials such as nanofibers, nanotubes, nanoparticles, or beads in the base fluid. In other words, nanofluids as a

kind of nanoscale colloidal suspensions made by mixing nanomaterials into a certain fluid. As a result they have two phases, a solid and a liquid phase.



Figure 1.2. Photograph of the real test set up.

There are a number of problems related to two-phased systems, the most important of which is the stability of the nanofluid. This is an old problem that has not been addressed yet despite the research on the area.

1.1. ESSENTIAL QUALITIES OF COOLANTS

Not any fluid would be a proper coolant in every situation, especially in the case of the combustion engine which produces tremendous amounts of heat. In addition, the nature of fluid should also be according to the environment in which the engine is used as well as the materials from which the engine is constructed. A proper coolant for a combustion engine would be required to have an elevated bubbling point as well as a low solidifying point temperature in order to function in any situation encountered during the engine's operation. In addition to freezing and boiling points, coolants perform a number of other essential functions such as engine's protection from corrosion and scale formation. The performance of engine coolants is primarily dictated by the following qualities: Oxidation Thermal Stability; since the engine coolants are hydrocarbon based, the ethylene glycol based fluid is susceptible to oxidation which involves reaction of ethylene glycol with oxygen to form glycol degradation acids. Certain additives in coolants such as nitrites which are used to protect cast iron-cylinders liners in more severe operating conditions such as high

temperature, aeration, pressure and any cooling system contaminants/corrosion metals in engines are factors that can accelerate oxidation and shorten coolant life.



Figure 1.3. Essential qualities of Coolants.

1.2. HISTORICAL OVERVIEW

Titanium oxide (TiO_2) has historically been used as a white pigment and it is obtained from rutile, an easy to obtain mineral. However, with the appearance of semiconductors and new applications of nanotechnology, TiO_2 found its usage in new fields, especially when it is in the anatase phase. A breakthrough came when Fujishima et al [2] discovered water photolysis by using TiO_2 in electrochemistry. They found that water could be split and hydrogen gas produced by using rutile electrodes. Since then, the studies on using TiO_2 based-materials as photocatalysts have increased drastically with different research groups exploring various aspects of them. Some looked at the possibility of using powder anatase TiO_2 in solution to split water but the effects were not as efficient as those involving electrodes. Further studies showed that the H_2 and O_2 produced by water splitting were recombined to produce water due to their proximity in suspended solution, something impossible when electrodes were used [3]. organic compound was added into the aqueous suspension of platinised TiO_2 [4, 5].

Other studies showed that H₂ can be generated from water by using anatase powder in metal dispersion [6]. According to them, in order to make the splitting efficient, the size of the metal dispersion should be less than 10 Å. Despite all the promising results, one of the greatest drawbacks of using TiO₂ is the fact that it can only perform these reactions under UV light, making the approach inefficient. As a result, focus shifted mostly on semiconductors such as CdS and CdSe with smaller band gap but lower efficiency as compared to TiO₂, closing here the chapter of TiO₂ usage for H₂ production in mid-80's [7].

1.3. NANOFUIDS

Nanofluids are a relatively new class of fluids that started to be used after the advent of nanotechnology, and their name comes from the nanoparticles they are mixed with. More formally they may be defined as engineered colloidal suspensions of nanoparticles such as metals, carbides, oxides or carbon nanotubes in a base fluid, which in turn could be water, oil or ethylene glycol.

1.4. SYNTHESIS OF NANOFUIDS

Production of nanofluids is carried out by two approaches: the first is called the single-step strategy in which the nanoparticles are straightforwardly dissipated into the base liquid. The other is called the two-step strategy, in which nanoparticles are to begin with arranged by an idle gas condensation or chemical vapor decomposition techniques, and then they are dispensed into the base fluid. A summarized scheme is shown on figures 1.4 and 1.5.

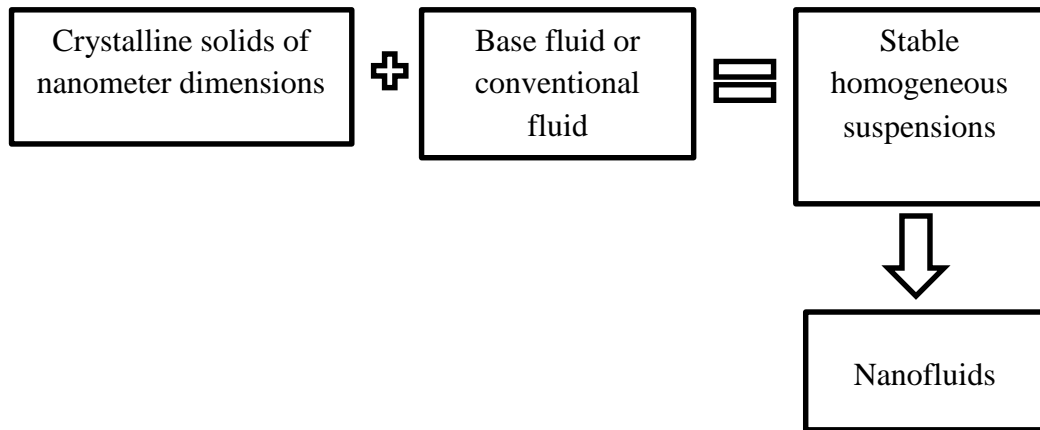


Figure 1.4. Nanofluid synthesis.

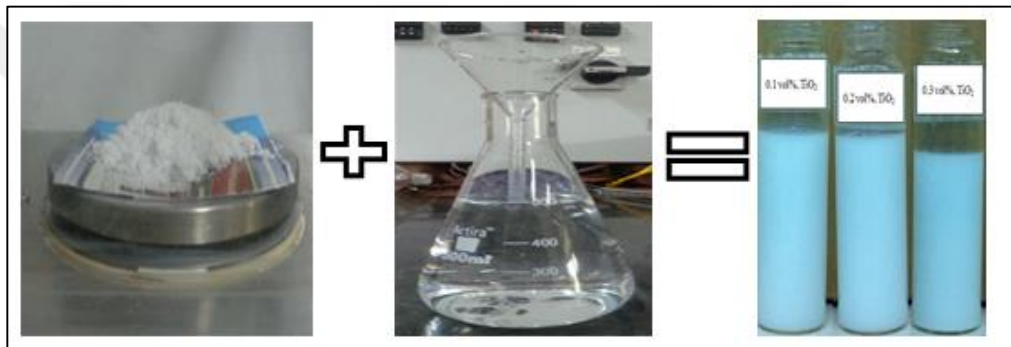


Figure 1.5. TiO₂-water nanofluid.

1.5. PARTICLE MATERIAL AND BASE FLUID

A variety of materials are utilized as a source of particles for nanofluid planning, such as Al₂O₃, CuO, Au, Cu, TiO₂, SiC, Ag, and TiC to mention just a few. In addition, carbon nanotubes are a preferred choice due to their special of having amazingly high thermal conductivity within the hub heading. On the other side, base fluids are common liquids utilized in heat-transfer applications such as water, ethylene glycol or engine oil. In addition, small amount of additives are included to the nanofluid suspension to increase the stability of nanoparticles in the base fluid.

1.6. PARTICLE SIZE

Nanoparticles to be used for preparation of nanofluids should have a diameter of less than 100 nm, and there are cases where particles as little as 10 nm have been effectively utilized in the area [7]. However, when the shape of particles is not spherical but tube or rod, the distance across still kept underneath 100 nm but the

length varies substantially, even reaching the range of micrometers. It ought to be famous though those particles of micrometer size may cluster together due to clustering phenomena, so caution is advised in such situations.

1.7. PARTICLE SHAPE

The most commonly used particles in nanofluids research are spherical in shape, however, as mentioned above, tube and rod-shaped ones are also common. Clusters shaped by nanoparticles may have fractal like shapes.

1.8. PREPARATION OF NANOFLUID

As mentioned in a previous section, nanofluids can be prepared by suspending solid particles with sizes of less than 100 nanometers inside a base fluid. The terms “synthesis and Characterization” are widely used in literature, describing the preparation phase of nanofluids. In general terms, it could be stated that nanofluids include nanometer measured strong particles, filaments, bars or tubes suspended in numerous base fluids [8]. Together with basefluids and nanoparticles, additives are also utilized to increase the solidness of nanofluids and to improve their dispersion behavior. The more common nanoparticles and basefluids exploited in nanofluid synthesis would be tabulated as in figure 1.6 [9]:

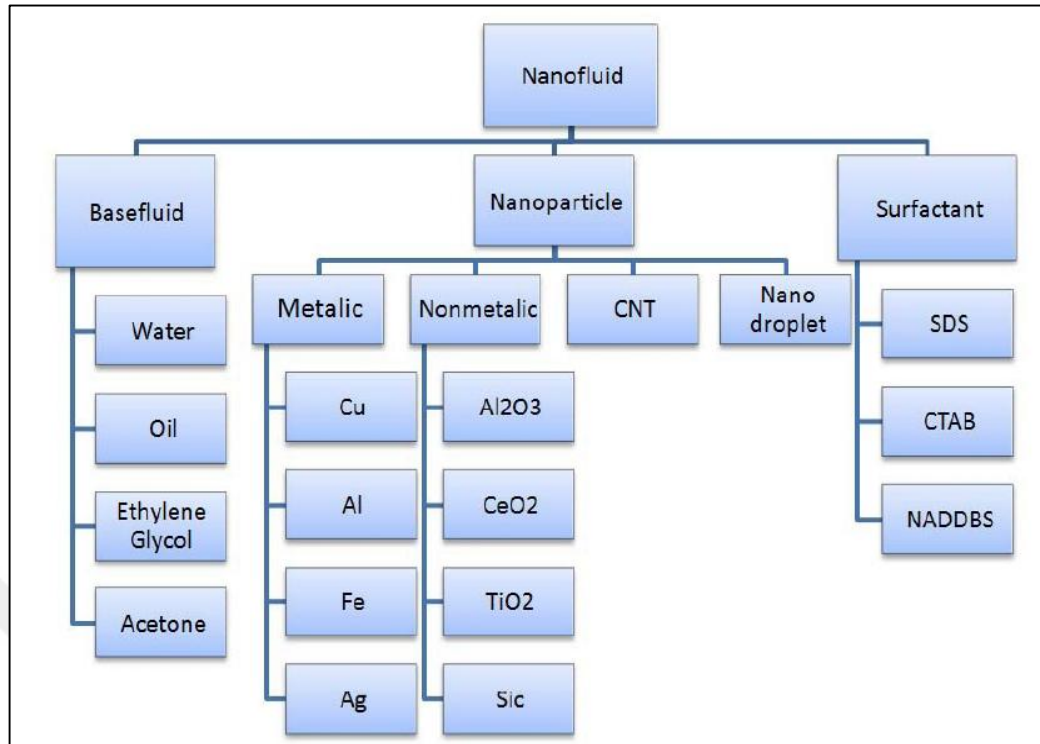


Figure 1.6. Common basefluids, nanoparticles, and surfactants for synthesizing nanofluid.

In general, two production methods for preparation and dispersion of nanoparticles, namely one and two-step methods are used. The key to critical increment in warm conductivity of nanofluids is synthesis, within which non-agglomerated nanoparticle are suspended in basefluid [10]. In the single-step method, preparing nanoparticles and dispersing inside basefluid occurs simultaneously. In two-step method, nanoparticles are first processed by some other techniques first, and then dispersed into basefluid. Most nanofluids, including oxide nanoparticles are produced by means of the two step method, but for metallic nanoparticles or particles with high thermal conductivity, one-step method is preferred [10]. For instance, Hong prepared Fe/ethylene glycol nanofluid by taking advantage of the two step method [11, 12]. In this case, synthesis of Fe nanoparticles was performed by the process of chemical vapor condensation and then they were dispersed in basefluid.

Using additives is another effective technical application to enhance heat transfer performance of liquids. Suspension of metallic or nonmetallic particles changes both, heat transfer characteristics and the transport properties of base fluids [13]. An

effective approach for improving base fluids' thermophysical properties is to suspend small solid particles in them. Recent reports on nanofluid research are pointing at particles clustering as a possible instrument for the abnormal augmentation of thermal conductivity when nanoparticles are suspended in liquids [14]. Samples of nanofluids are arranged by scattering pre-weighed amounts of dry particles in a base fluid. Extraordinary consideration must be paid to the pH of each aqueous mixture to ensure that no changes occur in the nanofluid volume fraction. In order to break up any particle aggregates, the mixtures are subjected to ultrasonic mixing for a short time [15].

1.9. VISCOSITY OF NANOFLUID

The efficiency of nanofluid convective heat transfer depends on the relationship between the increase of both thermal conductivity and viscosity. As such, it is critical to study nanofluid viscosity when a system has adopted fluid flow. The increase of fluid viscosity requires the addition of more particles, regardless of whether the particles are rotating or non-rotating in the flow field.

1.10. THERMAL CONDUCTIVITY OF NANOFLUID

Due to the rapid developments in industrial and nanotechnology approaches, the production of nanoparticles has become easier and more efficient [16]. The effectiveness of nanofluid has been observed to be greater than expected of thermal conductivity with small nanoparticle volume fraction [17]. Since then, investigators have shown interest in using nanoparticles for heat transfer enhancement and thermal performance [18].

1.11. FRICTION FACTOR AND HEAT TRANSFER

In the last ten years, there has been more attention on enhancing the efficiency of convective heat exchange of nanofluids due to their increasing acceptance for practical applications. However, the coefficient (h) of nanofluid convective heat transfer, also known as Nusselt number (Nu) is incompatible throughout the literature. Test ponders of the friction factor and nanofluid heat exchange upgrade with the flow velocity and nanofluid volume division interior warmed tube beneath

laminar stream condition have been introduced by Ali, H.M et al, and Kundan, L. et al [18, 19].

1.12. ADVANTAGES OF NANOFLUIDS

Nanofluids which are prepared according to sound engineering principles include the following advantages:

1. They have a bigger specific surface area, which means better heat exchange between the fluids and particles suspended in it.
2. High stability of dispersion, which relies primarily on Brownian motion.
3. Require less pumping energy to achieve the same efficiency as compared to pure liquid.
4. They have less particle clogging in comparison to other liquid-particle mixtures, making system miniaturization possible.
5. By changing particle concentration, their thermal conductivity and wet surface ability can be controlled according to the application's needs.

1.13. PROBLEM STATEMENT

Conventional fluids such as water and ethylene glycol (EG) have been utilized as coolants in automotive cooling systems since the beginning of the industry. However, the limited thermophysical properties of these fluids hamper heat transfer across the car radiator. The increasing demand for energy efficiency and better performance has led to increased interest on other alternative methods. Space constraints is another key issue in the automotive cooling system. Sometimes overheating occurs in the engine because the radiator is not functioning up to the standard expectations. The reasons for using nanofluids as a coolant within the car cooling framework are as takes after:

1. They reduce the amount of circulating water of an automobile radiator.
2. Help engineers optimize the design of a car radiator.
3. Decreases the operation time of the radiator's fan.

1.14. AIM OR GOAL OF THIS WORK

The point of this consider is to improve the heat transferring capacity of car radiators by means of nanofluids utilizing the following approach:

1. Analyze and compare heat transfer rates from car radiator using nanofluids with different base fluid, nanoparticles sizes and concentration.
2. Experimental work to assess the physical properties of different nanofluids.
3. Experimental setup on real car engine using nanofluid coolants to compare heat exchange of car radiator with and without nanofluids.
4. Study the effects of average particle size on the execution of heat exchanger by using nanoparticles of different sizes.
5. Study the effect environment surrounding to car radiator.



Figure 1.7. Photograph of the Auto Lab.

1.15. ORGANIZATION OF THE THESIS

This thesis is organized under six chapters, each covering different aspects as shown in the summary below.

Chapter 1: Introduction

Background of the research, importance of the research, problem statement of the dissertation, aim and objectives of the Doctor of Philosophy (PhD)'s dissertation.

Chapter 2: Literature study

Background of basic fluid mechanics, theory behind natural convection, detailed discussion of nanofluids and the models available to determine their properties, as well as discussion of past experimental works.

Chapter 3: Theoretical Analysis

The theoretical background gives a detailed account on suspension viscosity models, namely, classical, new theoretical and empirical models. The review of the experimental studies that have identified key factors that affect nanofluid viscosity and Thermal conductivity.

Chapter 4: Methodology (Experimental setup)

An experimental investigation into a TiO₂ deionised water nanofluid. Selecting the models and methods used to determine the nanofluid's thermophysical properties.

Chapter 5: Results and Discussion

Discussion and results that show the thermal conductivities and viscosities of nanofluids, Thermal conductivity of TiO₂ nanofluid at various volume fraction and viscosity of TiO₂-water nanofluid at various temperatures, and normal heat exchange coefficient as a work of Reynolds number.

Chapter 6: Conclusion and recommendation

Concluding the investigation by summarizing the various sections of the study and their respective results, as well as providing recommendations for further studies.

CHAPTER 2

LITERATURE REVIEW

The purpose of this literature survey is to provide information on different areas of nanofluid research such as the various factors that influence the thermal conductivity and viscosity of nanofluids, the behaviour of TiO₂-water nanofluids in car radiator field configurations, and the preparation of a stable nanofluid.

Extraordinary endeavors have been went through to progress the warm proficiency of a number of forms with blended victory until the later rise of a promising modern course of nano-coolants with a fluid component such as water blended with nanoparticles begun to form their way into a heap of designing applications. Although they are anticipated to supply substitutes of ordinary coolants within the close future, a number of advancements are still to be made. Endeavors are still being made, on one hand to diminish the equipment's measure and increase the warm trade surface by utilizing blades, and on the other to extend the warm conductivity of liquid exchangers. Enhancements in nanotechnology have upgraded our capacities to synthesize nano-scale materials, such as distinctive sorts of nanoparticles counting non-metallic, carbon-based and metallic ones, which have begun to be utilized in ordinary liquids such as water, ethylene glycol and oil, making a modern lesson of liquids called nanofluids [20]. Awesome endeavors have been went through to progress the warm effectiveness of a number of forms with blended victory until These nanofluids have been appeared to have improved warm properties and potential applications in different areas such as pharmaceutical, hardware and transportation [21].

TiO₂ nanofluids were first proposed by Oliveira et al.[22], and since then, studies on their thermal properties for various concentrations and particle sizes have been on the raise. Table 2.1 provides a summary of the most recent papers studying various ways to enhance thermal conductivity of TiO₂ nanoparticles and figure 2.1 provides a

glimpse on the surging number of research articles on this particular area on 2004-2017 period based on the data from the web of science.

Table 2.1. The articles on thermophysical properties of TiO₂ nanofluids.

Base fluid	Size (nm)	Temperature (°C)	Enhancement of thermal conductivity (%)	Concentration	Reference
Water	22	16, 26, 36	Not informed	0.3–3 vol%	[23]
Oil	5.8	26–61	43.7% at 0.06 vol% (26 °C)	0.02–0.06 vol%	[24]
Diathermic oil	11	21–51	8% at 2 vol% (51 °C)	0.2–2 vol%	[25]
Water	<99	31–51	8.4% at 41 ppm (32 °C)	0–101 ppm	[26]
Water and water/EG	22	31–71	Water: 6.02% at 2.1 vol% (31 °C)	0.3–2.0 vol%	[27]
Deionized water (DI)	11	6–46	13% at 5 vol%	0.2–6 vol%	[28]
Water/EG	51	30–70	Maximum at 2.7 vol%	0.6–2.6 vol%	[28]
Water	14	16–31	52.2% at 1.6 vol% (31 °C)	0.2–1.6 vol%	[29]
Water	41	26	12.5% at 4.6 vol%	0.6, 3.6 and 5.6 vol%	[30]
Water	31–51	11–41	17%	1.9–7 vol%	[31]
Water	50	30–60	27%	0.6–4.0 vol%	[32]

Titanium dioxide (TiO₂), a steady and non-toxic fabric has been broadly utilized in nanofluids inquire about. It has three crystalline stages, to be specific brookite, rutile and anatase, the final one being the foremost vital and utilized for distinctive purposes such as gas sensors, colors, nanofluids and catalysis. Liu Yang, and Yuhan Hu et al [33, 34] have summarized later investigate on TiO₂ nanofluids in two audits. The first part of their reviews summarizes recent progresses on preparation, stability, what's more, physical properties of TiO₂ nanofluids, with the area of TiO₂ nanofluids physical properties concentrated on the consistency and surface pressure. The utilization of TiO₂ nanofluids and their warm conductivity were presented in the

second piece of the reviews. According to them, TiO₂ nanofluids have shown good results in various applications in many energy-related filed.

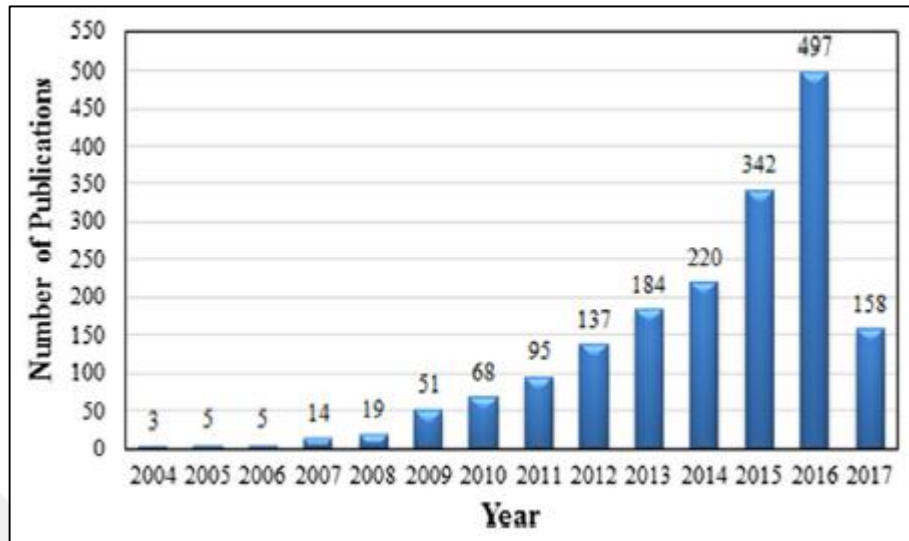


Figure 2.1. Number of distributions including TiO₂ nanofluids within the writing concurring to distribution year.

In a ponder by Minsta et al. (2009), information were collected which built up the reliance of warm conductivity on temperature for alumina and copper oxide based nanofluids [12]. The comes about appeared an generally anticipated impact of a raise in warm conductivity by expanding the division of molecule volume and diminishing molecule measure. In expansion, they too found that the relative increment in warm conductivity was of more prominent importance at higher temperatures [12]. Another study by Liu Yang et al. [35] was done to move forward the suspending capacity of smelling salts water based TiO₂ nanofluids employing a energetic circulating gadget, and the energetic characteristics of smelling salts water based TiO₂ nanofluids counting suspending capacity, thickness and surface pressure were explored. The ponder found that the energetic circulating handle has small impact on the thickness of TiO₂ nanofluids, and the surface pressure is basically decided by the expansion of sodium dodecyl benzene sulfonate (SDBS).

Numerous viewpoints of nanoparticles such as volume division, measurement, shape and other physical properties influence nanofluid's warm conductivity, which is expectedly measured by the hot-wire strategy. Estimations have appeared the increment in nanofluids' warm conductivity to be connected with the volume

division of ultra-fine particles [36]. A unused relationship to appraise the warm conductivity of Al_2O_3 and CuO nanofluids based on test information was created and it was appeared that the increment in warm conductivity for both cases was emphatically connected with temperature [37].

However, one of the foremost vital instruments in deciding the thermo-physical properties of half breed nanofluids are numerical models. They are, in expansion, utilized to approve and diminish the blunder between anticipated and exploratory information [38]. Factors included in such numerical relationships incorporate thickness, warm conductivity, grinding components, Nusselt number etc. Such models appear that crossover nanofluids' exhibitions are decided by volume concentration, scattering soundness and blending proportion.

Utilization of nanofluids in cooling frameworks of electronic gadgets offers a number of focal points and the advancement of this innovation may well be an vital figure in encourage miniaturization as well as the increment in vitality proficiency of such contraptions [39]. One of the well-studied frameworks by implies of Atomic Energetic Reenactments (MDS) is the layering marvel in which shell-like arrangements of water particles cover nanoparticles' surfaces. In these frameworks, metal nanoparticles (Cu) and their oxide shapes (CuO) are invigorated concurring to the parameters of a water environment [40]. Comes about appear requested water particles shaping layers around nanoparticles to play an basic part in clarifying test comes about of warm conductivity for such nanofluids.

In another consider, the impact of water- Al_2O_3 nanofluid on the execution of sun based collectors was decided beneath genuine climate conditions. The advancement within the productivity of the sun oriented collector was appeared to be subordinate on the concentration of nanoparticles; tall nanoparticle concentration essentially decreased the device's temperature, which was at the same time related with expanded warm proficiency [41].

Consistency and warm conductivity of a number of metallic oxides such as CuO , ZnO , SiO_2 and Al_2O_3 at diverse temperatures, nanoparticle concentration and shapes (circular, platelets, edges, bricks and round and hollow) have as of now been

modeled and decided [42]. Such things about have appeared that shape features a extraordinary impact on nanofluids thermophysical properties. More imperatively, warm conductivity was improved by expanded temperature and thickness was emphatically related with expanding the molecule volume divisions, two properties with promising applications in present day innovation.

Nanofluid solidness and the impact of surfactant concentration amid test planning and sedimentation was considered to assist move forward the suspension steadiness as e implies of applying it to sun based plants. The long-term steadiness of nanofluids is amplified by certain surfactants which make chemical bonds with nanoparticles within the liquid, but their warm conductivity isn't influenced. Ponders have appeared that nanofluids in both nearness and nonappearance of surfactants appear non-Newtonian behavior and they gotten to be more gooey with expanding the cluster measure [43].

In another ponder by Gu et al. (2013) on three water based nanofluids (NFs) comprising of expansive viewpoint proportion fillers - carbon nanotubes (CNTs), silver nanowires and copper nanowires, it was found that the shape of nanoparticle had a critical impact on the suspension's warm compelling conductivity [44]. They concluded that molecule shape is a basic figure causing huge changes among exploratory values of warm conductivity. Their comes about show that materials with higher warm conductivity are not the as it were definitive variables in moving forward warm transport profiles of nanofluids.

In 2017, Liu Yang et al. [45] carried out an vital and comprehensive audit of both the test and hypothetical inquire about on the thickness, warm conductivity and surface pressure of nanofluids. They concluded that fabric sort includes an awesome impact in warm conductivity of nanofluids since warm conductivity of Graphene, CNTs, Au; Ag etc. nanofluids is significantly higher than that of other sort, such as TiO₂, SiC, SiO₂ nanofluids. In expansion, the fabric sort has small impact in consistency of nanofluids since no relationship can be concluded between diverse molecule materials. Most comes about appear that thickness and warm conductivity increment as an increment in molecule stacking.

A new application of nanofluids is utilizing them as a substitute for schedule coolants in car radiators, a crucial component of the car motor. Radiators serve as heat-exchangers for cooling the car motor expectedly utilizing water as trade medium. Vehicle engine's warm execution beneath the impact of nanofluids has been considered by numerous analysts, and The most important applications of nanofluids have been as coolers and oils in car radiators in an endeavor to extend the warm expulsion proficiency. Comes about have appeared that warm exchange coefficient can be made strides by more than 50% as compared to the routine coolants but it is constrained by the drop on liquid's weight. In any case, may specialists concur that an ideal execution can be accomplished at moo nanoparticle volume division of less than 1% ($\phi < 1\%$) [46]. After the nanofluid TiO_2 in a water base was selected, a detailed study was done into previous worked in this field with a focus on characteristic convection warm exchange in a walled in area.

Moradi, et al. [47] explored the impact of the geometric shape of the cylindrical enclosure on the heat transfer of Ti and Al_2O_3 nanofluids. They found that the lower surface of the enclosure had a constant heat flux. It was additionally found that the heat transfer coefficient of TiO_2 nanofluid was smaller than that of the base fluid under the same conditions. In addition, Hu et al. [48] performed a number of experiments and numerical analysis on the heat transfer of a TiO_2 -water nanofluid with mass fractions of 3.85%, 7.41% and 10.71% in a square enclosure. The numerical analysis was based on a Lattice- Boltzmann model coupling transfer. Results showed a good fit between experimental and theoretical results, but no improvement of heat transfer was found between nanofluid and its base control.

A study done by Ganji et al. [49] Added the aspect of a uniform magnetic field. The theoretical study investigated water-based Ti and Al nanofluids in a vertical enclosure. In this study, it was observed that the particles within the fluid tend to migrate from the heated walls towards the cold walls, creating a non-uniform distribution of within the fluid. Another numerical study based on the Lattice-Boltzmann model was done by Sheikholeslami et al.[50]. They simulated heat transfer and nanofluid flow of alumina, Cu, TiO_2 and Ag-water-based nanofluids inside a square enclosure with a rectangular heated body. In order to calculate effective viscosity, Brinkmann model was utilized, while the thermal conductivity

was determined using the Maxwell-Garnett model. The study showed that the effect of the nanoparticle volume fraction is more noticeable for low Rayleigh numbers.

Ouyahia et al. [51] carried out a numerical examination on warm and hydrodynamic characteristics of a TiO₂-water nanofluid in a cavity with a triangular cross-section. The base wall was kept at a high temperature, while the other sides were at constant cold temperature throughout. Then they used the SIMPLER algorithm to do the calculations for heat transfer and fluid flow rate and found the heat transfer to be enhanced, especially on the case of higher Rayleigh number.

In another case, Nieh et al. [52] utilized the nanofluids of Al₂O₃ and TiO₂ with pure water radiators cooled by air to enhance their performance. Their approach consisted of assessing the nanofluids' thermo-physical properties for different nanoparticle concentrations, and then measuring the drop of pressure and Reynolds numbers. Results showed a significant improvement in efficiency and heat dissipation rate as compared to the controls which consisted of ethylene glycol or pure water. Furthermore, they confirmed a greater efficiency of TiO₂-water as compared to the Al₂O₃ counterpart. Briefly, there was an increase by 25.6% in heat dissipation rate and 6.1% in pressure drop, 2.5% increase in pumping power and 27.2% enhanced efficiency as compared to the conventional ethylene glycol and water mixture.

Mohammed et al. [53] reviewed the effect of nanofluids on the heat transfer in micro channel heat exchanger. They concluded that the rate of heat transfer can be significantly enhanced at the cost of increased friction factor. Further, they recommended further studies for a way better understanding of the heat transfer phenomenon of nanofluids as well as their preparation techniques.

In a study carried out by Leong et al. [54], the effect of another nanofluid, Cu- EG on the execution of car radiators was examined.. To compare the comes about, Reynolds number =s for air and coolant were taken as 6000 and 5000, separately. Results appeared an increment in warm exchange rate of 3.8% when 2% Cu nanoparticles were added and a dependency of the heat exchanger's thermal performance on Reynold's number such that, an increase of this number from 4000 to 6000 caused an increase by 42.7 % and 45.2 % in radiator's thermal performance

for ethylene glycol and Cu-EG, respectively. On the other hand, when the Reynold's number for coolant was increased from 5000 to 7000, thermal performance was only enhanced by 0.9 % and 0.4 %, respectively. In addition, the heat exchanger's frontal area was decreased by 18.7 % by when 2% of Cu-EG particles were added. Furthermore, fluids pumping power was enhanced by 12.13 % as compared to ethylene glycol while the nanofluid's volumetric flow rate was kept constant at m^3/s .

Ebrahimi et al. [55] investigated the characteristics of heat transfer by forced convection in car radiator using SiO_2 -water nanofluids as coolant. The heat exchanger employed in the cooling system was compact heat exchanger. In their study, they concentrated on a number of important parameters such as nanofluids' flow rate, inlet temperature of nanofluids and particle volume concentration was studied by experiments. They found a direct positive correlation between the Nusselt number and inlet temperature, Reynolds number and nanofluid's particle volume concentration. Inlet temperature was varied by 43°C , 52°C and 60°C . They concluded that in the nanofluid, increasing the volume concentration of the particle by 0.04 %, led to an enhancement by 3.8% in heat transfer rate compared to base fluid.

In an important study, TiO_2 -water nanofluid's properties, such as pressure drop and convective heat transfer were investigated by Amani et al. [56]. Nanofluids were prepared using TiO_2 nanoparticle of 30 nm particle size by dispersing them in de-ionised water. The value of Reynolds number was varied from 8000 to 51000. Nusselt number was expanded by expanding the Reynolds number. Unfortunately higher values of Reynolds number tends to increase the pumping power. Experimental results showed that for a given Reynolds number, the value of Nusselt number increased with particle volume concentration.

In another study by Sheikhzadeh et al. [57] copper/ethylene glycol was used as coolant in assessing the thermal performance of a car radiator and they found that increasing nanofluid's particle volume fraction and the Reynold number driven to a significant increment within the overall heat coefficient of air side. More specifically, increasing particle volume concentration from 0-5% caused a raise in heat transfer rate of 26.9 % and overall heat transfer coefficient of 64.3 %. In addition, it was

observed that increasing the Reynold's number from 4000 to 6000 caused an increase of 12.4 and 4.5% in nanofluid and air heat transfer coefficient, respectively. The overall comes about of the study proved that the performance of the radiator's heat transfer was more efficient at 50°C as compared to that of 20°C weather conditions.

There have been also a number of theoretical as well as experimental studies assess fluid flow rate and heat transfer properties in horizontal tubes. The nanofluid of interest was the suspension of TiO₂ nanoparticles into distilled water prepared at various concentrations between 0.002 to 0.02 % by volume. The experiments were carried out in turbulent flow region for various Reynolds number of range 8000-51000. Results from numerical analysis were also validated by experimental data and good fit was observed between them. These studies showed that Nusselt number, which represents a dimensionless heat transfer coefficient, was positively correlated with particle volume concentration and Reynolds number, but pressure drop also increased with increasing volume concentrations. At the end, the authors concluded that the efficiency in heat transfer can be made strides drastically, but at the expense of pumping power [58].

Hussein et al. [59] did a set of experiments further understand the effect of tube's cross section on heat transfer execution of a car radiator in order to advance its heat transfer capacity. Fluent software was used on developed CFD by using the finite volume technique. For experimentation, TiO₂-water nanofluids were prepared at 1 %, 1.5 %, 2 % and 2.5% nanoparticle volume concentration. Circular, elliptical and flat tube geometries were considered having length 500 mm and hydraulic diameter of 3mm. Results revealed that circular cross section had higher values of friction factor as compared to elliptical and flat counterparts, but if the value of Reynolds number was increased, friction factor decreased. Heat transfer coefficient was found to be the highest in flat tube cross configuration due to higher area involved in heat transfer.

Another study by Mohammed, et al. [60] was concentrated on the effect of Reynold's number and volume fraction on heat transfer and weight drop in laminar flow conditions. They used a set of nanofluids of Al₂O₃, SiO₂, Ag and TiO₂ and pure water as a control. The values of Reynold's number varied from 100 to 800 and volume

fraction from 2% to 10%. On micro channel heat exchanger consisted of 25 channels for hot and cold fluid, respectively. Their results showed silver to have the lowest pressure drop, while alumina was shown to have the most noteworthy heat transfer coefficient.

The prepared nanofluid by scattering TiO_2 nanoparticles with an average particle size of 21 nm supplied by Sigma-Aldrich Chemicals Ltd. To guarantee uniform scattering of nanoparticles in the base fluid 0.5 ml of oleic acid and cetyl trimethyl ammonium bromide (C-TAB) equal to 1/10th weight of TiO_2 nanoparticles were added [61].

Thermal performance of TiO_2 nanoparticles was studied by using a heat exchanger having multiple twisted tapes. In addition, different particle concentrations of 21 nm average size were used. Results showed that the tube carrying 0.21% nanoparticle concentration by volume had the best performance factor of 1.59, and the rate of heat transfer and friction factor were expanded by 3.52 and 11.7 times, respectively, as compared to the tube with pure water as fluid [62].

The car radiator heat exchange improved by utilizing SiO_2 and TiO_2 nanoparticles scattered in plain water. The convective heat transfer of both SiO_2 and TiO_2 base fluid was increased. There was a reduction of friction factor with volume centralization of SiO_2 -water and TiO_2 -water with expand in coolants melting temperatures for the car radiator. Significant expanded in heat transfer were noticed for the case of increased nanoparticle by volume fraction. A maximum Nusselt number up to 17.6 for TiO_2 - water and 18.27 for SiO_2 - water were measured, respectively. The results proved that TiO_2 and SiO_2 nanofluid have the greatest ability to enhance heat transfer. Hydrodynamic flows are exceedingly appropriate to industrial and practical applications. The range of volume fraction and Reynolds number are 1.0-2.5% and 250-1750, respectively. The vitality rate and adequacy of nanoparticles scattered in water were also assessed. Results showed 20% and 32% increase in the flow rate as well as 24% and 29.5% viability improvement for each TiO_2 and SiO_2 nanofluids, respectively. This amount of heat transfer exchanged out by cooling will help the engine increase its productivity and efficiency [63].

The effect of expanding particle concentration and agglomerate size on fluid stability were studied using sodium dodecyl sulfate (SDS) which directly increases the viscosity of carbon nanotubes (CNT) [64]. They started with the assumption that the zeta potential for the SDS - CNTs nanofluids was higher than that of the uncovered CNTs, and therefore proposed that the electrostatic shock between the oppositely charged surfaces had an important role in CNT adjustment [64]. It was observed that SDS drastically affected the outright estimation of zeta potential in titanium and alumina nanofluids by the mass part of 0.01% and 0.05% correspondingly [65]. On the thermal conductivity and consistency of a car motor coolants based silicon carbide (SiC) nanofluids, the homogeneous and stable nanofluids with volume part up to 0.5 % (vol/vol) were set up by the two-stage strategy with the expansion of surfactant made of oleic corrosive. Data showed that temperature and volume fraction had drastic effects on nanofluids thermal conductivity improvement by up to 53.81% for 0.5 % (vol/vol) nanofluid at the temperature 50°C [66].

Finally, in another study they used an Al_2O_3 and TiO_2 particles to upgrade the heat dispersal execution of an air cooled radiator. Results showed that the nanocoolant's heat dissemination limit was the highest for TiO_2 followed by the Al_2O_3 , while mixture of water with ethylene glycol showed the lowest heat dissipation capacity. The best results for heat transfer capacity, pumping power and pressure drop were around 6.1%, 27.2% and 25.6%, respectively, as compared to the control. By large, the nanocoolant enhances the heat dissemination limit of the cooling system [52].

2.1. BASE FLUID

Concurring to the established theory on conductivity models, particularly that of Maxwell, there is an inverse correlation between a fluid's thermal conductivity and thermal conductivity ratio, which is characterized as the thermal conductivity of the nanofluid which contains nanoparticles, divided by that of the base fluid, in most of the cases pure water [67]. However, for the case of nanofluids, the situation is even more complicated because given the particles nanometer size, their movement (Brownian motion) is heavily affected, and as a result, their thermal conductivity may change drastically [68].

In a study carried out by Lee et al.[69], the effect of the electric double-layer which envelopes nanoparticles on their thermal conductivity was studied. They found out that the thickness of this layer around the particle and their thermal conductivity depends on the base fluid and it is very difficult to exactly assess their quantitative effects. The best approach is to carry out a series of experiments studying the problem from various angles in order to build an overall picture. Therefore, some of the most important experimental studies on this field are summarized below.

In a landmark study by Wang et al. [70], Al_2O_3 and CuO nanoparticles were mixed with a variety of base fluids such as ethylene glycol, water, engine oil and vacuum pump liquid to prepare nanofluids for further studies. Al_2O_3 nanoparticle fluid showed the best thermal conductivity when mixed with ethylene glycol, followed by engine oil, and finally water and pump oil. CuO nanoparticles was mixed only with water and ethylene glycol, and both cases showed the same thermal conductivity values when their volumes were the same.

Another important set of experiments on the effects exerted on nanofluid's thermal conductivity by base fluids was performed by Xie et al. [71]. They used a set of base fluids such as deionized water, pump oil, ethylene glycol glycerol, water-ethylene glycol and water-glycerol mixtures and mixed them with Al_2O_3 nanoparticles. Comes about appeared a diminish in thermal conductivity ratio as the base fluids thermal conductivity increased. Furthermore, exploratory comes about were compared with theoretical calculations from another study [72] and they were found to be incompatible with each other. However, it should be kept in mind that the information gotten from the experiments are in great understanding with the Maxwell model. In addition, experimental results showed that water-based nanofluids had a higher thermal conductivity ratio as compared to other base fluids. [72, 73].

The impact of base liquids on warm conductivity was examined in a think about utilizing MWCNT nanofluids where ethylene glycol and engineered motor oil were utilized as base fluids. In these experiments, thermal conductivity was measured by a method called transient hot-wire approach. Results showed that 1vol.% MWCNT in ethylene glycol base fluid led to 12.5% increase in thermal conductivity whereas

2 vol.% MWCNT in synthetic engine oil led to 30% increase, making the later a better choice [74].

2.2. METHODS OF PRODUCING NANOFUIDS

There are two widely-accepted methods for nanofluid preparation, and either of them can be adopted, depending on the aim of the study:

1. The to begin with one could be a single-step strategy involving evaporation in which nanoparticles are formed inside the base fluid directly [75].
2. The second method is a two-step approach, with the first step involving nanoparticle formation, and the second their dispersion into the base fluid. To ensure homogenous dispersion, the fluid must be carefully treated with a number of treatment devices such as stirrers, high-pressure homogeniser, ultrasonic disruptor or ultrasonic bath. All these methods are critical in preventing nanoparticle cluster formation inside the fluid [75].

2.3. APPLICATIONS OF NANOFUIDS

In this section, a diagram of some of the later thinks about on thermophysical properties of nanofluids and their enhancement of heat exchange will be presented. In addition, we will mention the relationship between Nusselt Number, thermal conductivity and viscosity of the nanofluids. Nanofluids are applied on a number of different heat exchangers involving different designs, such as plate, sell-and-tube, compact and double-pipe warm exchangers [76]. studied the applications including peristaltic micro pumps and novel drug delivery systems in pharmacological engineering [77]. A creative combination of nanoparticles and base fluids are shown in Figure 2.2.

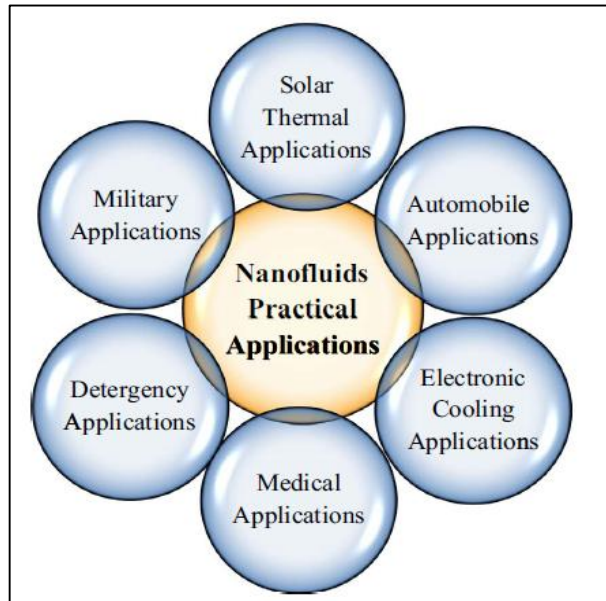


Figure 2.2. Some possible combinations of nanoparticles and base fluids [77].

In one study involving $\text{TiO}_2\text{-Ag}$ and $\text{Al}_2\text{O}_3\text{-Ag}$ composite nanoparticles dispersed in an epoxy matrix, preliminary tests showed promising results on their antimicrobial activity, findings that are of increasing relevance given the current need for more effective methods to control microbial infection [78]. In another case, CuO and Fe_2O nanoparticles mixed with water as a base fluid were studied in a car radiator and their overall heat transfer coefficient was measured, in this way avoiding the need of measuring the radiators wall temperature. In order to have a more complete picture, different variables were changed such as the types of base liquid, flow rates through the tubes, and particle concentrations and inlet temperatures were used for testing [79].

Table 2.2. Application of nanofluids and description of the field of potential application.

Field of potential application	Description
Heat transfer applications	<p>Cooling in Industrial applications: Replacing the water used in cooling and heating processes by nanofluids has the potential to conserve significant amounts of energy [80].</p> <p>Smart fluids: Can be used in controlling heat flow [81].</p> <p>Nuclear reactors: Water-cooled nuclear systems show improvements in both performance and productivity by using nanofluids. However, more research is necessary in this field [82].</p>
Automotive applications	<p>Nanofluid coolant: A smaller size and better positioning of the radiator can be achieved by using nanofluids as coolants. It gives higher efficiency of heat transfer [82].</p> <p>Brake and other vehicular nanofluids: Brakes generate a considerable amount of heat due to friction, which has a big impact on break oil. Therefore, nanofluids can be used to maximize performance in heat transfer [83].</p>
Biomedical applications	<p>Nano-drug delivery: Whole integrated micro- or nano-drug delivery systems can be used to control and monitor in real time the response of target cells and tissues to certain drugs. In this way we can understand better drug activity and improve their effectivity [84].</p> <p>Cancer therapeutics: Nanofluids are used both in cancer imaging technology and drug delivery systems, taking advantage of their advantageous properties. A magnetic nanofluid is useful when guiding the particles up the blood stream with magnets to a tumour [84].</p>

2.4. SURFACTANT

For chemical stability, a surfactant (also known as dispersant) such as ammonium hydroxide, sodium hydroxide, hydrazine hydrate or sodium borohydrate, is added to the nanofluid [85]. Hwang et al., [86] found that the stability of the nanofluid depends on the suspended nanoparticles and the base fluid where particles are dissolved. To estimate a certain nanofluid's stability, the UV-vis spectrum is used. The addition of sodium dodecyl sulphate (SDS) improves the stability of the nanofluid because the SDS increases the zeta

potential (surface charge) of nanoparticles and creates the repulsion force between them. Wang et al., [87] added the sodium dodecylbenzene sulfonate (SDBS) to TiO₂, Al₂O₃ and CuO-water nanofluid to enhance the stability of the nanofluid. They found that the SDBS made a helped difference the scattering of nanoparticles in the base fluid as well as helping to increase its thermal conductivity. Yang et al., [88] found the optimum stability of Al₂O₃-water nanofluid by adding a 0.3% mass fraction of polyacrylic acid (PAA) and cetyl-trimethyl ammonium bromide (CTAB). Anandan et al., [89] mixed CTAB with CuO- nanofluid by using ultrasonication and found that CTAB enhances the stability of the nanofluid. Chopkar et al., [90] added 1 vol.% of tetramethylammonium hydroxide (TMAH) into the nanofluid for better dispersion and observed an improvement in its heat transfer characteristics with a low volume concentration of the TMAH surfactant in a pool boiling heat transfer. The lauric acid surfactant is commonly used in magnetic nanofluid for steric stabilization purposes as no heat transfer effect is observed in it [91, 92]. A summary of the most widely-used surfactants with brief descriptions of their main properties is shown on table 2.3.

Table 2.3.Surfactants used for nanofluid stability.

Surfactant	Nanofluid	Effect	Reference
SDS	Various nanofluids [Multi-walled carbon nanotubes (MWCNT), fullerene, CuO, SiO ₂]	Improves stability for all nanofluids.	[86]
SDBS	Al ₂ O ₃ and Cu-water	Thermal conductivity increases with the increment in surfactant,	[87]
CTAB	CuO-water	Thermal conductivity increases when there is a proper dispersion of nanoparticles in the bas fluid.	[89]

Table 2.3. (continued)

TMAH	Zirconium dioxide (ZrO ₂)	The addition of 1.0 vol.% of TMAH in a nanofluid gives better dispersion.	[90]
PAA CTAB	Al ₂ O ₃ -water	PAA is the most stable surfactant with 0.3% mass fraction of the nanoparticle.	[88]

2.6. SEDIMENTATION

The sedimentation of nanoparticles in their respective base fluids can be observed visually. If nanoparticles are not well mixed and distributed, they have a tendency to precipitate, thus shaping a lean layer of nanoparticles at the bottom. The weight of the nanoparticles precipitating is measured during certain time periods and the volume or weight settling indicates their stability in a particular base fluid. It is common practice to take photographs or video footage in order to observe nanoparticle sedimentation over long periods of time [93].

2.7. PH ADJUSTMENT

The idea behind adjusting the pH of a nanofluid to increase its stability is based on the fact that a nanofluid having a pH value equal or close to the isoelectric point (IEP) which is defined as the pH value at esteem at which a specific particle carries no net electric charge, gets to be unsteady. The IEP is also the point at which the zeta potential is zero. Therefore, increasing the pH of the nanofluid leads to an increases in the hydration forces, allowing for a more stable fluid [94].

In a study, Li et al. [95] explored the effects of pH on the stability Cu-water nanofluid. It were found them the pH of the nanofluid had a definite effect on its stability, with a pH of 9.5 showing the most stable case. The increase in stability was approved to charge build-up on the surface of the Cu particles due to the addition of a stabilizer. In this study, NaOH and HCI were used as factors for raising and lowering the pH of the nanofluid respectively.

Wen et al. [96] also studied the effects of pH adjustment on TiO₂-water

nanofluids. The particle sizes used in this study were between 30 nm and 40 nm, but it was later found that the mean particle size was 170 nm due to particle agglomeration. They used a supersonic mixer to disperse the particles into the base fluid, after which the fluid was processed in a high-shear homogenizer. The measured zeta potential for a 0.024% volume concentration nanofluid was presented as a function of pH and it was shown that the pH has significant impact on zeta potential. It was also found that for pH values lower than 3, the zeta potential was close to 50mV. In addition, IEP (zeta potential of 0mV) of this fluid was close to a pH of 6.5. For a pH larger than 8, the zeta potential was found to be in the range between -25mV and -50mV. At the end, they chose to use a pH of 3 for further studies, and after several hours, a thin layer of sedimentation was found. However, it was believed that these were agglomerates that were simply not broken down. Disregarding the initial sedimentation, the nanofluids were found to be steady for a number of weeks after the initial preparation.

Finally, Murshed et al., [97] examined the impact of pH on thermal conductivity. They reported that small increments in pH cause reduction in thermal conductivity. They tested TiO₂ thermal conductivity inside water and it should be pointed out that they observed only 2% reduction when pH was changed from 3.4 to 9.

2.8. TEMPERATURE

Temperature is discussed in literature as a major variable affecting fluid viscosity; however there is a big controversy on it. Prasher et al. [97] carried out some experiments and concluded that nanofluids' relative viscosity is not strongly affected by their temperature, while Li et al., [98] on the other hand showed a decrement of apparent viscosity by increasing the temperature for CuO. In addition, Nguyen et al. [99] measured the viscosity of Al₂O₃ and CuO for different particle sizes including 29, 36 and 47 nm and showed a dependency of viscosity on the temperature. Ding et al. [100] experimentally proved that the CNT viscosity in different volume concentrations decreases with temperature. On the other side, Chen et al. [101] studied MWCNTs behavior in distilled water and found no significant change in viscosity of nanofluid with increase of temperature up to 55°C. Surprisingly, sudden

increment occurred in range of 55 to 70°C. On the other side, Lee et al.,[102] studied SiC nanofluid and found a decrease in viscosity with decrease of temperature.

There are some other contradictory reports where a number of studies have found the viscosity to be strongly dependent on temperature [103, 104], yet Prasher et al. [105] and Chen et al. [101] defend the view that viscosity is a temperature-independent phenomenon. Anoop et al. [106] measured Al₂O₃ and CuO on ethylene glycol and Al₂O₃ on water base fluids for different volume concentrations of 0.5, 1, 2, 4 and 6%. The temperature was shifted between 20°C and 50°C and a reduction in viscosity with temperature increase was observed. Their comes about are in assention with Duangthongsuk et al. [107] who studied TiO₂ behavior in temperature range 15-50°C and obtained similar result to Anoop et al. [106].

Turgut et al. [108] also selected TiO₂-deionized water to investigate the influence of temperature on viscosity and thermal conductivity. For a range of 13-55°C, results showed a reduction of viscosity by temperature. Additionally, Kole et al. [109] who was concentrated on the usage of nanofluids as coolants in an ICE, concluded that the viscosity of alumina based nanofluid of up to 1.5 vol % became lower as the temperature increased for shifted of 10-50°C.

Pastoriza et al. [110] measured water-based CuO in temperatures of 10.5°C -50.5°C, with a step of 10 K and pressure range from 1 to 45 MPa. They observed a reduction in nanofluid's viscosity with increasing the temperature.

Finally, in another case Namburu et al. [111] studied the viscosity of SiO₂ nanofluid in water and ethylene glycol and watched non-Newtonian behavior (exponential) watched in the shifted 35°C to 50°C. In another investigation [112] they found that mixing CuO with water and ethylene glycol appears Newtonian behavior within the same temperature extend, contrary to their previous results. Both cases show that viscosity is reduced with temperature. To prove the case, Naik et al. [113] also found that the viscosity of CuO/PG particles mixed with ethylene glycol appears Newtonian behavior within the same temperature extend 15°C to 62°C.

2.9. VOLUME FRACTION

Nanofluids' volume concentration is another important property which directly influences not only their viscosity, but their thermal properties as well. There have been many studies on the relationship between particles' wt% and nanofluid viscosity. The results are almost unanimous on the fact that the higher wt% is, the more viscous the nanofluid. Thus, the tradeoff between thermal properties and rheological properties is an essential issue to consider. Concerning this, some experiments have shown that the volume concentration can significantly affect the viscosity of nanofluids [98, 105]. Studies of Lee et al., [102] on volume concentration found that the viscosity thickness increments relatively with particles' volume fraction. Ding et al. [100] also appeared an increment in nanofluids' viscosity with increasing CNT concentration. Chen et al. [101] found the increments of volume concentration (fractions of 0.002, 0.004, 0.006, 0.008 and 0.010) lead to higher viscosity for MWCNTs.

Das et al. [114] measured Al_2O_3 viscosity for different nanoparticle concentration and showed that they are positively correlated. In addition, they claim there is a strong dependency between volume concentration and nanofluids non-Newtonian behavior. Kole et al. [109] measured different volume concentration Al_2O_3 and TiO_2 in deionized water and found 82% and 86% increase, respectively. Chen et al. [101] in agreement with other researchers showed an increase in viscosity in accordance with nanoparticle loading for MWCNTs. Kim et al., [115] also measured TiO_2 in distilled water and appeared that the volume concentration increases the viscosity of nanofluids. However, studies from some other groups have contradicted the above results showing that increasing particle volume leads to decreased viscosity of the nanofluids [116].

2.10. CLUSTERING OF NANOPARTICLES

Clustering may be defined as the aggregation of small particles into larger size aggregates. This phenomenon is critical in the field of nanofluid since it affects their thermal conductivity among many other properties. As a result, numerous studies have been carried out by different groups to better understand the process and take steps into reducing or get rid of it completely. Hong et al., [117] studied aggregation

on Fe-ethylene glycol nanofluid and they found that this nanofluid's thermal conductivity was related to the duration of ultrasonic disturbance, which in turn varied from 0 to 70 minutes maximum. In addition, they also checked the changes in nanofluid's thermal conductivity after ultrasonic application, and they found that thermal conductivity decreased with time. Furthermore, they also showed that the size of clusters was dependent on the time, in other words, the more time passed post ultrasonic application, the bigger the cluster size became. Moreover, it was moreover found that the connection of warm conductivity with molecule volume division was nonlinear, and this observation was interpreted to be the effect of higher particle volume leading to faster aggregation. On the same line, but concentrating on a different aspect, Zhu et al. [118] examined the effects of pH on nanofluids thermal conductivity using Fe_3O_4 water and concluded that the main variable leading to unexpected increase of thermal conductivity in that nanofluid was the clustering of nanoparticles.

A schematic representation of particle clustering is shown in figure 2.3 where a number of particle cluster configuration can be observed, such as irregular and monodispersed cases. In addition, a real image from Transmission electron microscopy (TEM) is shown in figure 2.4 where the average size of the nanoparticles is 15 nm as indicated by the provider and cluster morphology is generally spherical. There is one common approach to break clustering, that of sonication and addition of surfactant. They both break the aggregates and solubilize the particles into single units or smaller aggregate sizes [119].

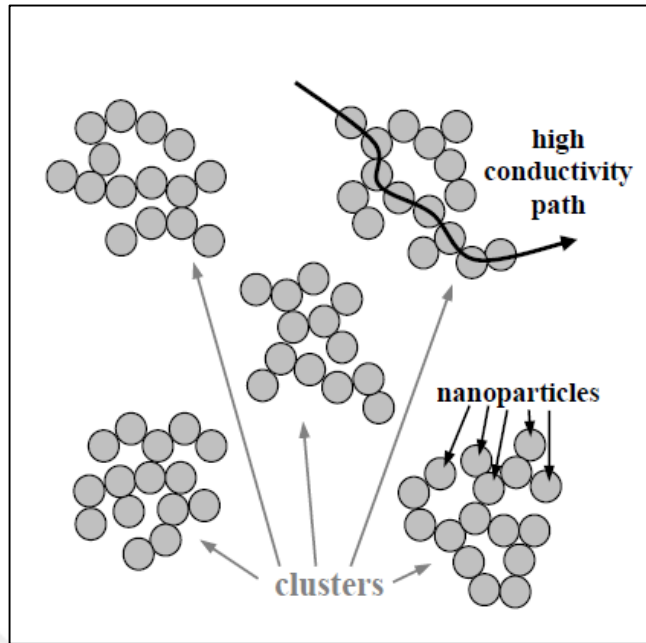


Figure 2.3. Schematic layout representing the clustering marvel [119].

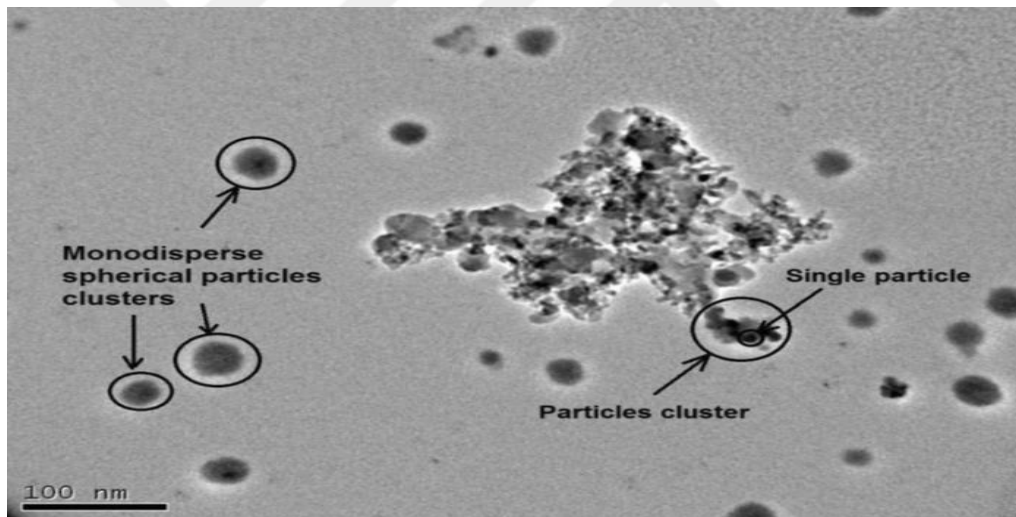


Figure 2.4. TEM nanograph of 15 nm TiO_2 nanoparticles.

2.11. RHEOLOGICAL CHARACTERISTICS OF NANOFUIDS

Rheology involves the study of materials flow and deformation when a certain force is applied on them. Rheological properties are measured for materials of all kinds and states such as dilute solutions, surfactants, semi-solids, and even solid polymers. Therefore, measurement of materials' rheological properties is indispensable and involves every stage of their processing and development. In the following subsections, the rheological properties of nanofluids will be briefly summarized.

2.11.1. Viscosity

Viscosity is defined as the resistance of a fluid to deformation by the stress, and it is more commonly known as a fluid's thickness. Viscosity is a very important variable in the field of nanofluids, and there have been great efforts to understand its impact on nanofluids properties. Thus, Sundar et al [120] found a positive relationship between a nanofluid's viscosity and particle volume concentration, but an inverse relationship with nanofluids temperature. Particularly, they found that absolute viscosity for water temperatures of 20°C and 60°C was 1.063 and 2.09 times bigger for 0.2% volume concentration. When concentration was increased to 2%, it became 1.1 and 2.96 times for the same temperatures.

In another study by Reddy et al., [61], they calculated heat transfer coefficient in TiO₂ nanofluid which was passed through a double-pipe heat exchanger for two cases, one involved helical coil inserts, while the other case did not. Comparisons with base fluid showed a 10.73% increase in heat transfer coefficient for 0.02% volume concentration for the tube without helical coils, and it increased by 13.85% for the same concentration involving helical coils.

Furthermore, Mahbubul et al., [121] examined viscosity of Al₂O₃ particles and observed it to be 179 times higher than that Base fluid concentrations of 6 ° C and 2 percent volume. Therefore, optimal concentrations of nanoparticles with refrigerants should be dispersed in view of thermal conductivity and viscosity in order to achieve better heat transfer efficiency. Finally, Yiamsawas et al [122] determined the viscosity of a mixture of ethylene glycol and water where TiO₂ and Al₂O₃ nanoparticles were suspended. They found that Al₂O₃ nanofluid had higher viscosity than TiO₂ and this difference was interpreted to be due to the larger particle size of the former.

2.11.2. Nanofluid Viscosity Dependent on Nanoparticle Material

As it was shown in the previous sections, nanoparticles make up only a tiny percentage by volume concentration of nanofluids. Despite that, they are the main factor behind the special properties of these classes of fluids, making the understanding of their behavior critical for further advancements in the field. Figure

2.5 shows a chart representing the various nanoparticle source materials used in various nanofluids used in different studies. The figure clearly shows that TiO_2 are the most widely used nanoparticles, followed by Al_2O_3 and CuO used in 17.9 and 7 studies respectively, out of a total 41 studies involving nanoparticles.

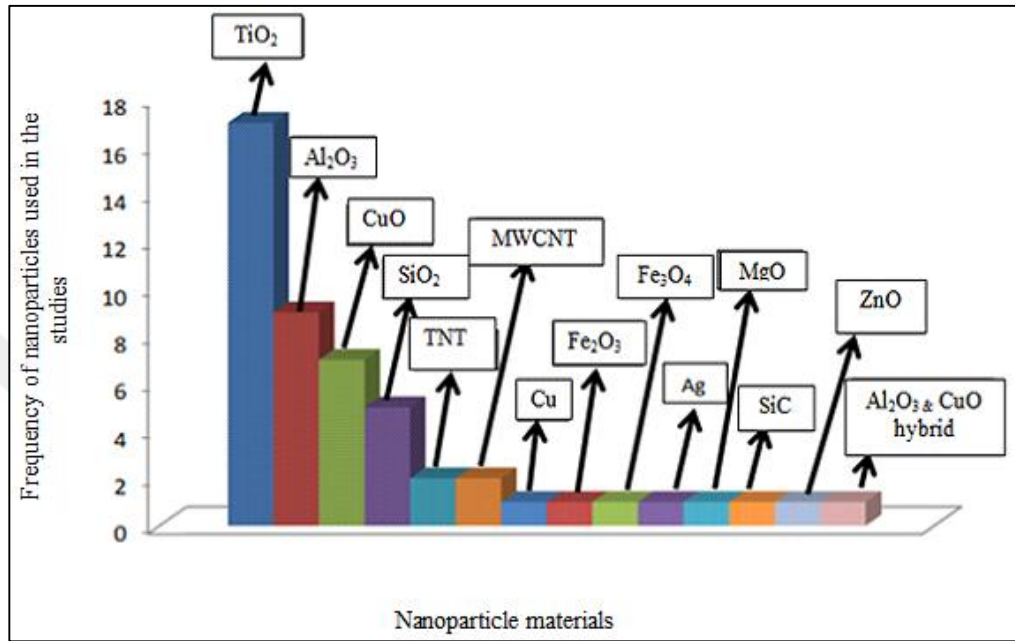


Figure 2.5. Nanoparticle repeat plot gotten from the composing think about.

2.11.3. Nanofluid Thermal Conductivity Dependent on Nanoparticle Material

Some of the most important systematic studies to understand the behavior of nanoparticles were carried out by Yu et al., [123]. They analyzed many nanoparticles in different particles and made extensive tabulations of their results (table 2.6). Closer study of the table shows many differences between experimental data, and the major factor leading to such differences are thought to be the various experimental approaches followed by each research group. As a proof of principle, Kundan et al., [19] carried out some experiments where they compared the results obtained by two different methods, namely transient hot-wire and steady-state cut-bar strategies and found no differences in the data when experiments were carried out at room temperature. However, when the same tests were performed at higher temperatures, the differences between them became more significant. Their explanation for this phenomenon by calling in natural convection phenomenon, which affects the hot-wire method more than the other, causing divergences between the two approaches.

Table 2.4. Rundown of exploratory ponders of warm conductivity improvement.

Particle Type	Base Fluid ^b	Particle Volume Fraction (%)	Maximum Enhancement t (%) ^a	Particle Size (nm)	Notes	Reference
TiO ₂	water	3.10–4.30	10.8	27	31.85°C – 86.85°C	[14]
Al ₂ O ₃	water	1.30–4.30	32.4	13		
SiO ₂	water	1.11–2.41	1.1	12		
TiO ₂	water	0.51–6.00	30	15 sphere	Room temperature	[124]
TiO ₂	water	0.51–6.00	33	11x41 rod		
TiO ₂	water	0.2–3.0	7.4	21	13°C– 55°C	[108]
MWCNT	water	0.06–0.50	79	40 nm (diameter)	21°C– 31°C	[100]
DWCNT	water	0.75–1.00	8	5(diameter)	Effect of sonication time was examined.	[125]
MWCNT	water	0.60	34	130x10000		
MWCNT	EG / EO	0.20–1.00 / 1.00–2.00	12/30	20~50 (diameter)	Room temperature	[74]
CuO	water	2.00–6.00	51	29	28.9°C –33.4°C	[126]
Al ₂ O ₃	water	2.00–10.00	29	36	27.5°C -34.7°C	
Al ₂ O ₃	water	1.86–4.00	20	8 – 282	Effect of particle size was examined.	[127]
Al ₂ O ₃	EG	2.00–3.01	19	12 – 282		

^aThe percentage values indicated are according to the expression $100(k_{nf} - k_f) / k$

^bEG: ethylene glycol, EO: engine oil.

Another important study on the same subject was performed by Ju et al., [128] who appeared that on the off chance that the measurements are taken immediately after sonication, hot-wire method gives erroneous results due to temperature increase in the solution caused by the sonication procedure. In addition, they showed that this high temperature effect due to sonication continued for about 50 minutes after sonication was over. According to them, another source of error are successive measurements if the in-between heating pulses intervals are 5 seconds. Therefore, even if Kundan et al., [19] reported consistent thermal conductivity data, there still may be discrepancies in literature due to the factors mentioned above [128].

Another important factor causing differences between different experiments is the phenomenon of clustering, which was explained in more detail in its appropriate section. Although there is no consensus on the quantitative effects yet, it is well established that clustering has a contains a major part on nanofluids' thermal

conductivity [129]. The degree of clustering depends on a number of parameters, some of them not well understood yet, however adjusting the pH of the solution as well as adding certain amounts of surfactants are proven ways to decrease clustering [87]. As a result, having the same nanofluids with the same parameters can give radically different results due to clustering. Therefore, researchers should be careful and strictly control not only nanoparticle concentration and type, but also pH and additives [18].

One of the most effective technique to get rid of clustering is to use ultrasonic vibrations, the duration and intensity of which heavily affect nanoparticles dispersion in solution. Since nanoparticles start to cluster again after sonication is stopped and increase with time [130], controlling for the time between measurements, sonication intensity and duration, are important factors affecting nanofluid thermal conductivity, therefore giving different, and sometimes conflicting results between experiments [131].

2.12. STABILITY OF NANOFLUIDS

An important parameter to be tightly controlled in experiments involving nanofluids is their stability because it can drastically affect the data obtained. Meyer et al., [132] have defined a stable nanofluid as a solution in which nanoparticles are in continuous Brownian motion without impediment and interaction with each other, in other words, there is no flocculation which leads to agglomeration and ultimately to particle sedimentation at the bottom of the container.

The duration of the period during which a nanofluid is stable can be described as a function dependent on various components, such as the nature of the nanoparticle, its volume concentration, surfactant origin and concentration, particle shape, whether the system is dynamic or stationary, the temperature of solution, its preparation method as well as the contrast between the densities of nanoparticles and the base fluid [132]. Given its importance, a number of methods are used to study nanofluid stability, such as visually following up sedimentation, measuring sedimentation rate, solution turbidity, zeta potential etc. [132]. Most of these methods however, have their inherent limitations when used in practice.

2.13. OTHER EXPLORATORY INVESTIGATE ON NANOFLUID FOR ENGINE COOLING

In addition to the experiments performed in real car engines, many other studies are carried out in conditions that mimic those of the actual vehicle engines. There have been a number of considers including ethylene glycol as the base fluid. In one of them, Teng et al., [133] investigated MWCNT performance and observed a 14.1% increase in heat exchange efficiency. Their experimental setup was based on a 50 by 50 proportion of nanofluid and ethylene glycol and moo volume concentration of nanoparticles. An important finding was the fact that increasing nano-coolant's concentration did not lead to better performance because nanoparticles had a tendency to disperse unevenly. Additionally, Nieh et al. [52] calculated the efficiency of TiO₂ nanofluid (0.2 vol%) to increase 28.2%. The list of such experiments is long [76-80] and beyond the scope of this study, however an outline is given in table 2.5.

Table 2.5. Exploratory thinks about of nanofluid for vehicle framework cooling.

Nanofluids	Results	Reference
CuO, SiC, Al ₂ O ₃ , TiO ₂ -EG/water (80% water, 20% EG)	Maximum heat transfer rate improvement for SiC was 15.34%, whereas for Al ₂ O ₃ was 14.33%, for TiO ₂ was 14.03%, and for CuO was 10.20% with 1.0 vol% of nanoparticle concentration compared to pure base fluid.	[134]
TiO ₂ -water, SiO ₂ -water	The heat transfer rate enhancement was 20% and 32% for TiO ₂ and SiO ₂ nanofluids respectively.	[135]
SiO ₂ -water, TiO ₂ -water	Maximum Nusselt number enhancements for TiO ₂ and SiO ₂ nanofluids were 11% and 22.5% respectively compared to pure water.	[136]
MWCNT-EG/water (50 vol% of EG)	Maximum enhancement of thermal conductivity of the MWCNT-EG/W nanofluids was 49.6% with 0.4 vol% of nanoparticles compared to EG/W. Maximum efficiency factor was 14.1% at low concentration of MWCNT nanoparticle.	[133]
MWCNT-engine oil	Maximum enhancement of thermal conductivity of the nanofluids was 12.7% with 0.5 vol% of MWCNT nanoparticles at 20 °C.	[137]

Table 2.5. (continued)

CuO–water, Fe ₂ O ₃ –water	Heat transfer coefficient was enhanced up to 9% at 0.65 vol.% nanoparticle concentration in comparison with water.	[79]
Al ₂ O ₃ –EG	Maximum enhancement of thermal conductivity of 4.5% with 1.5 vol% of Al ₂ O ₃ nanoparticles was at 50 °C.	[138]

As it was stated previously, an important component of nanofluid studies are also theoretical studies involving numerical analysis [81-84]. A list of those studies is given in table 2.6.

Table 2.6. Outline of numerical thinks about on nanofluid for vehicle framework cooling.

Nanofluids	Findings	Reference
Al ₂ O ₃ , Au, CuO, TiO ₂ –water/vapor	Heat transfer coefficient decreases along the flow as the vapor quality increases. In two-phase flow, the heat transfer coefficient enhancement for Al ₂ O ₃ was the highest followed by TiO ₂ , Au, and CuO nanofluids	[139]
Al ₂ O ₃ –water, Al ₂ O ₃ –EG	Nusselt number for two-phase approach was 10–45% greater and closer to the experimental data than the single-phase approach	[140]
CuO–water, Fe ₂ O ₃ – water, TiO ₂ –water, EG/water (50:50)	TiO ₂ -water nanofluid can enhance 10% of heat recovery without any pressure drop followed by Fe ₂ O ₃ - water and CuO-water nanofluid compared to EG/water	[141]
Cu–water, Cu–oil engine	Heat transfer coefficient and heat dissipating capacity enhancement of Cu-water nanofluid with 5.0 vol% of nanoparticle concentration were about 46% and 43.9% more than pure water.	[142]

CHAPTER 3

THEORETICAL ANALYSIS

3.1. THERMOPHYSICAL PROPERTIES OF THE NANOFLUID

The thermophysical properties of any nanofluid depend on a number of components such as molecule estimate, shape, whether it is metallic or non-metallic (oxide), chemistry of the arrangement, particularly pH, and arrangement age. For occasion, the warm conductivity of circular formed nanoparticles is lower as compared to round and hollow ones, whereas littler estimate particles have way better warm conductivity when compared to those of more prominent measure. Moreover, metallic nanoparticles have way better warm conductivity than non-metallic ones [107].

Table 5.1 appears the thermo-physical properties of TiO₂ and immaculate water at temperatures extend between 20 and 80°C. The taking after conditions were utilized to appear the consistency with respect to consistency, particular warm, warm conductivity and thickness [143].

Nanofluid density is calculated as takes after:

$$\rho_{nf} = \varphi\rho_p + (1 - \varphi)\rho_w \quad (3.1)$$

3.2. VISCOSITY CALCULATION AND MEASUREMENT

Nanofluid viscosity is additionally decided by a number of variables such as the volume division of nanoparticles, their measure and shape, base liquid, thickness of the nanolayer, scattering method, temperature and pH value, and nanoparticles' Brownian movements [14, 108, 144-147]. by and large measured by rebellious such as viscometer or rheometer, and the compiled information are compared to known

relationships. The primary demonstrate to degree thickness was created by Einstein in 1902.

(Equation 2). Particle's circular shape and less volume division are the constraining variables of this condition [148].



Figure 3.1. Pycnometer used for measuring density of nanofluids.

$$\mu_{nf} = (1 + 2.5\varphi)\mu_w \quad (3.2)$$

A more compelling equation was afterward determined by the Brickman Model [149].

$$\mu_{nf} = \frac{\mu_{bf}}{(1-\varphi)^{2.5}} \quad (3.3)$$

Another show considered to be more appropriate for nanoparticles with volume division more noteworthy than 2% was determined by Nelson in 1970 and appeared in condition (3.4) [150].

$$\mu_{nf} = \left[(1 + 1.5\varphi) e^{\frac{\varphi_p}{(1-\varphi_m)}} \right] \mu_{bf} \quad (3.4)$$

Where φ_p and φ_m stand individually for volume concentration and greatest volume division. Analysts have as of late altered these models by presenting more parameters

in arrange to extend their precision. One such show is the Corcione show which features a number of preferences such as giving comes about with 1.84% of standard deviation as well as taking after boundaries of nanoparticles with distances across between 20-200 nm and volume division of 0.0001–0.071 [151].

$$\mu_{nf} = \left[\frac{1}{1 - 34.87 \left(\frac{d_p}{d_f} \right)^{-0.3} \varphi^{1.03}} \right] \mu_{bf} \quad (3.5)$$

$$d_f = 0.1 \left(\frac{6M}{N\pi\rho_{bf}} \right)^{1/3} \quad (3.6)$$

where ρ_{bf} denotes the mass density of base fluid at 20°C

Recently, with the increase in computation power, there have been concentrated efforts by researchers to develop better theoretical models by increasing the number of parameters, as summarized in table 3.1.

In this ponder, nanofluid viscosity was measured by using a Brookfield Viscometer (DV-2 + Pro Programmable Viscometer) and in arrange to diminish instability, the measured values were compared with the information in ASHARE Handbook [152].

Table 3.1. Viscosity models for TiO₂ nanofluids.

Derived Model	Reference																
$\mu_{nf} = A\varphi^B T^C \mu_{bf}^D$ <p>$A = 0.837831, B = 0.189264, C = 0.098069$ and $D = 1.100955$</p>	[147]																
$\mu_{nf} = (a + b\varphi + c\varphi^2)\mu_{bf}$ <table border="1" data-bbox="520 651 1067 860"> <thead> <tr> <th>$T (^{\circ}C)$</th> <th>a</th> <th>b</th> <th>c</th> </tr> </thead> <tbody> <tr> <td>15</td> <td>1.0226</td> <td>.0477</td> <td>-0.0112</td> </tr> <tr> <td>25</td> <td>1.013</td> <td>0.092</td> <td>-0.015</td> </tr> <tr> <td>35</td> <td>1.018</td> <td>0.112</td> <td>-0.0177</td> </tr> </tbody> </table>	$T (^{\circ}C)$	a	b	c	15	1.0226	.0477	-0.0112	25	1.013	0.092	-0.015	35	1.018	0.112	-0.0177	[107]
$T (^{\circ}C)$	a	b	c														
15	1.0226	.0477	-0.0112														
25	1.013	0.092	-0.015														
35	1.018	0.112	-0.0177														
$\mu_{nf} = (13.47e^{35.98\varphi})\mu_{bf}$	[153]																
$\mu_{nf} = \mu_{bf} \left[1 - \frac{\varphi}{\varphi_m} \left(\frac{d}{D} \right)^{1.2} \right]^{-2}$ <p>where φ = particle concentration; D = average diameter of aggregates; φ_m = crowding factor ($\varphi_m \approx 0.66$) in case of arbitrary pressing of circles; d = distance across of suspended particles</p>	[154]																



Figure 3.2. Brookfield Viscometer (DV-2 + Professional Programmable Viscometer).



Figure 3.3. Photographic view of Cone and plate assembly.

3.3. SPECIFIC HEAT CAPACITY OF NANOFLUID

Specific heat is characterized as the sum of warm per unit mass of a fabric to raise the temperature by one degree centigrade. It is one of the basic properties impacting the rate of warm exchange in nanofluids. Studies have appeared it to differ with molecule estimate and since littler particles have bigger particular surface ranges, decreasing particles measure increments the impact of the surface vitality on viable particular heat capacity [70, 155]. In arrange to decide the particular warm capacity of TiO₂ nanofluid, condition (3.7) was utilized:

$$Cp_{nf} = \frac{\varphi \rho_p Cp_{p,n} + (1-\varphi) \rho_w Cp_{bf}}{\rho_{nf}} \quad (3.7)$$

3.4. THERMAL CONDUCTIVITY OF NANOFLUID

Thermal conductivity is the capacity of a fabric to conduct heat and it depends of numerous variables such as the warm conductivities of base liquid and nanoparticles, surface range, nanoparticle shape, temperature and volume division. A number of hypothetical and experimental models have been inferred to foresee the thermal conductivity of nanofluids [156-158], with conditions (3.8-3.10) representing the ones utilized within the current think about to compare with the exploratory comes about gotten by measuring it by KD2 Professional heat property analyzer (Decagon, USA). This gadget comprises of a sensor for measuring liquids thermal conductivity by employing a transitory line warm source and a hand-held controller. To carry out the estimations, nanofluid test was immersed for 11 minutes in water shower at the specified temperature until it comes to balance with the medium. Four readings were taken with 16 minutes interims between each at a temperature extend of 20-80°C.

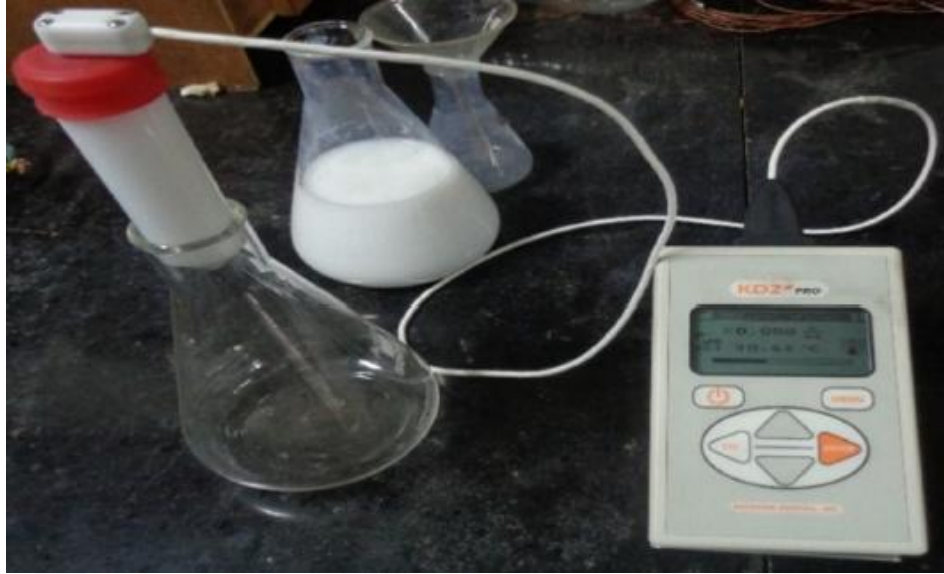


Figure 3.4. KD2 Pro with KS-1 needle.

Maxwell model
$$k_{nf} = \frac{k_p + 2k_{bf} + \varphi(k_p - k_{bf})}{k_p + 2k_{bf} - \varphi(k_p - k_{bf})} k_{bf} \quad (3.8)$$

Hamilton-Crosser model
$$k_{nf} = \frac{k_p + (n-1)k_{bf} - \varphi(n-1)(k_{bf} - k_p)}{k_p + (n-1)k_{bf} + \varphi(n-1)(k_{bf} - k_p)} \quad (3.9)$$

Yu and Choi model
$$k_{nf} = \frac{k_{pe} + 2k_b + 2(k_{pe} - k_b)(1 + \beta)^3 \varphi}{k_{pe} + 2k_b - 2(k_{pe} - k_b)(1 + \beta)^3 \varphi} k_b \quad (3.10)$$

Scientists used different parameters to derive a numbers of models in order to estimate nanofluids' thermal conductivity. Some of those models with a short description are shown in in a summarized way in (Table 3.2).

Table 3.2. Thermal conductivity models of TiO₂ nanofluid.

Derived Model	Discussion	Reference
$k_{eff} = k_{bf} \left[\frac{3fq(p)/p_0}{1 - fq(p)/p_0} \right]$	The created comprehensive demonstrate included the nanolayer thickness, molecule measure, temperature, volume division and the interaction between adjoining nanoparticles.	[159]
<p>Model 1: $k_{nf} = k_{bf} \left[\left(\frac{C_{P,nf}}{C_P} \right) \left(\frac{\rho_{nf}}{\rho} \right)^{1.33} \left(\frac{M}{M_{nf}} \right)^{0.33} \right]$</p> <p>Model 2: $k_{nf} = k_{bf} \left[\frac{k_p + (n-1)k_{bf} + (n-1)(k_p - k_{bf})(1+\beta)^3 \varphi}{k_p + (n-1)k_{bf} - (k_p - k_{bf})(1+\beta)^3 \varphi} \right]$</p>	<p>Model 1: utilized to decide the warm conductivity of nanofluid over a huge extend of molecule concentration, estimate and distinctive base liquids and molecule materials.</p> <p>Model 2: made a difference to imagine the rate commitment of layer thickness, molecule shape, Brownian movement to the improvement in warm conductivity of nanofluids.</p>	[154]
$k_{nf} = k_{bf} \left[\frac{k_p + (n-1)k_{bf} - (n-1)(k_p - k_{bf})\varphi_{eff}}{k_p + (n-1)k_{bf} + (k_p - k_{bf})\varphi_{eff}} \right]$ $\varphi_{eff} = \varphi \left(1 + \frac{h}{r} \right)^3$	Considered the fluid layer thickness, warm conductivities of base liquid and nanoparticles but not the interface between particles and particle appraise.	[160]
$k_{nf} = 1 + 4.4Re^{0.4}Pr^{0.66} \left(\frac{T}{T_{fre}} \right)^{10} \left(\frac{k_p}{k_{bf}} \right)^{0.03} \varphi^{0.66}$	The experimental relationship of Corcione is appropriate with 1.91% of standard deviation mistake over a wide extend of temperature (20–80°C), nanoparticle distance across (11–149 nm) and volume division (0.003–0.8)	[151]

3.5. CALCULATION OF HEAT TRANSFER COEFFICIENT

In arrange to assess heat transfer coefficients within the radiator, the taking after conditions for the coolant and discuss were utilized [161].

$$Q = h A \Delta T = h A (T_b - T_w) \quad (3.11)$$

$$Q = \dot{m}C_p (T_{in} - T_{out}) \quad (3.12)$$

Where, Q is the rate of warm exchange rate in Watts (W). C_p is the particular heat capacity of working liquid [J/kgK], m speaks to the mass flow rate of working liquid [kg/s], T_{in} , and T_{out} stand for channel and outlet temperatures of coolant liquid [$^{\circ}C$], individually, T_b is the bulk temperature which was expected to be the normal esteem of channel and outlet temperatures of the liquid moving through radiator, and at last T_w is the tube divider temperature which is the normal esteem of two surface thermocouples..

$$h_{exp} = \frac{Q}{A(T_b - T_w)} \quad (3.13)$$

Where, h_{exp} is the heat transfer coefficient [$W/m^2 \cdot K$].

Nusselt number (Nu) is determined as:

$$N_u = \frac{hD_h}{K} \quad (3.14)$$

Where, D_h stands for the hydraulic diameter of the tube [mm]. Finally, Reynolds number (Re) is determined as

$$R_e = \frac{\rho \vartheta D_h}{\mu} \quad (3.15)$$

Where, ϑ is Velocity at inlet radiator [m/s]

3.6. RELATIONSHIPS FOR NUSSELT NUMBER DETERMINATION FOR SINGLE PHASE FLUIDS

Relationships for the laminar flow through channels [162] and for the flow in the compact heat exchanger at $550 \leq Re \leq 1850$ range were decided by conditions (3.16) and (3.18) respectively [163].

$$Nu = 1.86 \left(\frac{Re_D Pr}{L/D_h} \right)^{1/3} \left(\frac{\mu}{\mu_s} \right)^{0.14} \quad (3.16)$$

$$Nu = 0.951 \times Re_D^{0.173} \times Pr^{1/3} \quad (3.17)$$

$$Nu = 1.953 \left(Re Pr \frac{d}{L} \right)^{1/2} \quad (3.18)$$

Where Re_D represents tube-side Reynolds number which is based on tube hydraulic diameter whereas Pr is Prandtl number.

In spite of the fact that, we utilized a tall Reynolds number as an input parameter, exploratory comes about were compared by utilizing the conditions for contact (Equation (3.19)).

$$f = \frac{64}{Re} \quad (3.19)$$

3.7. UNCERTAINTY ANALYSIS

The accuracy of test setup is pivotal for any think about, but of the same significance is the gathering of precise information with the right measuring gadgets. Awfully capable devices in planning tests are moreover instability investigation since they are utilized to degree test mistakes which may be negative to information precision. No matter the precision of measuring gadgets, instability investigation is continuously utilized to decide blunders developing from environment, test conditions, measuring gadgets or experimenter. In arrange to calculate the entire vulnerability for these tests, condition (3.20)[164, 165] was used as follows:

$$G = G(x_1, x_2, x_3, \dots) \xrightarrow{f} W_s = \left[\left(\frac{\partial G}{\partial x_1} w_1 \right)^2 + \left(\frac{\partial G}{\partial x_2} w_2 \right)^2 + \dots + \left(\frac{\partial G}{\partial x_n} w_n \right)^2 \right]^{1/2} \quad (3.20)$$

To calculate add up to instability, S is the fundamental amount to be decided with n free factors influencing the quantity G as $x_1, x_2, x_3, \dots, x_n$. The mistake rate for each of those free factors as well as the full instability examination are expressed as W_1, W_2, \dots, W_n and W_s respectively. The specialized capabilities, add up to vulnerability and precisions investigation of measuring hardware are shown in Table 3.3.

Table 3.3. Technical properties, precisions and total uncertainty analysis of the equipment.

Measuring device	Measuring range	Precision	Total Uncertainty
Flow meter	2-21 m ³ /h	± 2.6 %	± 0.0003136 %
Thermometer	0 - 121 °C	± 0.19 °C	± 0.076 °C
Thermocouple	0 - 1199 °C	± 0.18 °C	± 0.14 %
Anemometer (air velocity)	0 - 21 m/s	± 0.02 m/s	± 0.013 %

3.7. FLOW METERS

In order to calculate the heat transferred by the heat exchanger, the water flow rate through the tube and the shell is necessary. Flow meters positioned on the inlet and outlet pipes can be used to provide the volume flow rate. This, in turn, can be used to calculate the mass flow rate.



Ürün Kodu: EF301

Gövde: SS316 Paslanmaz Çelik

Ölçüm Tüpü: Cam

O-Ring: Viton

Max. P/T: 7 ila 15 bar / 150 C

Bağlantı: 1/2"BSP ...2 BSP

Hassasiyet: +/- %1 f.s.

Skala Uzunluğu: 310 mm

Debi: SU 1.6...16 l/h - 1...10 m3/h

HAVA 0.05...0.5 m3/h - 20...200 m3/h

Toplam Boy: 408...431 mm

Şamandıra: AISI 316 Paslanmaz Çelik

Bağlantı Rekorları: AISI 316 Paslanmaz Çelik

Muhafaza: Boyalı Çelik Saç

Figure 3.5. Flow meters (specifications in Turkish language).

3.8. THERMOCOUPLES

Temperature measurements at the entries and exits of the heat exchangers are necessary to decide the rate of warm exchange. Utilizing thermocouples that are precisely placed in the center of the tubes, the temperature measurements can be taken. More thermocouples are placed inside the walls of the heat exchangers to allow the precise measurement of the temperatures of the wall. Thermocouples can also be inserted in the cavity or submerged in the fluid in order to gather data for modeling fluid flow within the cavity.



Figure 3.6. Pico-thermocouple (display: TC-08) and Testo-thermometer (Display: 435).

CHAPTER 4

PREPARATION AND CHARACTERIZATION OF NANOFLUID

4.1. EXPERIMENTAL WORK

Nanofluid preparation is key, and there are two widely-accepted methods for nanofluid preparation, and either of them can be adopted, depending on the aim of the study:

- Single step method.
- Two step method.

As explained before, in single-step approach, nanoparticles are arranged through physical vapor deposition (PVD) strategy or fluid chemical strategy (figure 4.1). In the case of two-step approach, first nanoparticles are produced via certain other techniques, such as sol-gel, hydrothermal synthesis, micro emulsion etc., and then they are mixed with a base fluid of interest by using ball milling, ultrasonic vibration, magnetic force stirring or high shear mixing (figure 4.2) [18].

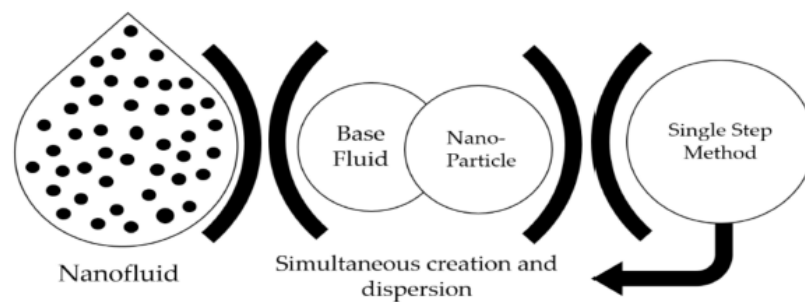


Figure 4.1. Single step method.

In this study, our concentration was on TiO₂-water nanofluid, and since the two-step strategy is the foremost broadly utilized approach for studying TiO₂ based

nanofluids, we used it. In addition, we used 0.1, 0.2 and 0.3 vol% TiO₂ nanoparticle concentrations.

A major advantage of the two-step method is scaling and the ability to produce nanofluid at large industrial scale. However, this is augmented by the drawback of high clustering rate, therefore using surfactants is essential.

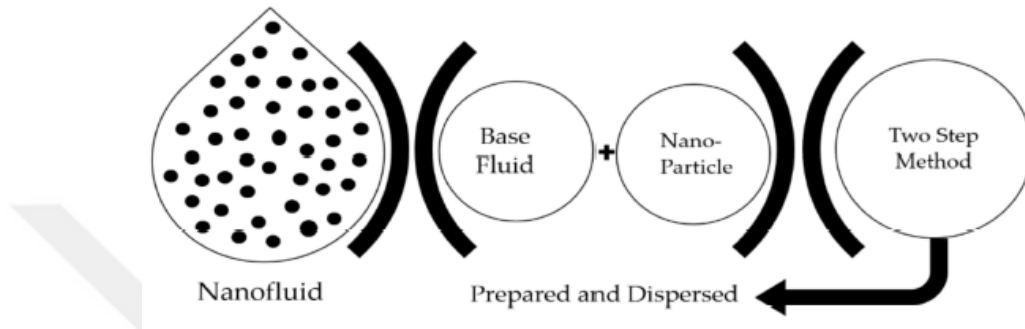


Figure 4.2. Two-step method.

4.2. CHARACTERISTICS OF EXPERIMENTAL TiO₂ NANOPARTICLES

As a first step in preparing our TiO₂ nanoparticles, nanoparticles of dry Titanium oxide with anatase nature having an average size of 32 nm distance across and particular surface area of (BET) of 54 m²/g were purchased from Alfa Aesar company (USA). They were mixed with deionized water. Titanium oxide of anatase nature is always found as small, isolated and sharply developed crystals. Anatase is kinetically stabilised; therefore it will maintain its stability and cool effectively while it flows over any hot system. The next step of our procedure was the homogenization of the mixture by sonication for 6 hours. This is a critical step to break clusters and make particle dispersion as evenly as possible. Figure 4.3 shows the titanium oxide dry powder and its specification as provided by Alfa Aesar Company. The dry titanium oxide powder to be used in further experiments was weighed using digital weighing machine of high accuracy. Figure 4.4 shows the weighing of titanium oxide dry powder used to produce the nanoparticles.

Figures 4.5 and 4.6 shows the X-ray diffraction (XRD) machine and the XRD spectra of our sample, respectively. The titanium powder XRD was carried out with a Rigaku X-ray diffract meter by Cu-k α 1 radiation in the range of 20°C-80°C.



Figure 4.3. TiO_2 nano powder.



Figure 4.4. Weighing of TiO_2 nano powder.



Figure 4.5. XRD.

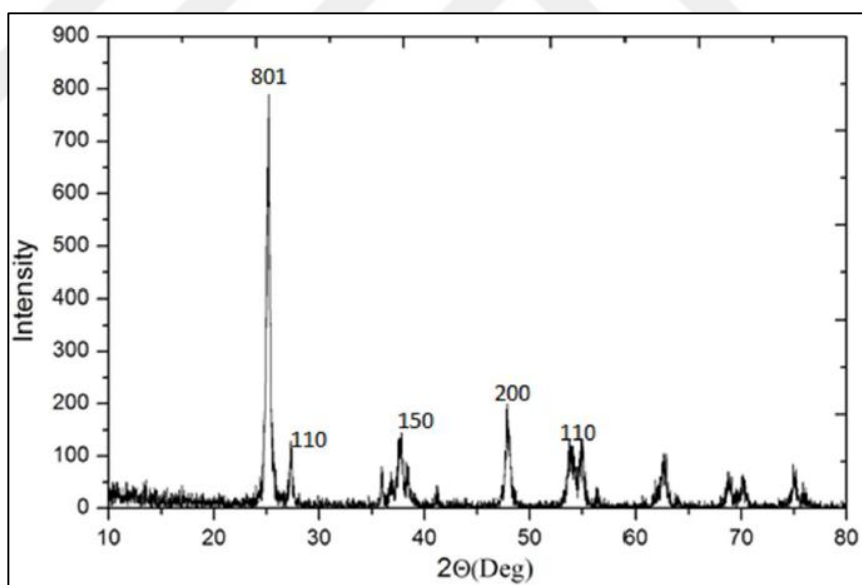


Figure 4.6.XRD analysis of TiO₂ nano particles.

Mechanical stirrers were used for at least one hour to produce a homogeneous mixture, followed by ultrasonic stirring for about two hours (figure 4.7). This is necessary to break any clustering of nanoparticles in solution and ensure even distribution [166].



Figure 4.7. Ultrasonic stirrer.

The lines of XRD spectra were indexed on the tetragonal phase of TiO_2 utilizing the Joint Committee on Powder Diffraction Measures (JCPDS). The XRD pattern of titanium dioxide nanoparticles shown in Figure 4.6 shows only the diffraction peaks of the pure anatase phase and nothing else; meaning that there were no impurity phases in the solution within the resolution power of XRD. Our XRD spectra shows strong diffraction peaks at 27.4 , 38 and 48° . These numbers are used to calculate grain size in the solution (in our case it was 32 nm) by applying the Sherrer formula [167] which is expressed as follows:

$$d = \frac{0.9\lambda}{\beta \cos \theta} \quad (4.21)$$

Where d represents the crystallite measure; λ the wavelength of X-Ray source; β stands for half width full maximum and θ for diffraction angle.

The Scanning Electron Microscope (SEM) and image of the prepared sample are represented in figures 4.8 and 4.9 respectively. Additionally, figures 4.10 and 4.11 show SEM images of TiO_2 particles under 50000X and 30000X magnifications respectively. These figures show the structure of Titanium oxide powder to be agglomerated at micrometer scale under atmospheric conditions. The shape of the

individual nanoparticles was close to spherical. The XRD and SEM analysis are used to find the crystal structure of TiO₂ nanoparticles and their surface morphology, respectively. Different magnifications of SEM images are used to identify the average diameter of the particle. Our characterization of dry titanium oxide powder confirm the specification given by the company from which it was purchased.

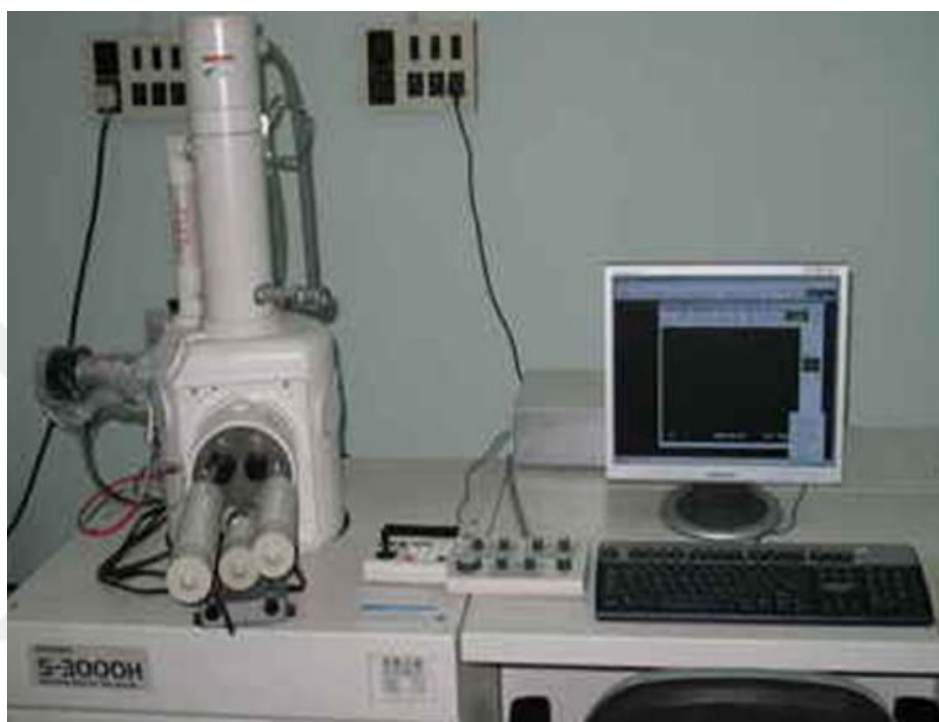


Figure 4.8. Scanning Electron Microscope.

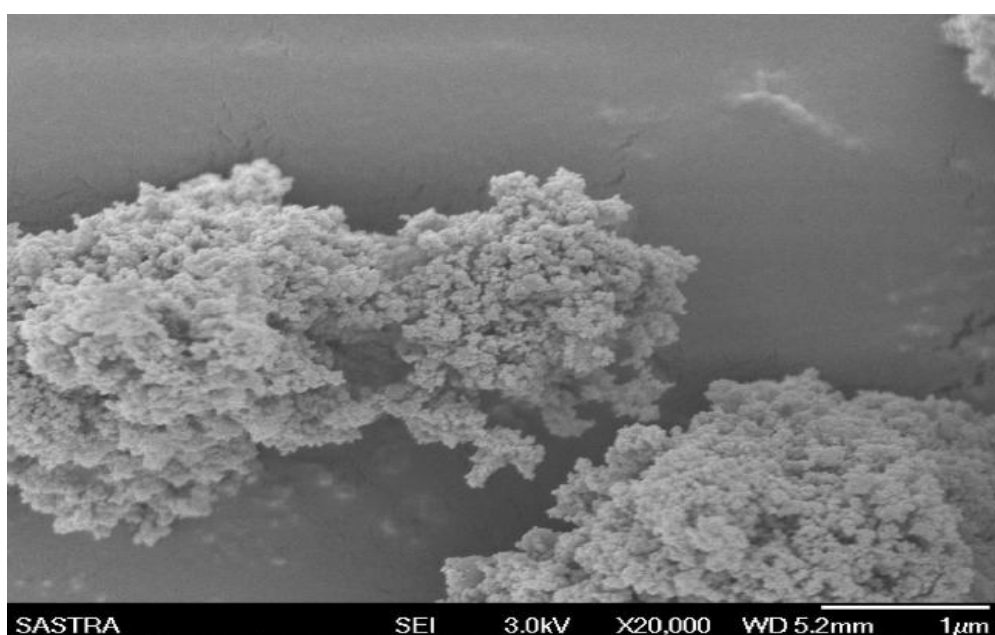


Figure 4.9. SEM picture of TiO₂ nanoparticles 20000X.

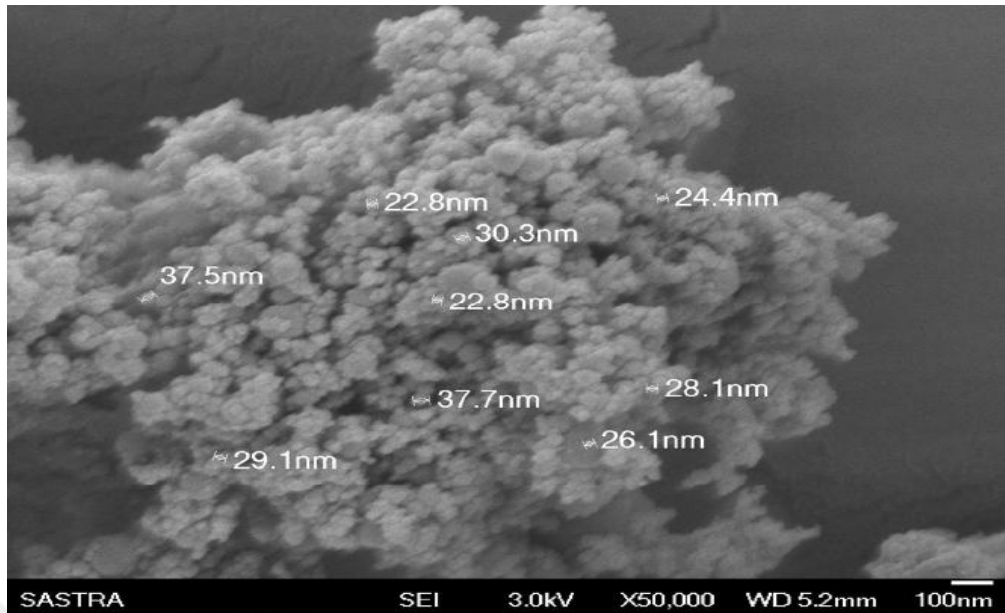


Figure 4.10.SEM image of TiO₂ nanoparticles 50000X.

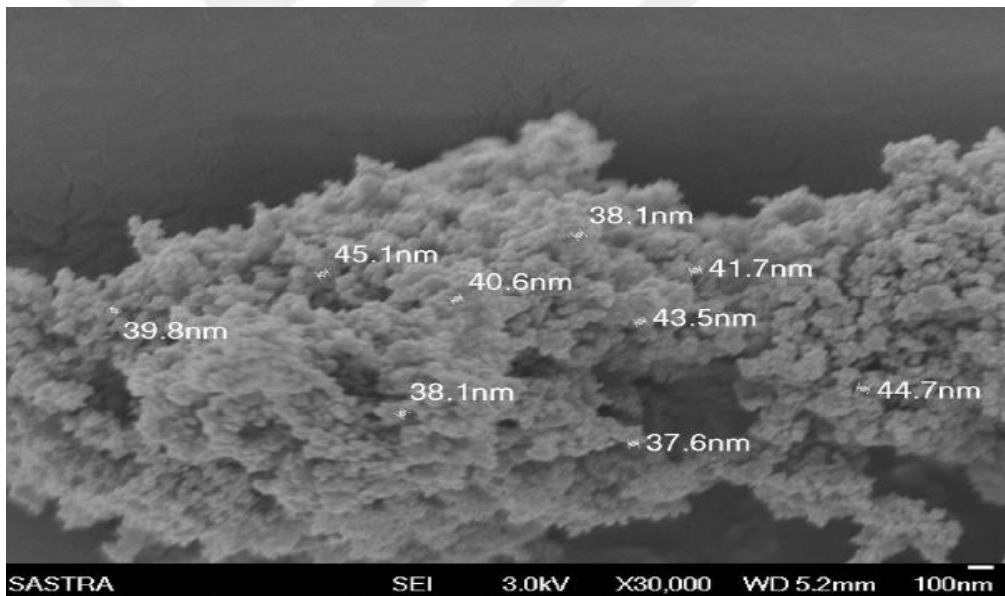


Figure 4. 11.SEM image of TiO₂ nanoparticles 30000X.

4.3. ARRANGEMENT OF TiO₂ NANOFLUID

Nanofluid test Arrangement was carried out in a two-step handle of spreading the basically orchestrated nanoparticles in refined water by implies of ultrasonication. Particles were to begin with decreased in estimate and after that chosen for a uniform breadth by Spex-8000 ball processing (Spex Businesses, Inc., Edison, NJ), giving an ordinary dissemination centered at an normal of 44 nm and a run from 30 to 60 nm (Fig. 5.2). Particles' surface morphology and microstructures were examined with

checking electron magnifying lens (SEM) and transmission electron magnifying lens (TEM). Numerous past thinks about have appeared that expanding the nanofluid's molecule proportion leads to an increment in their precipitation.

Indeed in spite of the fact that we utilized diverse molecule proportions in this think about, the ideal one is 2% at which precipitation remains at a negligible level. Nanoparticles were suspended in deionized water which has fundamental properties and the blend was assist moved forward by expansion of Triton X-100 (atomic equation: $C_{14}H_{22}O(C_2H_4O)_n$) to last concentrations of 0.1% 0.2% and 0.3%, individually, in arrange to improve the dissolvability of TiO_2 . Triton X-100 has surfactant properties and it has been broadly utilized in colors and cleansers for diminishing surface pressure and contact points, driving to an increment within the wetting capacity of the fabric. As a result, TiO_2 particulates can be suspended for longer time periods in liquids by using ball processing to supply tall vitality, expansion of surfactant and ultrasonic shower. In arrange to discover the ideal Triton X-100 sum, the nanofluid's solidness; frothing and accumulation were measured for diverse concentrations of the constituents. A concentration of 0.5% Triton X-100 was chosen for this ponders. Table 1 appears the characteristics of TiO_2 .

Titanium oxide TiO_2 nanoparticles scattering in deionized water was carried out by ceaseless beating through an ultrasonic processor (Bandelin Sonorex Super RK514H) at an ideal term. All through the planning handle of nanofluid, the holder was always cooled to dodge vanishing of surface dynamic operator.

Table 4.1. Characteristics of TiO_2 nanoparticles.

Parameter	Value
Purity	99 %
Color	White
Diameter	44/nm
SSA	10–45/m ² g
Shape	Spherical
Bulk density	0.460/g cm ³

4.4. STABILITY OF NANOFLUID

In arrange to anticipate nanofluid sedimentation amid the tests; a number of steps were taken: To begin with, TiO₂ molecule measure was diminished to nanoscale by utilizing tall vitality affected ball processing (Spex-8000) taken after by expansion of Triton X-100. In expansion, the nano-TiO₂ gotten from the over methods was broken up in water by utilizing ultrasonication. Given the tremendous thickness contrasts between metallic oxide nanoparticles and deionized water, two strategies have been proposed to anticipate sedimentation and consistently disperse nanoparticles in nanofluids; the primary one includes changing nanofluids pH and the other utilizing surfactants [168]. When the zeta potential value is smaller than a certain value, around 10 mV, the repulsive forces among the particles are quite weak, allowing the particles to approach each other and ultimately agglomerate. Agglomeration occurs nearby the isoelectric point or pH value where the zeta potential becomes zero [169]. Table 4.2 shows the colloid stability as related to the values of zeta potential. From the comparison between the table 4.1 and the figure 4.11, indicates the good stability of TiO₂-Water Nanofluid.

Table 4.2. Nanofluid stability for distinctive zeta potential values.

Zeta potential [mV]	Stability behavior of the colloid
0 to ±5,	Rapid coagulation or flocculation
±10 to ±30	Incipient instability
±30 to ±40	Moderate stability
±40 to ±60	Good stability
more than ±61	Excellent stability

Our nanofluid was arranged by utilizing 0.1 to 0.5% surfactant, the final one giving a negligible agglomeration. In expansion, molecule structure is an critical determinant of nanofluid soundness. Dynamic surface reagents have numerous characteristics such as structure, nearness of numerous sorts of metal oxides for moving forward warm conductivity as well as flocculation when they experience ultrasonication, all of them making TiO₂ more compelling as compared to other metal oxides [64]. One of the foremost vital highlights of TiO₂ is tall water adsorption capacity making a gelly surface which increments the oil esteem.

Our nanofluid kept up its solidness all through the test strategy in all temperatures attempted (Figure 4.12). The same was the case for TiO_2 -water nanofluid suspension which was steady and had no refining issues all through the total method. The three crucial thermophysical properties TiO_2 -water nanofluid were measured as appeared in (Table 5.1).



Figure 4.12. TiO_2 -water nanofluid.

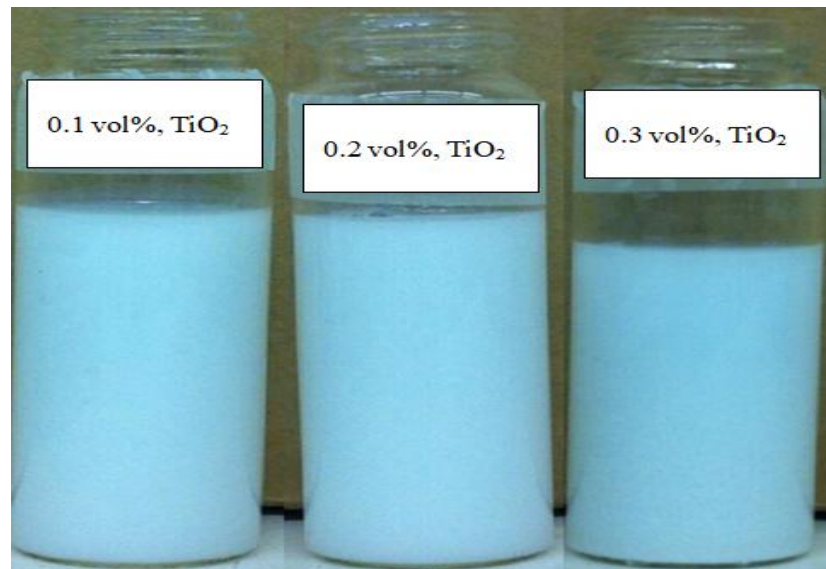


Figure 4.13. TiO_2 water nanofluid of sonication process.

4.5. EXPERIMENTAL SETUP

The vehicle motor framework (Show FIAT DOBLO 1300 cc. MJTD) utilized in this ponder incorporates stream lines, a centrifugal pump, a stream meter, anemometer, tank, thermocouples, a constrained draft fan and a cross stream warm exchanger, moreover known as vehicle radiator (Figure 4.14 & 4.15).

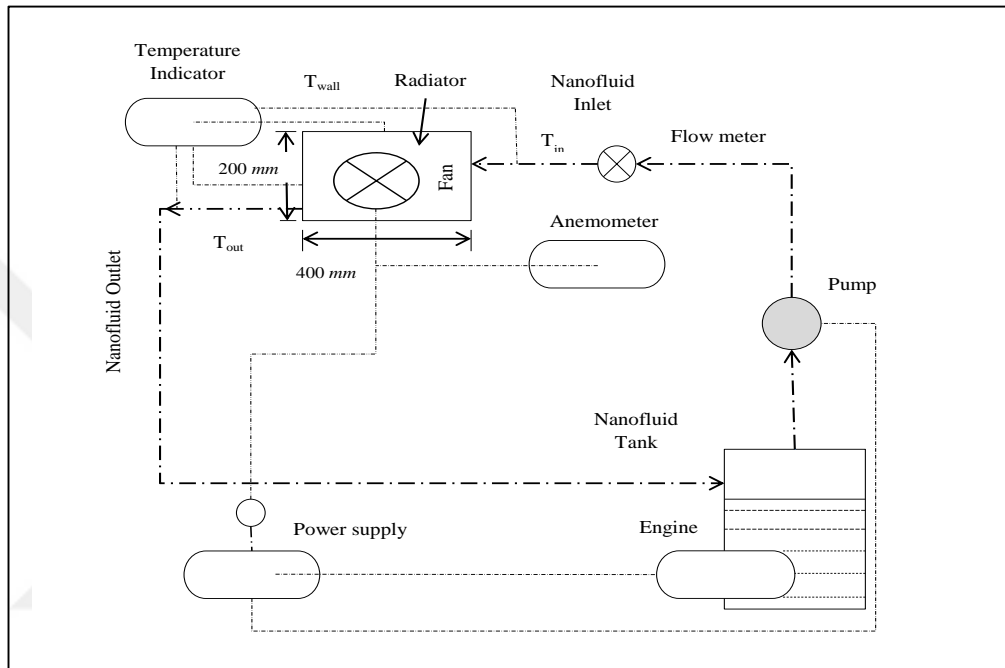


Figure 4.14. Schematic representation of experimental setup.

The measurements of the chosen car radiator are appeared in Table 4.3 and those of the car radiator tubes in Table 4.4. Figure 4.16 appears a schematic representation and measurements of the radiator level tube and Figure 4.17 that of car radiator.

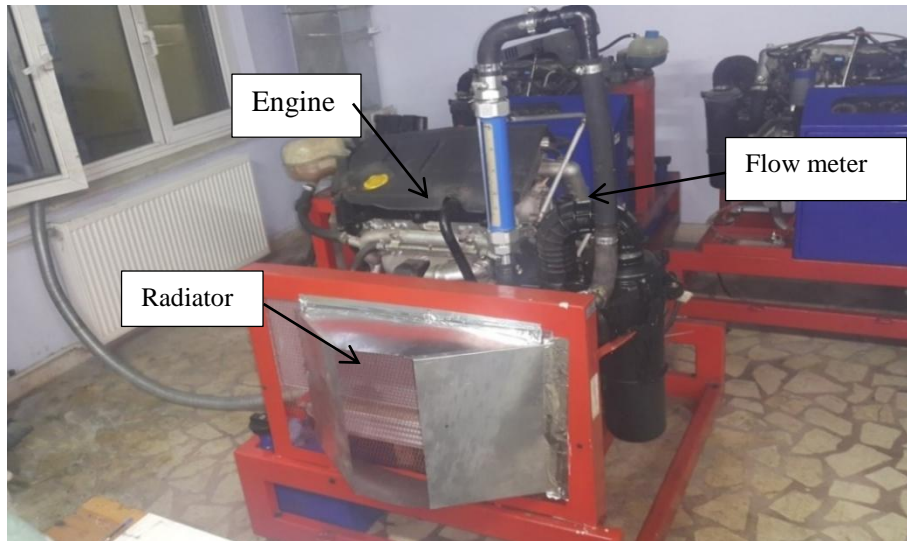


Figure 4.15. Photograph of the real test set up.

Table 4.3. The dimensions of the chosen car radiator.

Length	Height	Width
400mm	200mm	16mm

Table 4.4. The dimensions of the car radiator tubes.

Inward measurement	Material	Number of tube	Spacing	D_h
$18 \times 19.6 \times 295(\text{mm})$	Aluminum	33mm	8.06	3.35mm

D_h is the hydraulic diameter of the tube

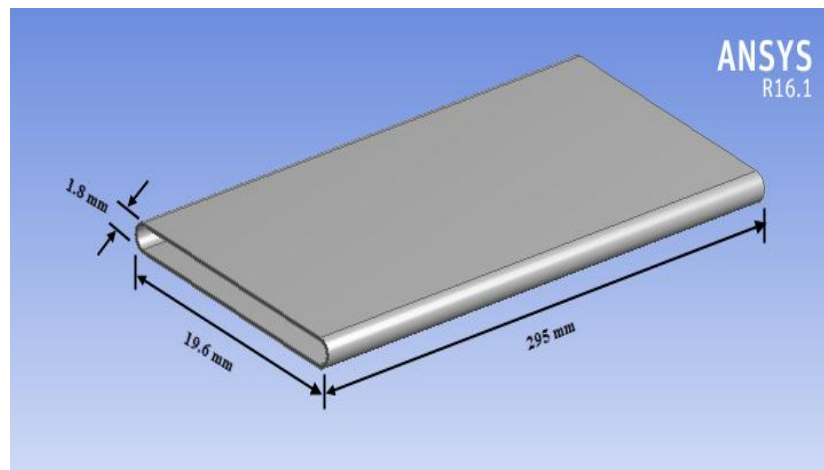


Figure 4.16. Schematic and dimensions of the radiator flat tube.



Figure 4.17. Photograph of car radiator.

Four Pico-thermocouple (show: TC-08) thermometers were utilized to degree the coolant temperature. In expansion, a Testo-thermometer (show: 435) was associated to degree air's input and yield temperatures of back and front surfaces of the radiator (Figure 4.18).



Figure 4.18. Pico-thermocouple (display: TC-08) and Testo-thermometer.

In arrange to dodge any potential issues amid experimentation; the setup was tried to begin with immaculate water (Figure 4.19). This was done to guarantee the steadiness of the test setup and legitimacy of test comes about. The strategy was as takes after: as the nanofluid goes through the pump, it is experienced by tall weights

and shear; in this way gathering is ousted [170]. Furthermore, tall stream rate within the radiator tubes and related channels upgrades the alteration of the nanofluid [64].

After conducting the try with immaculate water, the test framework was released totally and energized to take after the same method for TiO₂-water nanofluid. The nanofluid was utilized in three diverse concentrations: 0.1%, 0.2% and 0.3%, and was pumped through the radiator at diverse stream rates of 0.097m³/h and 0.68m³/h as working liquid. These tests, as in immaculate water case, were rehased and the information were recorded.



Figure 4.19. The experiment with pure water.

CHAPTER 5

RESULTS AND DISCUSSION

5.1. PROPERTIES OF NANOFLUID

Table 5.1 appears a normal specific heat of 0.09 J/kg.K and an increment in particular heat capacity for TiO_2 -water nanofluid as compared to pure water. Additionally, it moreover appears that viscosity and density of TiO_2 -water nanofluid are higher than unadulterated water. Given the truth that viscosity increments with temperature, the viscosity of TiO_2 - water nanofluid is marginally higher than pure water at all temperatures. This could be ascribed to the metal particles in nanofluid which increment the thickness of TiO_2 -water blend. Concurring to past considers [64, 170], as the density of nanofluid increments, there's an inclination for it to flocculate. This diminishes the assortment of homogeneous arrangements since the solidness of low-density nanofluid is generally superior then the nanofluid with a better density (Figure 5.1).



Figure 5.1. Real experimental setup.

Table 5.1. The properties of pure water and TiO₂.

Working fluid	Density <i>kg/m³</i>	Viscosity <i>m.Pa.s</i>				Specific heat <i>J/kg.K</i>	Thermal conductivity <i>W/m.K</i>	
		20 °C	40 °C	60 °C	80 °C			
TiO ₂	4259.8	-	-	-	-	6891	11.69	[143]
Pure water	986.9	0.969	0.738	0.578	0.468	4182.3	0.644	
TiO ₂ - water $\varphi = 1\%$	1043.5	1.02	0.819	0.647	0.529	4522.9	0.729	
TiO ₂ - water $\varphi = 2\%$	1064.9	1.03	0.838	0.677	0.557	4400.9	0.736	
TiO ₂ - water $\varphi = 3\%$	1092.8	1.05	0.868	0.709	0.609	4365.9	0.752	

In Figure 5.2, the dispersion chart of molecule measure within the nanofluid agreeing to escalate gotten by zeta-seizer on distinctive days is appeared. Figures 5.3 and 5.4 appear TEM and SEM pictures individually. The dispersion crest is at a nearly indistinguishable flat position but the escalated increments vertically showing an increment within the populace of totals. It can in this manner be concluded the measure of particles in TiO₂-water nanofluid extended from 30 to 60 nm with an normal estimate of 44 nm.

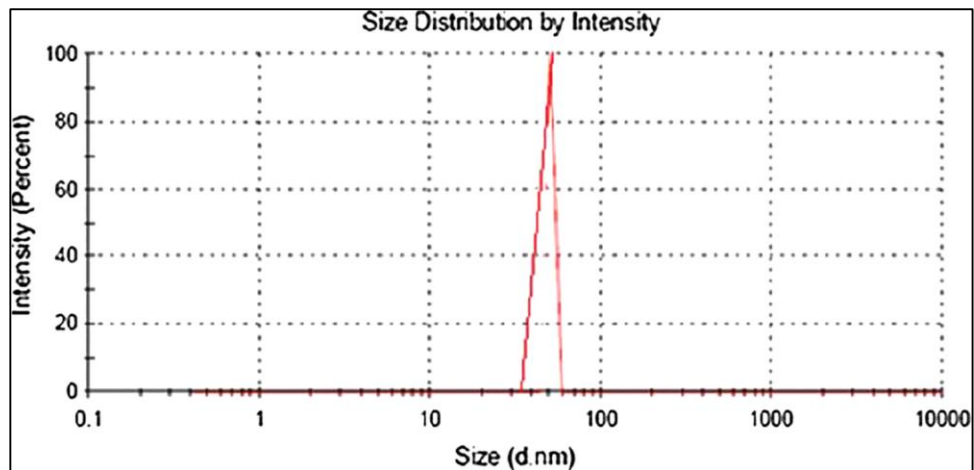


Figure 5.2. Nanoparticles Size distribution.

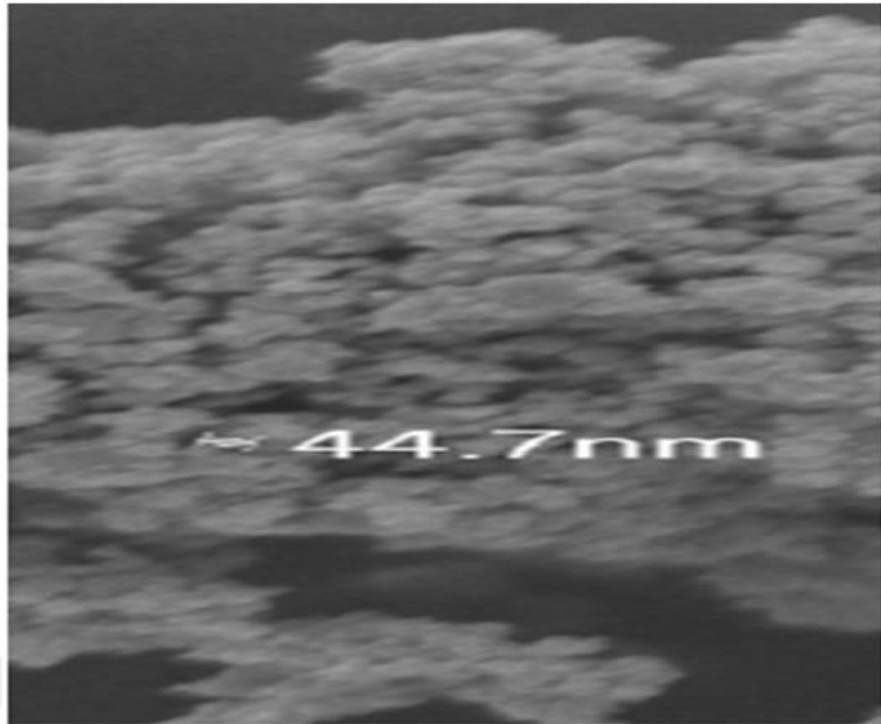


Figure 5.3. SEM morphology of TiO₂.

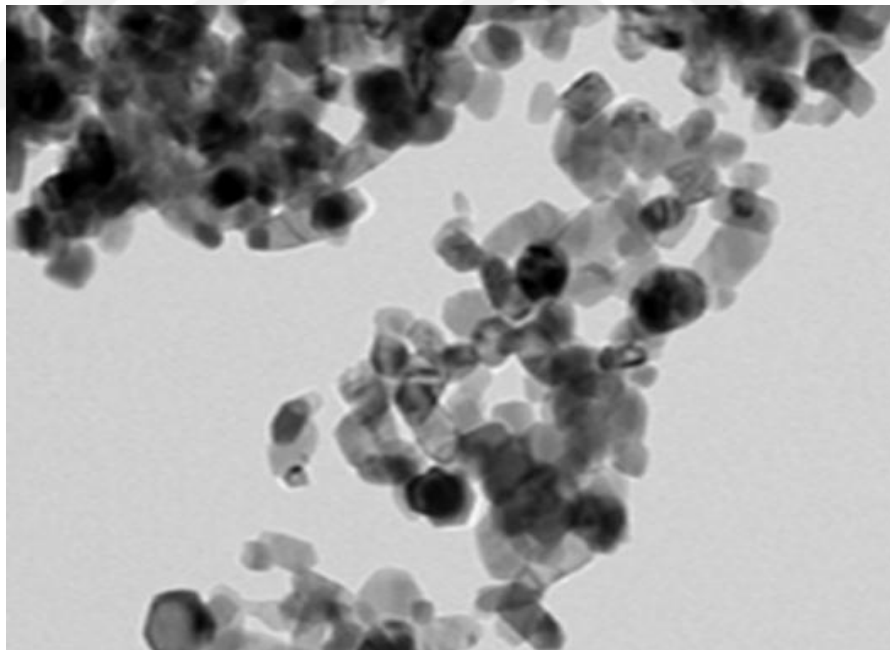


Figure 5.4. TEM of the TiO₂ nanoparticle.

5.2. VISCOSITY

Figure 5.5 appears viscosity for diverse volume concentrations of TiO₂ (0.1, 0.2, and 0.3%) at diverse temperatures in arrange to analyze the impact of temperature on nanofluid consistency. It can be clearly seen that expanding the channel temperature of the nanofluid diminishes its viscosity. Hence, ready to conclude that there exists a coordinate relationship between temperature and thickness for all tests beneath all conditions as compared to the base fluid.

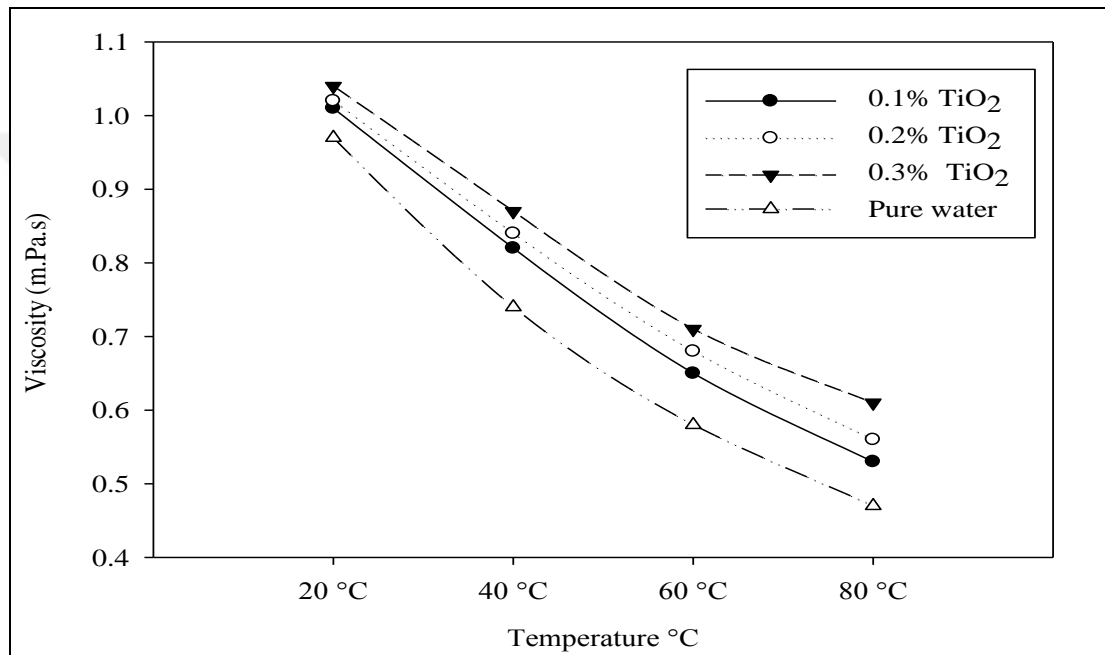


Figure 5.5. Viscosity of TiO₂-water nanofluid at distinctive temperatures.

5.3. THERMAL CONDUCTIVITY

The test values of nanofluid's warm conductivity are in great assention with that show in writing. It can be clearly seen from figure 5.6 that warm conductivity increments in a about straight mold with each incremental increment of volume division. The same figure moreover appears a connection of warm conductivity to volume concentration, once more in great assention with distributed information [44, 171, 172]. Exploratory values of thermal conductivity of TiO₂-water nanofluids appear tall deviation when compared to those assessed from Maxwell Show, but they are in great assention with estimations from Choi Model.

When comes about of TiO_2 and Al_2O_3 [173] frameworks are compared by taking the base liquid as reference, the previous appears essentially higher warm conductivity as compared to the afterward in spite of its bigger molecule estimate (cruel estimate of 44 nm and 13 nm, individually). These come about show that particle's warm conductivity has more impact than molecule measure. Agreeing to a ponder conducted by Eastman et al., (2001), metallic nanoparticle-based nanofluids appear a expansive increment in warm conductivity as compared to the oxide particle-based or base fluid partners [174]. Another ponder appeared that nanofluids thermal conductivity was not influenced by the suspended state of nanoparticles [175].

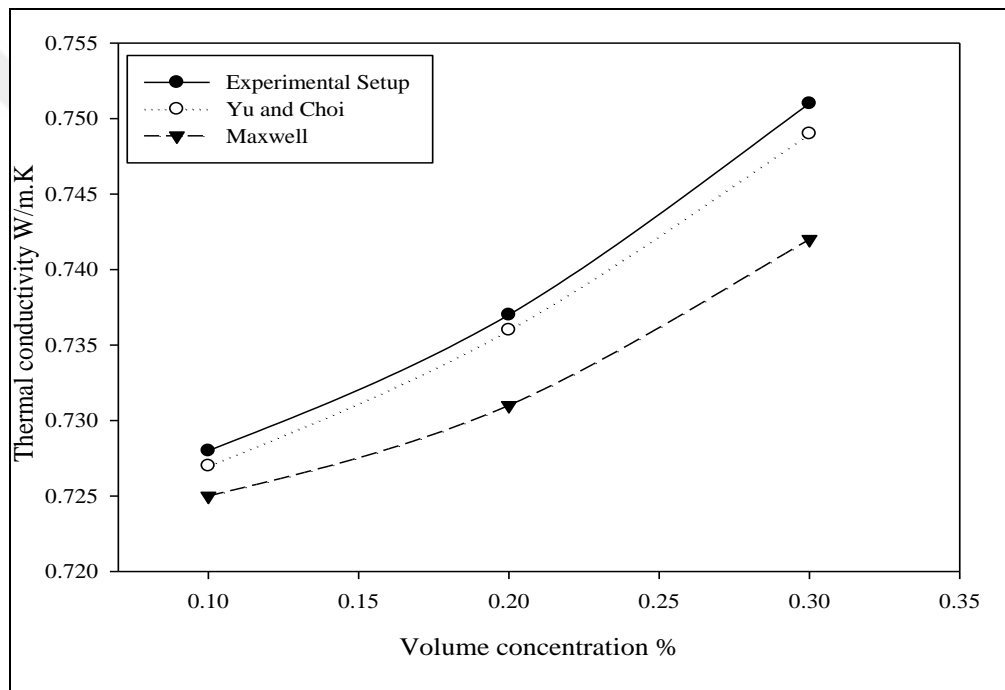


Figure 5.6. Thermal conductivity of TiO_2 nanofluid at distinctive volume fraction.

5.4. HEAT TRANSFER COEFFICIENT

In figures 5.7, nanofluid's generally warm exchange as a work of Reynolds number at consistent stream rate for diverse nanoparticle concentration is appeared. It can be clearly seen from the figure that by and large heat exchange coefficient increments with expanding Reynolds number as compared to the base liquid. The tentatively gotten by and large warm exchange esteem is $2050 \text{ W/m}^2\cdot\text{K}$ for 0.3% TiO_2 -water. These comes about are in great assention with anticipated values but somewhat lower when compared to vehicle radiator in which a multi-walled carbon nanotube

(MWCNT) based on water/ethylene glycol is utilized with nanoparticle volume concentration of 0.5%, and warm exchange coefficient increment from 986.8W/m².K to 2951W/m².K, for Reynolds number from 430 to 1400 (figure 5.8) [176].

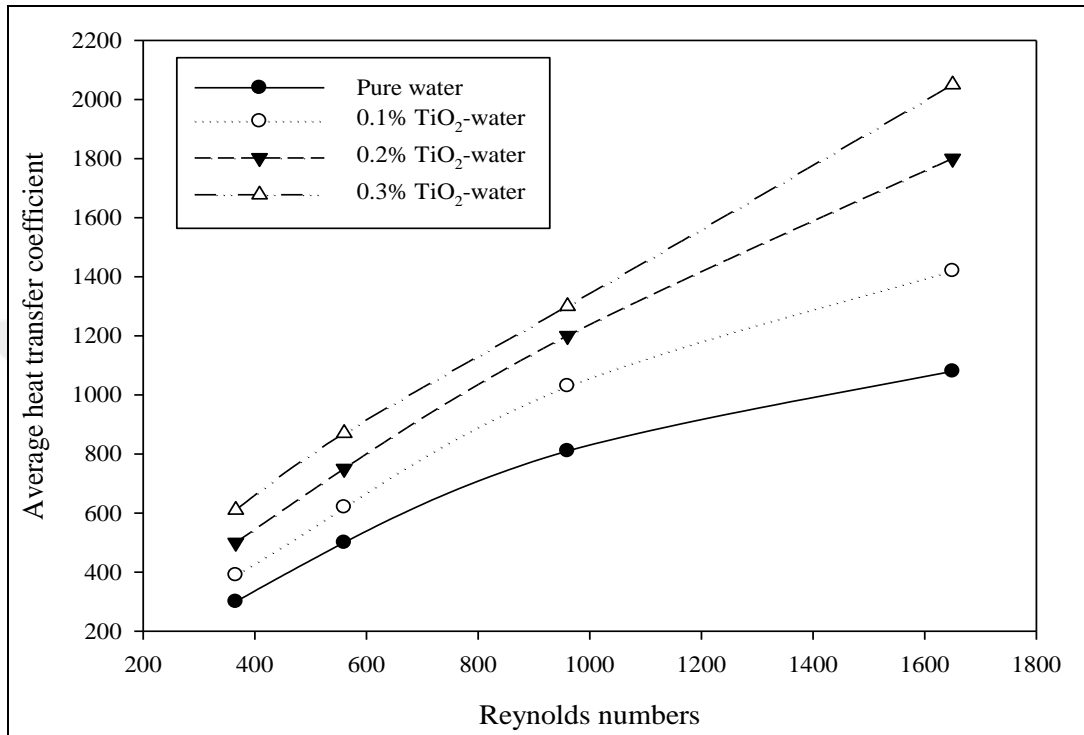


Figure 5.7. Average heat transfer coefficient as a function of Reynolds numbers.

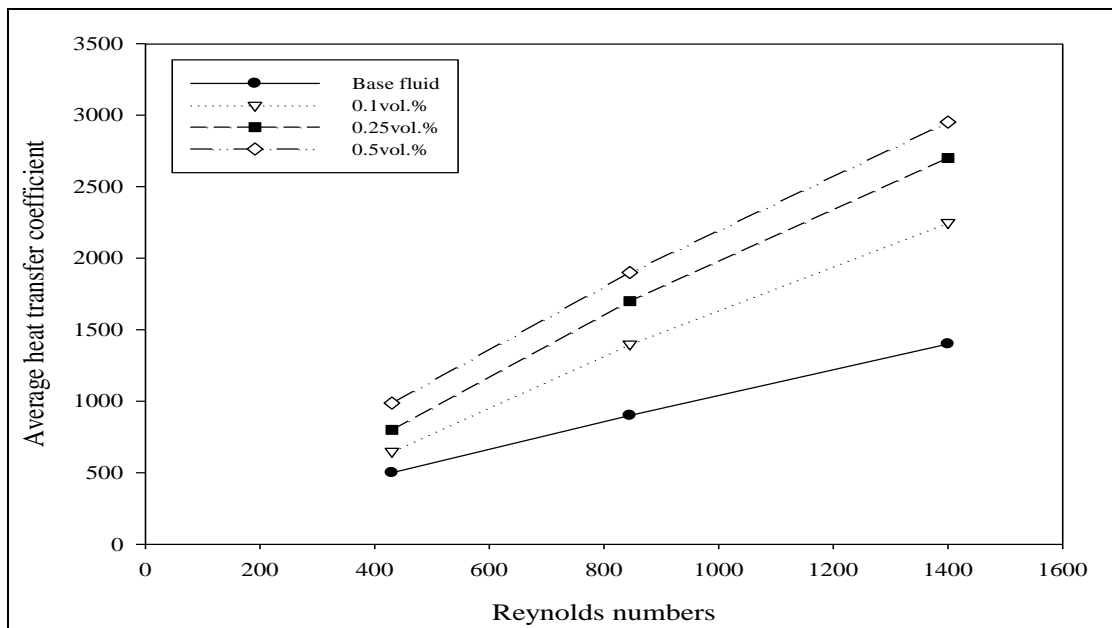


Figure 5.8. The experimental data of MWCNT nanofluid by [176].

5.5. EFFECT OF REYNOLDS NUMBER ON NUSSLETT NUMBER

First, in arrange to decide the relationship between Nusselt and Reynold Numbers, the experiment was carried out in an empty tube and the results were compared with theoretical expectations by using Shah Equation for laminar flow as a control [177]. As the graphs on figure 5.9 show, our experimental results fit nicely with the theoretical ones.

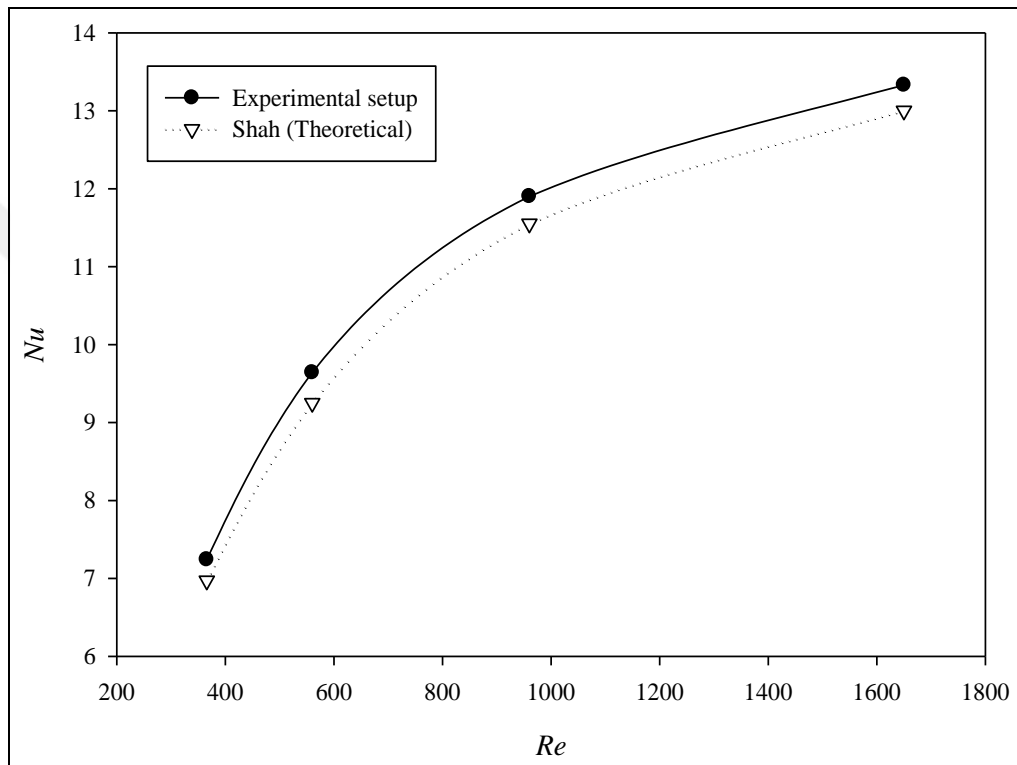


Figure 5.9. Nusselt Number verification.

There have been a number of models aimed at predicting the Nusselt number for nanofluids in laminar regime [162,163,178,180]. According to all these models, Nusselt number is a function of both, Reynold's number and the volume fraction of nanoparticles. Taking these into account, we established the relationship between Nusselt number and these two variables. The relationship between Reynold and Nusselt numbers is represented on figure 5.10. As the figure clearly shows, Nusselt numbers are higher for all nanofluid as compared to pure water. In addition, they also increase dramatically with each increase of Reynold numbers. This behavior of Nusselt number could be because of one or more of the following factors: either the

concealment of the boundary layer, nanoparticles' dispersion in the nanofluid, and/or the viscosity of the nanofluids.

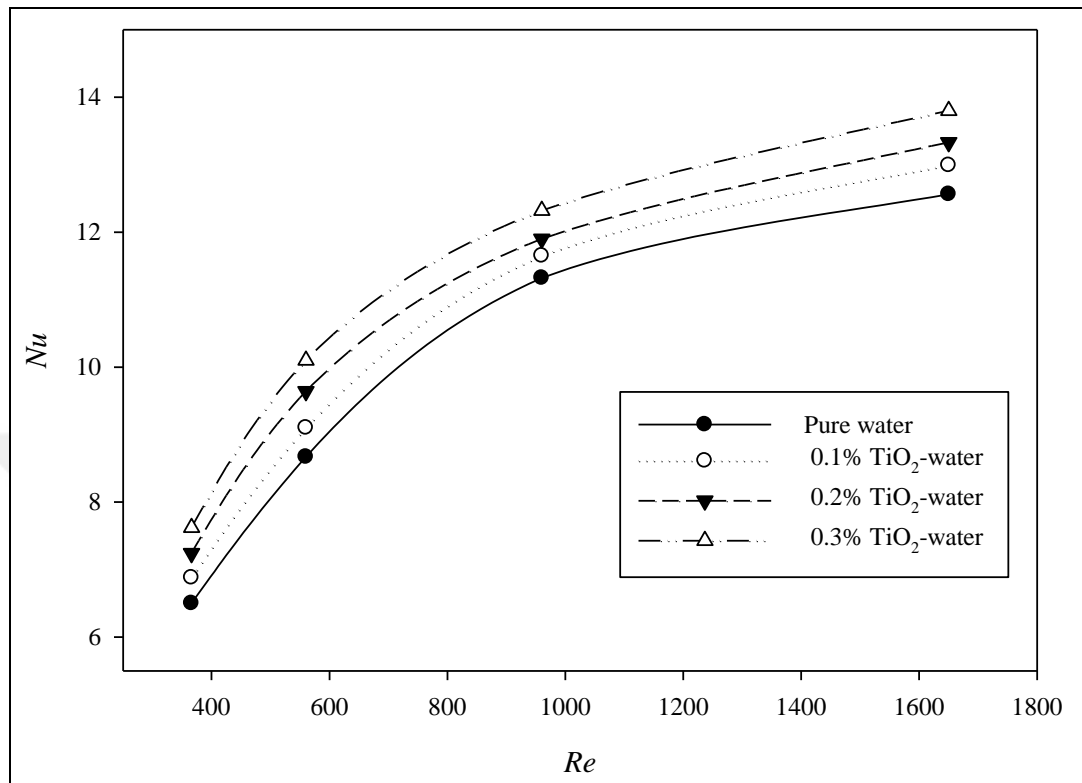


Figure 5.10. Nusselt number as a function of Reynolds numbers.

5.6. EFFECT OF VOLUME FRACTION ON NUSSELT NUMBER

Figure 5.11 represents the relation between Nusselt number and nanoparticles' volume concentration. The figure clearly shows a coordinate relationship between Nusselt number and volume concentration, and as a consequence Reynold's Number. In addition, nanoparticle concentration has an essential role in the rate of heat transfer; whenever nanoparticle concentration is increased, it is followed by an increase in heat transfer coefficient. Adding 0.3% nanoparticle by volume concentration at 80°C leads to a 47.3% increase in heat transfer coefficient as compared to the base fluid. Based on the equation representing the thermophysical properties of fluids, it is known that the calculated properties of nanofluids are different than those of the base fluid, especially the increment in thermal conductivity and density and the slight decrease in their specific heat. There is also a more significant increase in viscosity which favors heat transfer, but when all these

differences are taken into account, they can explain only about 5% of the 47.3% increment in heat exchange coefficient, while the rest is debt to the nanofluid itself.

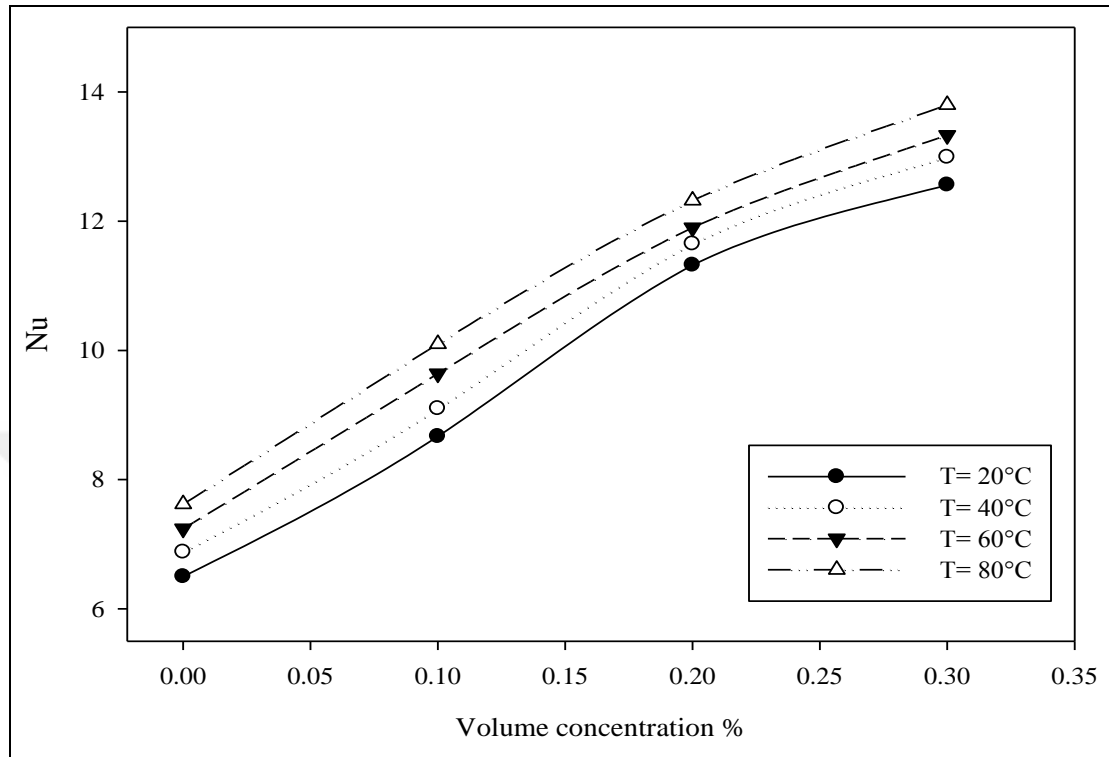


Figure 5.11. Nusselt number as a temperature of volume fractions.

5.7. DENSITY OF NANOFLUID

Figure 5.12 shows the graph for nanofluid density versus temperature. As it can be observed from the graph, the density of water-based TiO_2 nanofluid diminishes with the incrementing temperature. This is due to the expansion in fluid volume as the temperature increases. More to the point, when the temperature is raised from 20 to 80°C, the density of the base fluid increases by 1.9%. However, as the volume concentration of the nanofluid increases, its density increases accordingly, so it always has a higher density than the base fluid, a phenomenon caused by the increased volume of nanoparticles dispensed in it.

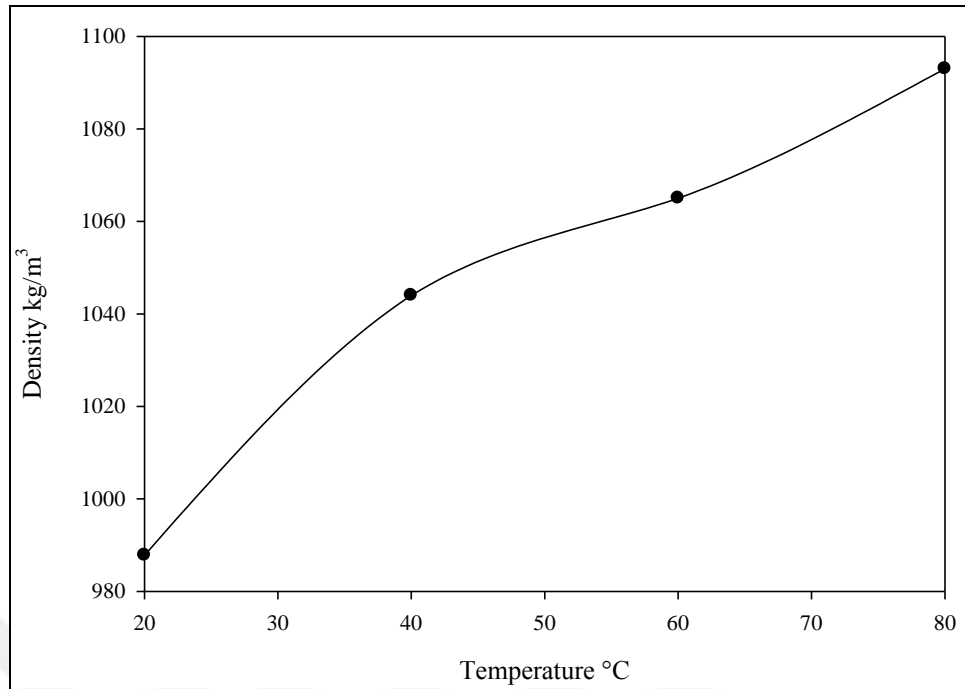


Figure 5.12. Density of water-based TiO₂ nanofluid as a function of temperatures.

Since there are no accessible exploratory information in writing on the radiator coolant nanofluid density, our experimental results were compared with theoretical calculation based on Pak and Cho [181] models for validation. The comparison between theoretical and experimental results is shown on figure 5.13, which clearly shows an almost perfect fit between theoretical calculations and our water-based TiO₂ nanofluid, except for a small deviation consistent throughout all the measurements' range.

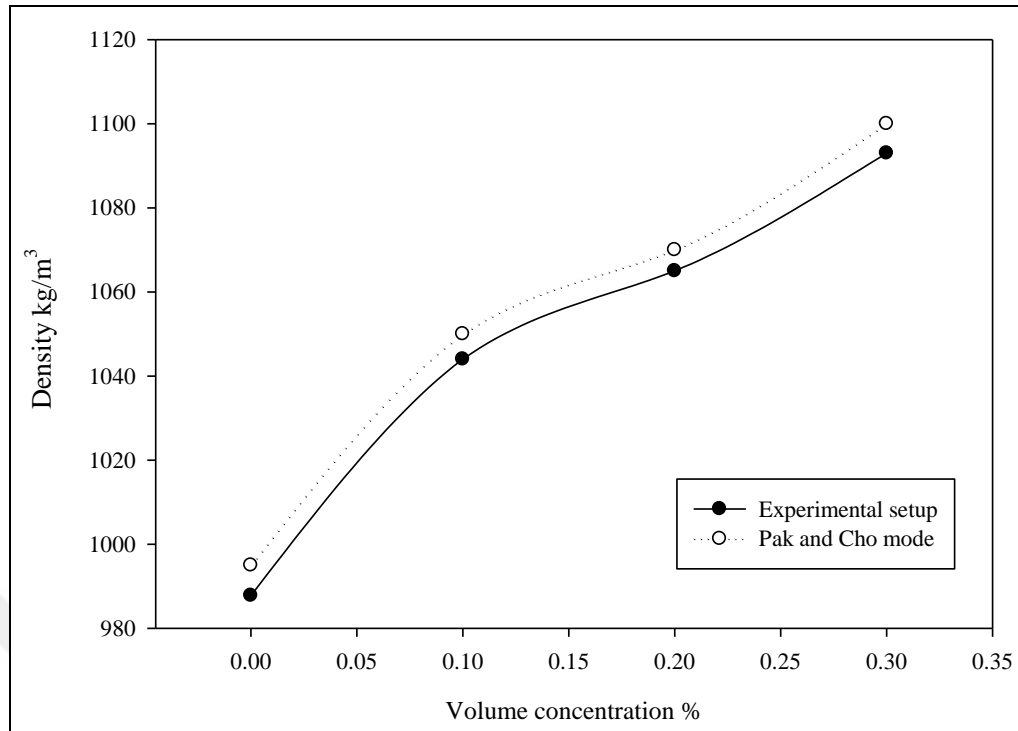


Figure 5.13. Density of TiO₂ nanofluid at different volume fraction.

5.8. SPECIFIC HEAT CAPACITY OF NANOFLUID

Figure 5.14 shows the relationship between specific heat and temperature for our water-based TiO₂ nanofluid. It can be inferred from the graph that the nanofluid's specific heat increases linearly as the temperature increases until 40°C, then it dropped again less dramatically.

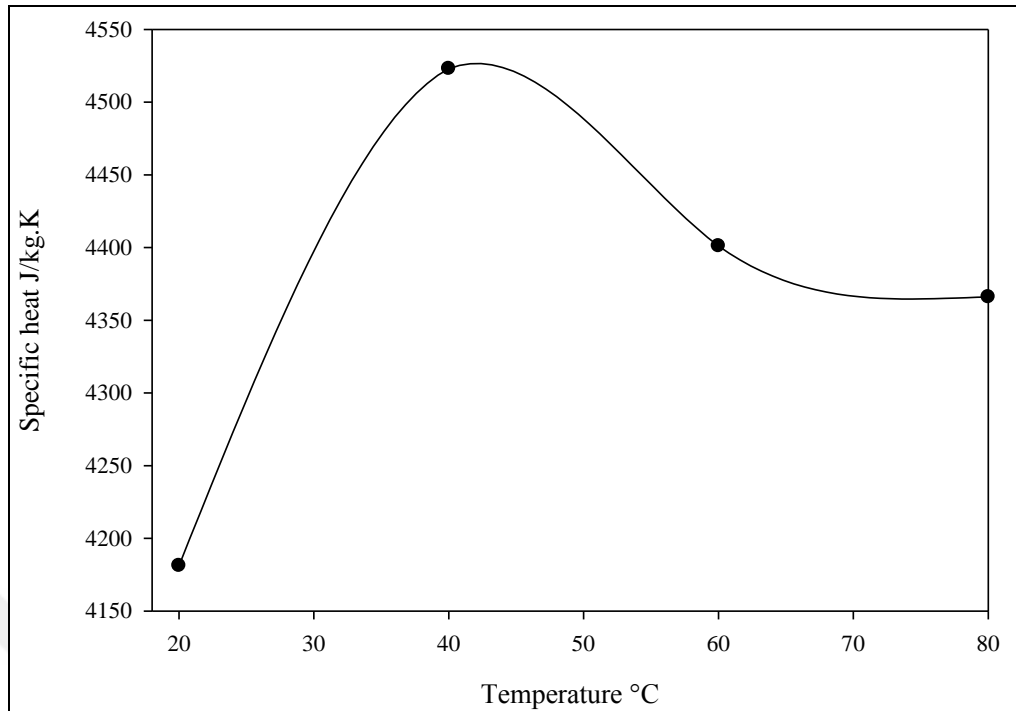


Figure 5.14. Specific heat of TiO_2 - water nanofluid as a function of temperature.

He et al. [182] portrayed two reasons which impact specific heat of nanofluids. To start with, the specific heat of jointly nanoparticles and base liquid impact the scattering. In the event that the nanoparticles' particular specific heat is not exactly the basic fluid, the specific heat of suspension will be diminished.

Figure 5.14 represents the relation between specific heat and particle concentration by volume in the nanofluid for both, theoretical and experimental data. The graphs do not fit perfectly with each other, in contrary; there is a widening gap with expanding volume concentration of the nanoparticles. This may be the best result of the experimental approach where a small amount of sample, a few milligrams equivalent of a fraction of a suspension drop, were used to measure the specific heat, leading to the observed changes.

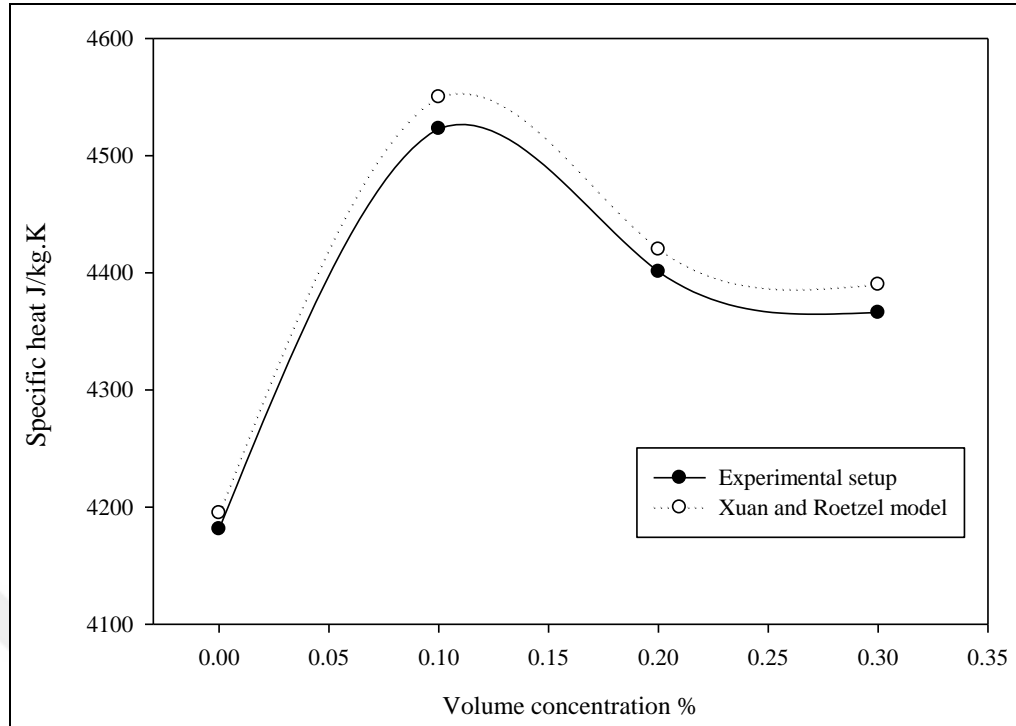


Figure 5.15. Specific heat capacity of TiO₂ nanofluid at different volume fraction.

The graphs on figure 5.15 show the differences between in the relationship between nanofluid's specific heat and nanoparticle volume concentration for experimentally-obtained results and those predicted by Xuan and Roetzel model [183] for 20°C temperature. The graphs clearly shows a decrease in nanofluid's heat capacity as the nanoparticles' volume concentration increases, a phenomenon attributed to the lower specific heat of nanoparticles as mentioned before. However, our experiments showed more decrease than the theoretical results, which means that the impact of nanoparticles on the specific heat of the nanofluid was bigger than expected. The deviation of our experimental results from those expected by the model was 4-5% only.

It is obvious from Figure 5.15 that the specific heat capacity of water-based TiO₂ nanofluid is conversely corresponding to the particles' volume concentration. It implies a smaller demand for heat to raise the nanofluid's temperature when nanoparticle concentration is higher. It also means that the lower the nanofluid's specific heat, the higher the convective heat transfer can become. Figure 5.15 shows that when nanofluid with $\psi = 0.1 \text{ vol}\%$ is used, the specific heat capacity increases compared with that of base fluid, It ought to moreover be famous that adding nanoparticles, in addition to leading to an increment in the heat transfer and

convective heat transfer coefficient, it also enhances the nanofluid's thermal conductivity.



CHAPTER 6

CONCLUSION AND RECOMMENDATIONS

6.1. CONCLUSION

Within the current think about, utilization of TiO₂-water nanofluid's as a cooler in car motor radiator was examined. Based on the exploratory results, TiO₂-water nanofluid offers distant better; a much better; a higher; a stronger; an improved a much better by and large execution than base liquid. The in general heat exchange coefficient of TiO₂ nanofluids in a car radiator was tentatively measured as a work of concentration and temperature. It was found that the nearness of TiO₂ nanoparticle can essentially improve radiator's heat exchange rate in a way subordinate on nanoparticle amount included to the base liquid. Heat transfer coefficient essentially progresses for 0.2% nanoparticle concentration as compared to unadulterated water. Typically due to the truth that TiO₂'s more noteworthy thermal conductivity, perspective proportion, lowers particular gravity, warm resistance and bigger specific zone as compared to pure water.

The results obtained from the experimental investigation were analysed and explained. There was found to be an increment in heat transfer with increment in the temperature, and TiO₂-water nanofluid with 0.2% concentration can improve the viability of car radiator by 47% as compared to 0.1 and 0.3% concentrations and pure water as a coolant.

6.2. RECOMMENDATIONS FOR FUTURE WORK

Based on the results obtained in this study, there are a number of recommendations to be made around future work on the field. We recommend that the experimental

and numerical investigations be extended to include different particle sizes as well as different particles from different materials such as copper, aluminum and platinum. This would make possible a better off understanding of the dependency of heat transfer enhancement on both the particle size and the nature of the material included to the base fluid.

The superiority of nanofluids to conventional fluids in thermal conductivity is a well-known fact, but their increased viscosity due to the nanoparticles is a limiting factor for real-life applications. Therefore, coming up with solutions on this aspect will require a lot of studies and will open new avenues for wider applications of nanofluids, replacing the less efficient conventional counterparts. Putting these recommendations into practice will require more studies and more innovative approaches than we have currently in hand.

Nanotechnology is an emerging multidisciplinary field which combines approaches from many sciences such as natural sciences, engineering, and medicine. It also requires advanced mathematics and statistics for building and testing advanced mathematical models, making inter-disciplinary collaboration indispensable for the future.

As a conclusion, the heat transfer of water is enhanced by up to 8.2% TiO_2 particles are suspended in it. If it is followed by more future studies, this heat transfer enhancement can be optimized for usage in heat exchanger applications in various field

REFERENCES

1. <https://vehiclemaintenanceandrepairs.com/>. *Car Cooling Systems*-101 (2017).
2. Fujishima, A. and K. Honda, Electrochemical photolysis of water at a semiconductor electrode. *nature*, 238, 37 (1972).
3. Kawai, T. and T. Sakata, Conversion of carbohydrate into hydrogen fuel by a photocatalytic process. *Nature*, 286, 474 (1980).
4. Colmenares, J.C., Selective redox photocatalysis: Is there any chance for solar bio-refineries? *Current Opinion in Green and Sustainable Chemistry*, (2018).
5. Sakata, T. and T. Kawai, Heterogeneous photocatalytic production of hydrogen and methane from ethanol and water. *Chemical Physics Letters*, 80(2): 341-344 (1981).
6. MERCER- SMITH, J.A. and D.C. Mauzerall, Photochemistry of porphyrins: a model for the origin of photosynthesis. *Photochemistry and photobiology*, 39(3): 397-405 (1984).
7. Bamwenda, G.R., et al., Photoassisted hydrogen production from a water-ethanol solution: a comparison of activities of Au • TiO₂ and Pt • TiO₂. *Journal of Photochemistry and Photobiology A: Chemistry*, 89(2): 177-189 (1995).
8. Choi, S., Enhancing conductivity of fluids with nanoparticles, *ASME Fluid Eng. Division*, 231: 99-105 (1995).
9. Li, Y., et al., A review on development of nanofluid preparation and characterization. *Powder technology*, 196(2): 89-101 (2009).
10. Das, S.K., et al., Nanofluids: science and technology. *John Wiley & Sons* 331:58-63 (2007).
11. Hong, T.-K., H.-S. Yang, and C. Choi, Study of the enhanced thermal conductivity of Fe nanofluids. *Journal of Applied Physics*, 97(6): 064311 (2005).
12. Mintsa, H.A., et al., New temperature dependent thermal conductivity data for water-based nanofluids. *International Journal of Thermal Sciences*, 48(2): 363-371 (2009).

13. Li, Q. and Y. Xuan, Convective heat transfer and flow characteristics of Cu-water nanofluid. *Science in China Series E: Technological Science*, **45**(4): 408-416 (2002).
14. Masuda, H., A. Ebata, and K. Teramae, Alteration of thermal conductivity and viscosity of liquid by dispersing ultra-fine particles. *Dispersion of Al₂O₃, SiO₂ and TiO₂ ultra-fine particles*. (1993).
15. Vinayan, B., et al., Synthesis of graphene-multiwalled carbon nanotubes hybrid nanostructure by strengthened electrostatic interaction and its lithium ion battery application. *Journal of Materials Chemistry*, **22**(19): 9949-9956 (2012).
16. Choi, Y.K., Y.H. Bae, and S.W. Kim, Block copolymer nanoparticles of ethylene oxide and isobutyl cyanoacrylate. *Macromolecules*, **28**(24): 8419-8421 (1995).
17. Devireddy, S., C.S.R. Mekala, and V.R. Veeredhi, Improving the cooling performance of automobile radiator with ethylene glycol water based TiO₂ nanofluids. *International communications in heat and mass transfer*, **78**: 121-126 (2016).
18. Ali, H.M., et al., Preparation techniques of TiO₂ nanofluids and challenges: a review. *Applied Sciences*, **8**(4): 587 (2018).
19. Kundan, L. and S.S. Mallick, Effect of time dependent morphological parameters of nanoclusters on perikinetic heat conduction and induced micro-convection mechanisms of oxide based nanofluids. *Experimental Heat Transfer*, **31**(3): 251-274 (2018).
20. Choi, S.U. and J.A. Eastman, Enhancing thermal conductivity of fluids with nanoparticles., *Argonne National Lab.*, IL (United States) (1995).
21. Leena, M. and S. Srinivasan, Synthesis and ultrasonic investigations of titanium oxide nanofluids. *Journal of Molecular Liquids*, **206**: 103-109 (2015).
22. Oliveira, L.R., et al., Thermophysical properties of TiO₂-PVA/water nanofluids. *International Journal of Heat and Mass Transfer*, **115**: 795-808 (2017).
23. Duangthongsuk, W. and S. Wongwises, An experimental study on the heat transfer performance and pressure drop of TiO₂-water nanofluids flowing under a turbulent flow regime. *International Journal of Heat and Mass Transfer*, **53**(1): 334-344 (2016).
24. Qin, Z.-B., et al., One-pot synthesis of ultrafine TiO₂ nanoparticles with enhanced thermal conductivity for nanofluid applications. *Advanced Powder Technology*, **27**(2): 299-304 (2016).

25. Wei, B., C. Zou, and X. Li, Experimental investigation on stability and thermal conductivity of diathermic oil based TiO₂ nanofluids. *International Journal of Heat and Mass Transfer*, 104: 537-543 (2017).
26. Naina, H.K., et al., Viscosity and specific volume of TiO₂/water nanofluid. *Journal of Nanofluids*, 1(2): 161-165 (2012).
27. Reddy, M.C.S. and V.V. Rao, Experimental studies on thermal conductivity of blends of ethylene glycol-water-based TiO₂ nanofluids. *International Communications in Heat and Mass Transfer*, 46: 31-36 (2013).
28. Hojjat, M., et al., Thermal conductivity of non-Newtonian nanofluids: Experimental data and modeling using neural network. *International Journal of Heat and Mass Transfer*, 4(5): 1017-1023 (2011).
29. Abdulwahab, M.I., S.M. Thahab, and A.H. Dhiaa, Experimental study of thermophysical properties of TiO₂ nanofluid. *Iraqi J. Chem. Petrol. Eng.*, 17(2): 1-6 (2016).
30. Najiha, M.S., M.M. Rahman, and K. Kadirgama, Performance of water-based TiO₂ nanofluid during the minimum quantity lubrication machining of aluminium alloy, AA6061-T6. *Journal of Cleaner Production*, 135: 1623-1636 (2016).
31. Longo, G.A. and C. Zilio, Experimental measurement of thermophysical properties of oxide-water nano-fluids down to ice-point. *Experimental Thermal and Fluid Science*, 35(7): 1313-1324 (2011).
32. Azmi, W.H., et al., Heat transfer and friction factor of water based TiO₂ and SiO₂ nanofluids under turbulent flow in a tube. *International Communications in Heat and Mass Transfer*, 59: 30-38 (2014).
33. Yang, L. and Y. Hu, Toward TiO₂ Nanofluids—Part 1: Preparation and Properties. *Nanoscale research letters*, 12(1): 417 (2017).
34. Yang, L. and Y. Hu, Toward TiO₂ Nanofluids—Part 2: Applications and Challenges. *Nanoscale research letters*, 12(1): 446 (2017).
35. Yang, L., et al., Dynamic characteristics of an environment-friendly refrigerant: ammonia-water based TiO₂ nanofluids. *International Journal of Refrigeration*, 82: 366-380 (2017).
36. Xuan, Y. and Q. Li, Heat transfer enhancement of nanofluids. *International Journal of heat and fluid flow*, 21(1): 58-64 (2000).
37. Sundar, L.S., et al., Experimental thermal conductivity of ethylene glycol and water mixture based low volume concentration of Al₂O₃ and CuO nanofluids. *International Communications in Heat and Mass Transfer*, 41: 41-46 (2013) .

38. Hamzah, M.H., et al., Factors affecting the performance of hybrid nanofluids: a comprehensive review. *International Journal of Heat and Mass Transfer*, 115: 630-646 (2017).
39. Colangelo, G., et al., Cooling of electronic devices: Nanofluids contribution. *Applied Thermal Engineering*, 127: 421-435 (2017).
40. Milanese, M., et al., An investigation of layering phenomenon at the liquid–solid interface in Cu and CuO based nanofluids. *International Journal of Heat and Mass Transfer*, 103: 564-571 (2016).
41. COLANGELO, G., M. MILANESE, and A. DE RISI, NUMERICAL SIMULATION OF THERMAL EFFICIENCY OF AN INNOVATIVE Al₂O₃ NANOFLUID SOLAR THERMAL COLLECTOR. *THERMAL SCIENCE*, 21(6B): 2769-2779 (2017).
42. Alawi, O.A., et al., Thermal conductivity and viscosity models of metallic oxides nanofluids. *International Journal of Heat and Mass Transfer*, 116: 1314-1325 (2018).
43. Colangelo, G., et al., Thermal conductivity, viscosity and stability of Al₂O₃-diathermic oil nanofluids for solar energy systems. *Energy*, 95: 124-136 (2016).
44. Gu, B., et al., Thermal conductivity of nanofluids containing high aspect ratio fillers. *International Journal of Heat and Mass Transfer*. 64: 108-114 (2013).
45. Yang, L., et al., Recent developments on viscosity and thermal conductivity of nanofluids. *Powder Technology*, 317: 348-369 (2017).
46. Sidik, N.A.C., M.N.A.W.M. Yazid, and R. Mamat, Recent advancement of nanofluids in engine cooling system. *Renewable and Sustainable Energy Reviews*,. 75: 137-144 (2017).
47. Moradi, H., et al., Influence of the geometry of cylindrical enclosure on natural convection heat transfer of Newtonian nanofluids. *Chemical Engineering Research and Design*, 94: 673-680 (2015).
48. Hu, Y., et al., Experimental and numerical investigation on natural convection heat transfer of TiO₂–water nanofluids in a square enclosure. *Journal of Heat Transfer*, 136(2): 022502 (2014).
49. Ganji, D. and A. Malvandi, Natural convection of nanofluids inside a vertical enclosure in the presence of a uniform magnetic field. *Powder Technology*, 263: 50-57 (2014).

50. Sheikholeslami, M., H. Ashorynejad, and P. Rana, Lattice Boltzmann simulation of nanofluid heat transfer enhancement and entropy generation. *Journal of Molecular Liquids*, 214: 86-95 (2016).
51. Ouyahia, S.-E., Y.K. Benkahla, and N. Labsi, Numerical study of the hydrodynamic and thermal proprieties of titanium dioxide nanofluids trapped in a triangular geometry. *Arabian Journal for Science and Engineering*, 41(5): 1995-2009 (2016).
52. Nieh, H.-M., T.-P. Teng, and C.-C. Yu, Enhanced heat dissipation of a radiator using oxide nano-coolant. *International Journal of Thermal Sciences*, 77: 252-261 (2014).
53. Mohammed, H., et al., Heat transfer and fluid flow characteristics in microchannels heat exchanger using nanofluids: a review. *Renewable and Sustainable Energy Reviews*, 15(3): 1502-1512 (2011).
54. Leong, K., et al., Performance investigation of an automotive car radiator operated with nanofluid-based coolants (nanofluid as a coolant in a radiator). *Applied Thermal Engineering*, 30(17-18): 2685-2692 (2010).
55. Ebrahimi, M., et al., Experimental investigation of force convection heat transfer in a car radiator filled with SiO₂-water nanofluid. *IJE Trans B: Appl*, 27(2): 333-340 (2014).
56. Arani, A.A. and J. Amani, Experimental investigation of diameter effect on heat transfer performance and pressure drop of TiO₂-water nanofluid. *Experimental Thermal and Fluid Science*, 44: 520-533 (2013).
57. Sheikhzadeh, G., M. Hajilou, and H. Jafarian, Analysis of thermal performance of a car radiator employing nanofluid. *Int. J. Mechanical Engineering and Applications*, 2(4): 47-51 (2013).
58. Davarnejad, R. and R.M. Ardehali, Modeling of TiO₂-water nanofluid effect on heat transfer and pressure drop. *International Journal of Engineering-Transactions B: Applications*, 27(2): 195-202 (2013).
59. Hussein, A.M., et al., The effect of cross sectional area of tube on friction factor and heat transfer nanofluid turbulent flow. *International Communications in Heat and Mass Transfer*, 47: 49-55 (2013).
60. Mohammed, H., et al., Influence of nanofluids on parallel flow square microchannel heat exchanger performance. *International Communications in Heat and Mass Transfer*, 38(1): 1-9 (2011).
61. Reddy, M.C.S. and V.V. Rao, Experimental investigation of heat transfer coefficient and friction factor of ethylene glycol water based TiO₂ nanofluid in double pipe heat exchanger with and without helical coil inserts.

- International Communications in Heat and Mass Transfer*, 50: 68-76 (2014).
62. Eiamsa-ard, S. and K. Kiatkittipong, Heat transfer enhancement by multiple twisted tape inserts and TiO₂/water nanofluid. *Applied Thermal Engineering*, 70(1): 896-924 (2014).
 63. Hussein, A.M., et al., Heat transfer augmentation of a car radiator using nanofluids. *Heat and Mass Transfer*, 50(11): 1553-1561 (2014).
 64. Minea, A.A., *Advances in New Heat Transfer Fluids: From Numerical to Experimental Techniques*. **CRC Press** (2017).
 65. Xian-Ju, W., et al., Stability of TiO₂ and Al₂O₃ nanofluids. *Chinese Physics Letters*, 28(8): 086601 (2011).
 66. Li, X., C. Zou, and A. Qi, Experimental study on the thermo-physical properties of car engine coolant (water/ethylene glycol mixture type) based SiC nanofluids. *International Communications in Heat and Mass Transfer*, 77: 159-164 (2016).
 67. Maxwell, J., *Electricity and Magnetism* Clarendon Press. **UK, Oxford**, (1873).
 68. Xuan, Y., Q. Li, and W. Hu, Aggregation structure and thermal conductivity of nanofluids. *AIChE Journal*, 49(4): 1038-1043 (2003).
 69. Lee, D., Thermophysical properties of interfacial layer in nanofluids. *Langmuir*, 23(11): 6011-6018 (2007).
 70. Wang, X.-Q. and A.S. Mujumdar, Heat transfer characteristics of nanofluids: a review. *International journal of thermal sciences*, 46(1): 1-19 (2007).
 71. Xie, H., et al., Dependence of the thermal conductivity of nanoparticle-fluid mixture on the base fluid. *Journal of Materials Science Letters*, 21(19): 1469-1471 (2002).
 72. Hasselman, D. and L.F. Johnson, Effective thermal conductivity of composites with interfacial thermal barrier resistance. *Journal of composite materials*, 21(6): 508-515 (1987).
 73. Chopkar, M., et al., Effect of particle size on thermal conductivity of nanofluid. *Metallurgical and Materials Transactions A*, 39(7): 1535-1542 (2008).
 74. Liu, M.-S., et al., Enhancement of thermal conductivity with carbon nanotube for nanofluids. *International communications in heat and mass transfer*, 32(9): 1202-1210 (2005).

75. Aybar, H.Ş., et al., A review of thermal conductivity models for nanofluids. *Heat Transfer Engineering*, 36(13): 1085-1110 (2015).
76. Huminic, G. and A. Huminic, Application of nanofluids in heat exchangers: a review. *Renewable and Sustainable Energy Reviews*, 16(8): 5625-5638 (2012).
77. Tripathi, D. and O.A. Bég, A study on peristaltic flow of nanofluids: Application in drug delivery systems. *International Journal of Heat and Mass Transfer*, 70: 61-70 (2014).
78. Bala, V., E. Duesterwald, and S. Banerjia, Dynamo: a transparent dynamic optimization system. *Acm Sigplan Notices*, 46(4):41-52 (2011).
79. Peyghambarzadeh, S.M., et al., Experimental study of overall heat transfer coefficient in the application of dilute nanofluids in the car radiator. *Applied Thermal Engineering*, 52(1): 8-16 (2013).
80. Wong, K.V. and O. De Leon, Applications of nanofluids: current and future. *Advances in Mechanical Engineering*, 2: 519659 (2010).
81. Das, S.K., S.U. Choi, and H.E. Patel, Heat transfer in nanofluids—a review. *Heat transfer engineering*, 27(10): 3-19 (2006).
82. Kim, S., et al., *Study of pool boiling and critical heat flux enhancement in nanofluids*. (2007).
83. Shawgo, R.S., et al., BioMEMS for drug delivery. *Current Opinion in Solid State and Materials Science*, 6(4): 329-334 (2007).
84. Kim, J.H., et al., *A benchmark study on the thermal conductivity of nanofluids*. (2009).
85. Sundar, L.S., et al., Empirical and theoretical correlations on viscosity of nanofluids: a review. *Renewable and sustainable energy reviews*, 25: 670-686 (2013).
86. Hwang, Y.-j., et al., Stability and thermal conductivity characteristics of nanofluids. *Thermochimica Acta*, 9 455(1-2): 70-74 (2007).
87. Wang, X.-j. and D.-s. Zhu, Investigation of pH and SDBS on enhancement of thermal conductivity in nanofluids. *Chemical Physics Letters*, 9 470(1-3): 9. 107-111(2009).
88. Yang, L., et al., Preparation and stability of Al₂O₃ nano-particle suspension of ammonia–water solution. *Applied Thermal Engineering*, 31(17-18): 3643-3647 (2011).

89. Anandan, D. and K. Rajan, Synthesis and stability of cupric oxide-based nanofluid: A novel coolant for efficient cooling. *Asian Journal of Scientific Research*, 5(4): 218-227 (2012).
90. Chopkar, M., et al., Pool boiling heat transfer characteristics of ZrO₂-water nanofluids from a flat surface in a pool. *Heat and Mass Transfer*, 44(8): 999-1004 (2008).
91. Vekas, L., D. Bica, and M.V. Avdeev, Magnetic nanoparticles and concentrated magnetic nanofluids: synthesis, properties and some applications. *China Particuology*, 5(1-2): 43-49 (2007).
92. Vékás, L., D. Bica, and O. Marinica, Magnetic nanofluids stabilized with various chain length surfactants. *Romanian Reports in Physics*, 58(3): 257 (2006).
93. Zhu, H., et al., Preparation and thermal conductivity of suspensions of graphite nanoparticles. *Carbon*, 45(1): 226-228 (2007).
94. Sharma, S. and S.M. Gupta, Preparation and evaluation of stable nanofluids for heat transfer application: a review. *Experimental Thermal and Fluid Science*, 79: 202-212 (2016).
95. Li, X., D. Zhu, and X. Wang, Evaluation on dispersion behavior of the aqueous copper nano-suspensions. *Journal of colloid and interface science*, 310(2): 456-463 (2007).
96. Wen, D. and Y. Ding, Formulation of nanofluids for natural convective heat transfer applications. *International Journal of Heat and Fluid Flow*, 26(6): 855-864(2005).
97. Kumar, M., Preparation and Characterization of Nanofluids. *Citeseer*, (2012).
98. Li, J., Z. Li, and B. Wang, Experimental viscosity measurements for copper oxide nanoparticle suspensions. *Tsinghua Science and Technology*, 7(2): 198-201(2002).
99. Nguyen, C., et al., Temperature and particle-size dependent viscosity data for water-based nanofluids-hysteresis phenomenon. *International Journal of Heat and Fluid Flow*, 28(6): 1492-1506(2007).
100. Ding, Y., et al., Heat transfer of aqueous suspensions of carbon nanotubes (CNT nanofluids). *International Journal of Heat and Mass Transfer*, 649(1-2): 240-250(2006).
101. Chen, L., et al., Nanofluids containing carbon nanotubes treated by mechanochemical reaction. *Thermochimica Acta*, 477(1-2): 21-24 (2008).

102. Lee, S.W., et al., Investigation of viscosity and thermal conductivity of SiC nanofluids for heat transfer applications. *International Journal of Heat and Mass Transfer*, 54(1-3): 433-438(2011).
103. Cabaleiro, D., et al., Rheological and volumetric properties of TiO₂-ethylene glycol nanofluids. *Nanoscale research letters*, 8(1): 286 (2013).
104. Chen, H., et al., *Rheological behaviour of ethylene glycol based titania nanofluids*. Chemical physics letters, **444**(4-6): 333-337 (2007).
105. Prasher, R., et al., Measurements of nanofluid viscosity and its implications for thermal applications. *Applied physics letters*, 89(13): 133108 (2006).
106. Anoop, K., et al., Rheological and flow characteristics of nanofluids: influence of electroviscous effects and particle agglomeration. *Journal of Applied Physics*, 106(3): 034909 (2009).
107. Duangthongsuk, W. and S. Wongwises, Measurement of temperature-dependent thermal conductivity and viscosity of TiO₂-water nanofluids. *Experimental thermal and fluid science*, 33(4): 706-714 (2009).
108. Turgut, A., et al., Thermal conductivity and viscosity measurements of water-based TiO₂ nanofluids. *International Journal of Thermophysics*, 30(4): 1213-1226 (2009).
109. Kole, M. and T. Dey, Viscosity of alumina nanoparticles dispersed in car engine coolant. *Experimental Thermal and Fluid Science*, 34(6): 677-683 (2010).
110. Lugo, L., J. Legido, and M. Piñeiro, Enhancement of thermal conductivity and volumetric behavior of Fe₃O₄ nanofluids MJ Pastoriza-Gallego. *J Appl Phys*, 110: 014309 (2011).
111. Namburu, P., et al., Experimental investigation of viscosity and specific heat of silicon dioxide nanofluids. *Micro & Nano Letters*, 2(3): 67-71 (2007).
112. Namburu, P.K., et al., Viscosity of copper oxide nanoparticles dispersed in ethylene glycol and water mixture. *Experimental Thermal and Fluid Science*, 32(2): 397-402 (2007).
113. Naik, M., et al., Experimental investigation into rheological property of copper oxide nanoparticles suspended in propylene glycol–water based fluids. *ARPJ Journal of Engineering and Applied Sciences*, 5(6): 29-34 (2010).
114. Das, S.K., N. Putra, and W. Roetzel, Pool boiling characteristics of nanofluids. *International journal of heat and mass transfer*, 46(5): 851-862(2003).

115. Kim, D., et al., Production and characterization of carbon nano colloid via one-step electrochemical method. *Journal of nanoparticle research*,10(7): 1121-1128(2008).
116. Chevalier, J., O. Tillement, and F. Ayela, Rheological properties of nanofluids flowing through microchannels. *Applied physics letters*, 91(23): 233103(2007).
117. Hong, K., T.-K. Hong, and H.-S. Yang, Thermal conductivity of Fe nanofluids depending on the cluster size of nanoparticles. *Applied Physics Letters*, 88(3): 031901(2006).
118. Zhu, H., et al., Effects of nanoparticle clustering and alignment on thermal conductivities of Fe₃O₄ aqueous nanofluids. *Applied Physics Letters*, 89(2): 023123(2006).
119. Prasher, R., P.E. Phelan, and P. Bhattacharya, Effect of aggregation kinetics on the thermal conductivity of nanoscale colloidal solutions (nanofluid). *Nano letters*, 6(7): 1529-1534(2006).
120. Sundar, L.S., M.K. Singh, and A.C. Sousa, Thermal conductivity of ethylene glycol and water mixture based Fe₃O₄ nanofluid. *International communications in heat and mass transfer*, 49: 17-24(2013).
121. Mahbubul, I.M., R. Saidur, and M.A. Amalina, Influence of particle concentration and temperature on thermal conductivity and viscosity of Al₂O₃/R141b nanorefrigerant. *International Communications in Heat and Mass Transfer*. 43: 100-104(2013).
122. Yiamsawas, T., et al., Experimental studies on the viscosity of TiO₂ and Al₂O₃ nanoparticles suspended in a mixture of ethylene glycol and water for high temperature applications. *Applied energy*, 111: 40-45(2013).
123. Yu, W., et al., Review and comparison of nanofluid thermal conductivity and heat transfer enhancements. *Heat transfer engineering*, 29(5): 432-460 (2008).
124. Murshed, S., K. Leong, and C. Yang, Enhanced thermal conductivity of TiO₂—water based nanofluids. *International Journal of thermal sciences*. 44(4): 367-373 (2005).
125. Assael, M., et al., Thermal conductivity enhancement in aqueous suspensions of carbon multi-walled and double-walled nanotubes in the presence of two different dispersants. *International Journal of Thermophysics*. 26(3): 647-664 (2005).
126. Li, C.H. and G. Peterson, Experimental investigation of temperature and volume fraction variations on the effective thermal conductivity of

- nanoparticle suspensions (nanofluids). *Journal of Applied Physics*,. 99(8). 084314 (2006).
127. Beck, M.P., et al., The effect of particle size on the thermal conductivity of alumina nanofluids. *Journal of Nanoparticle Research*, 11(5): 1129-1136 (2009).
 128. Ju, Y.S., J. Kim, and M.-T. Hung, Experimental study of heat conduction in aqueous suspensions of aluminum oxide nanoparticles. *Journal of Heat Transfer*. 130(9): 092403(2008).
 129. Ueki, Y., K. Ueda, and M. Shibahara, Thermal conductivity of suspension fluids of fine carbon particles: Influence of sedimentation and aggregation diameter. *International Journal of Heat and Mass Transfer*. 127: 138-144 (2018).
 130. Zeng, J.-L., et al., Study on reduction of thermal conductivity of composite phase change material using Cu nanoparticles. *Energy Sources, Part A: Recovery, Utilization, and Environmental Effects*: 1-6 (2018).
 131. Özerinç, S., S. Kakaç, and A.G. Yazıcıoğlu, Enhanced thermal conductivity of nanofluids: a state-of-the-art review. *Microfluidics and Nanofluidics*. 8(2): 145-170 (2010).
 132. Meyer, J.P., et al., The viscosity of nanofluids: a review of the theoretical, empirical, and numerical models. *Heat Transfer Engineering*. 37(5): 387-421(2016).
 133. Teng, T.-P. and C.-C. Yu, Heat dissipation performance of MWCNTs nano-coolant for vehicle. *Experimental Thermal and Fluid Science*.49:22-30(2013).
 134. Sarkar, J. and R. Tarodiya, Performance analysis of louvered fin tube automotive radiator using nanofluids as coolants. *International Journal of Nanomanufacturing*. 9(1): 51-65 (2013).
 135. Hussein, A.M., et al., Heat transfer augmentation of a car radiator using nanofluids. *Heat and Mass Transfer*. 50(11):1553-1561 (2014).
 136. Hussein, A.M., et al., Heat transfer enhancement using nanofluids in an automotive cooling system. *International Communications in Heat and Mass Transfer*. 53: 195-202 (2014).
 137. Etefaghi, E.-o.-l., et al., Preparation and thermal properties of oil-based nanofluid from multi-walled carbon nanotubes and engine oil as nano-lubricant. *International Communications in Heat and Mass Transfer*. 46: 142-147(2013).

138. Kole, M. and T. Dey. Experimental investigation on the thermal conductivity and viscosity of engine coolant based alumina nanofluids. in *AIP Conference Proceedings*. AIP (2010).
139. Abbasi, M. and Z. Baniamerian, Analytical simulation of flow and heat transfer of two-phase nanofluid (stratified flow regime). *International Journal of Chemical Engineering*, (2014).
140. Delavari, V. and S.H. Hashemabadi, CFD simulation of heat transfer enhancement of Al₂O₃/water and Al₂O₃/ethylene glycol nanofluids in a car radiator. *Applied Thermal Engineering*. 73(1): 378-388 (2014).
141. Hatami, M., D.D. Ganji, and M. Gorji-Bandpy, CFD simulation and optimization of ICEs exhaust heat recovery using different coolants and fin dimensions in heat exchanger. *Neural Computing and Applications*. 25(7): 2079-2090 (2014).
142. Lv, J., et al., Numerical simulation of the improvement to the heat transfer within the internal combustion engine by the application of nanofluids. *Journal of Enhanced Heat Transfer*. 17(1) (2010).
143. Devireddy, S., C.S.R. Mekala, and V.R. Veeredhi, Improving the cooling performance of automobile radiator with ethylene glycol water based TiO₂ nanofluids. *International Communications in Heat and Mass Transfer*. 78: 121-126 (2016).
144. Bahiraei, M., et al., Using neural network for determination of viscosity in water-TiO₂ nanofluid. *Advances in Mechanical Engineering*. 4: 742680 (2012).
145. Fan, X., et al., Potential of 'nanofluids' to further intensify microreactors. *Green Chemistry*. 10(6): 670-677 (2008) .
146. Ghadimi, A. and I.H. Metselaar, The influence of surfactant and ultrasonic processing on improvement of stability, thermal conductivity and viscosity of titania nanofluid. *Experimental Thermal and Fluid Science*. 51: 1-9 (2013).
147. Yiamsawas, T., et al., Measurement and correlation of the viscosity of water-based Al₂O₃ and TiO₂ nanofluids in high temperatures and comparisons with literature reports. *Journal of dispersion science and technology*. 34(12): 1697-1703 (2013).
148. A., E., Eine neue Bestimmung der Moleküldimensionen. *Annalen der Physik*. 324(2): 289-306 (1906).
149. Brinkman, H., The viscosity of concentrated suspensions and solutions. *The Journal of Chemical Physics*. 20(4): 571-571(1952).

150. Nielsen, L.E., Generalized equation for the elastic moduli of composite materials. *Journal of Applied Physics*. 41(11): 4626-4627(1970).
151. Corcione, M., Empirical correlating equations for predicting the effective thermal conductivity and dynamic viscosity of nanofluids. *Energy Conversion and Management*. 52(1): 789-793 (2011).
152. Handbook, A.F., American society of heating, refrigerating and air-conditioning engineers. *Inc.: Atlanta, GA, USA*,(2009).
153. Tseng, W.J. and K.-C. Lin, Rheology and colloidal structure of aqueous TiO₂ nanoparticle suspensions. *Materials science and engineering: A.* 355(1-2): 186-192 (2003).
154. Chevalier, J., O. Tillement, and F. Ayela, Structure and rheology of SiO₂ nanoparticle suspensions under very high shear rates. *Physical Review E*, 80(5): 051403 (2009).
155. Eiamsa-Ard, S., K. Kiatkittipong, and W. Jedsadaratanachai, Heat transfer enhancement of TiO₂/water nanofluid in a heat exchanger tube equipped with overlapped dual twisted-tapes. *Engineering Science and Technology, an International Journal*. 18(3): 336-350 (2015).
156. Maxwell, J.C., A treatise on electricity and magnetism, Clarendon Press, *Oxford* (1873).
157. Hamilton, R.L. and O. Crosser, Thermal conductivity of heterogeneous two-component systems. *Industrial & Engineering chemistry fundamentals*. 1(3): 187-191(1962).
158. Yu, W. and S. Choi, The role of interfacial layers in the enhanced thermal conductivity of nanofluids: a renovated Maxwell model. *Journal of Nanoparticle Research*. 5(1-2): 167-171(2003).
159. Wei, W., A comprehensive model for the enhanced thermal conductivity of nanofluids. *Journal of Advanced Research in Physics*. 3(2)(2017).
160. Avsec, J. and M. Oblak, The calculation of thermal conductivity, viscosity and thermodynamic properties for nanofluids on the basis of statistical nanomechanics. *International Journal of Heat and Mass Transfer*. 50(21-22): 4331-4341 (2007).
161. Hussein, A.M., et al., Experimental measurement of nanofluids thermal properties. *International Journal of Automotive and Mechanical Engineering*. 7: 850 (2013).
162. Sieder, E.N. and G.E. Tate, Heat transfer and pressure drop of liquids in tubes. *Industrial & Engineering Chemistry*. 28(12): 1429-1435 (1936).

163. Dehghandokht, M., et al., Flow and heat transfer characteristics of water and ethylene glycol–water in a multi-port serpentine meso-channel heat exchanger. *International Journal of Thermal Sciences*.50(8):1615-1627 (2011).
164. Holman, J.P. and W.J. Gajda, Experimental methods for engineers. 8 ed. Vol. 8.: *McGraw-Hill New York* (2012).
165. Aktaş, M., et al., Performance analysis and modeling of a closed-loop heat pump dryer for bay leaves using artificial neural network. *Applied Thermal Engineering*. 87: 714-723 (2015).
166. Garg, D., et al., Direct trajectory optimization and costate estimation of finite-horizon and infinite-horizon optimal control problems using a Radau pseudospectral method. *Computational Optimization and Applications*. 49(2): 335-358 (2011).
167. Monshi, A., M.R. Foroughi, and M.R. Monshi, Modified Scherrer equation to estimate more accurately nano-crystallite size using XRD. *World Journal of Nano Science and Engineering*. 2(3): 154-160 (2012).
168. Sözen, A., et al., Utilization of fly ash nanofluids in two-phase closed thermosyphon for enhancing heat transfer. *Experimental Heat Transfer*., 29(3): 337-354 (2016).
169. Said, Z., et al., New thermophysical properties of water based TiO₂ nanofluid—The hysteresis phenomenon revisited. *International communications in heat and mass transfer*. 58: 85-95 (2014).
170. Nasiri, M., S.G. Etemad, and R. Bagheri, Experimental heat transfer of nanofluid through an annular duct. *International Communications in Heat and Mass Transfer*. 38(7): 958-963 (2011).
171. Abdul Hamid, K., et al., Thermal conductivity enhancement of TiO₂ nanofluid in water and ethylene glycol (EG) mixture. *Indian Journal of Pure & Applied Physics (IJPAP)*. 54(10): 651-655 (2016).
172. Arulprakasajothi, M., et al., Heat transfer study of water-based nanofluids containing titanium oxide nanoparticles. *Materials Today: Proceedings*.2(4-5): 3648-3655 (2015).
173. Usri, N., et al., Thermal conductivity enhancement of Al₂O₃ nanofluid in ethylene glycol and water mixture. *Energy Procedia*. 79:397-402 (2015).
174. Eastman, J.A., et al., Anomalously increased effective thermal conductivities of ethylene glycol-based nanofluids containing copper nanoparticles. *Applied physics letters*. 78(6): 718-720 (2001).

175. Yoo, D.-H., K. Hong, and H.-S. Yang, Study of thermal conductivity of nanofluids for the application of heat transfer fluids. *Thermochimica Acta*. 455(1-2): 66-69 (2007).
176. M'hamed, B., et al., Experimental study on thermal performance of MWCNT nanocoolant in Perodua Kelisa 1000cc radiator system. *International Communications in Heat and Mass Transfer*. 76:156-161 (2016).
177. Shah, R. Thermal entry length solutions for the circular tube and parallel plates. in Third national heat mass transfer conference, *Indian Institute of Technology*, Bombay, India. (1975).
178. Anoop, K., T. Sundararajan, and S.K. Das, Effect of particle size on the convective heat transfer in nanofluid in the developing region. *International journal of heat and mass transfer*. 52(9-10): 2189-2195 (2009).
179. Asirvatham, L.G., et al., Experimental study on forced convective heat transfer with low volume fraction of CuO/water nanofluid. *Energies*. 2(1): 97-119 (2009).
180. Esmaeilzadeh, E., et al., Experimental investigation of hydrodynamics and heat transfer characteristics of γ -Al₂O₃/water under laminar flow inside a horizontal tube. *International Journal of Thermal Sciences*, 63: 31-37 (2013).
181. Pak, B.C. and Y.I. Cho, Hydrodynamic and heat transfer study of dispersed fluids with submicron metallic oxide particles. *Experimental Heat Transfer an International Journal*, 11(2): 151-170 (1998).
182. He, Q., et al., Experimental study on thermophysical properties of nanofluids as phase-change material (PCM) in low temperature cool storage. *Energy conversion and management*, 64:199-205 (2012).
183. Xuan, Y. and W. Roetzel, Conceptions for heat transfer correlation of nanofluids. *International Journal of heat and Mass transfer*, 43(19). 3701-3707 (2000).

RESUME

Siraj Ali Ahmed was born in Tripoli in 1984. I graduated first and elementary education in Libya, and completed high school education, (SULAIMAN KHATER HIGH SCHOOL) in 1998-1999. I got BSc. In Mechanical Engineering from (ALMEARGAB NATIONAL UNIVERSITY - Libya) in 2007-2008. My MSc. In Advanced Manufacturing Systems from (TEESSIDE UNIVERSITY-Middlesbrough, UK) in 2010- 2011. I got licenses in Internal Quality Auditor (ISO 9001:2008 & ISO 19011:2002).In 2010, and I-DEAS Software courses.

I worked in Mechanical Engineering in the (Atomic Energy Establishment) from 2009, then in The Financing and Supporting Research and in the (Libyan Authority for Research, Science and Technology) form 2010. I worked in The Planning Administration at the (Libyan Authority for Research, Science and Technology) form 2012.

CONTACT INFORMATION

Address: ANKARA, CANKAYA

ATA MAH, LIZBON CAD

D.77, NO. 3

E-mail: serajaliomer1984@gmail.com; 2015738132602@ogrenci.karabuk.edu.tr